Modeling the 'Smart Well' in Noardburgum

An uncertainty analysis of the sustainability of the Smart Well

K.R.A. Geul

Technische Universiteit Delft

TU Delft Delft University of Technology

KWR Watercycle Research Institute

Vitens LAAT WATER VOOR JE WERKEN

Challenge the future

Modeling the 'Smart Well' in Noardburgum

An uncertainty analysis of the sustainability of the Smart Well

by

Koen Rudolf Antonius Geul

to obtain the degree of Master of Science

at the Delft University of Technology,

to be defended publicly on Thursday November 17, 2016 at 14:00 PM.

Student number:	4085973	
Project duration:	October 19, 2015 – November 17, 2016	
Thesis committee:	Prof. dr. ir. M. Bakker,	TU Delft
	Dr. ir. W. J. Zaadnoordijk,	KWR / TNO GDN
	ir. A.T. Oosterhof,	Vitens
	Prof. dr. ir. L.C. Rietveld,	TU Delft
	Dr. ir. G.H.W. Schoups,	TU Delft

An electronic version of this thesis is available at `http://repository.tudelft.nl/`.

Delft University of Technology

Preface

First of all, I would like to thank Willem Jan Zaadnoordijk for all his advice and help during this thesis. Without him this thesis would not have been possible. I would also like to thank Ate Oosterhof, for his help and advice during this thesis. Furthermore, I would also like to thank Mark Bakker, for thoroughly reading the report and giving useful tips and feedback. I would like to thank Luuk Rietveld and Gerrit Schoups for being part of the thesis committee. Furthermore, I would like to thank Annemieke van Doorn (KWR) and Sjoerd Rijpkema (Vitens) for their useful insight and feedback. Finally, I want to express my gratitude to my partner Laura, and my parents, for their support during this thesis and their support throughout my study.

K.R.A. Geul
Delft, October 2016

Abstract

The well field in Noardburgum has been closed since the year 1993, due to the salinization of the groundwater. Upconing and lateral attraction of brackish groundwater caused the salinization of the groundwater. Currently, Vitens is looking for ways to reinstate the Noardburgum well field without the risk of salinization. The Fresh Keeper is proposed as a solution. The Fresh Keeper extracts fresh and brackish water at different depths in the aquifer, thus preventing the upconing of brackish water. The extracted brackish water is infiltrated into a deeper aquifer. The Smart Well is a further development of the Fresh Keeper, which monitors the concentration of the brackish water and automatically adjusts the brackish extraction. Currently, a single Smart Well is installed in the Noardburgum well field. Plans exists for a full-scale well field in Noardburgum, including 4 Smart Wells, to be operational by the year 2018.

Another well field, called Ritskebos, is located 1.3 kilometer Southeast of Noardburgum. The chloride content of the extracted water has been increasing over the last decades. 800 meters North East of Ritskebos a hole exists in the aquitard, which separates the first aquifer from the brackish second aquifer. This hole is important to the salinization of the Ritskebos well field. The Smart Well is a potential risk for the Ritskebos well field, since it can increase the amount of groundwater flowing through this hole. It can also enhance the amount of seepage through the aquitard separating the aquifers. This is not beneficial, since groundwater with a high chloride concentration is located in the second aquifer.

The objective of this study is to analyze the effects of the Smart Well and the full-scale design on the regional geohydrology. An uncertainty analysis is performed to assess the reliability of the results. The sustainability is measured using different indicators, including the chloride concentration and the origin of the extracted groundwater. The computed values of the indicators give a measure of the sustainability of the system and the corresponding confidence intervals.

The results of this study show that the probability of salinization, noted as an exceedance of the 0.15 g L^{-1} chloride concentration limit within the coming 50 years, of the full-scale design in Noardburgum is 0-2%. The probability of salinization at Ritskebos without any extractions in Noardburgum is 5-36%, and increases in case of the full-scale design at Noardburgum to 42-66%. There is a 31-55 % probability the mixed water of Noardburgum and Ritskebos will be salinized. The Smart Well increases the probability of salinization at Ritskebos, and poses a substantial threat to the sustainability of the Ritskebos well field. The computed values of the sustainability show that there is almost 50% probability that the full-scale design may lead to an unsustainable situation.

Contents

List of Figures

List of Tables

1 Introduction

Coastal areas around the world are affected by salinization of groundwater, including the coastal areas in the Netherlands. The creation of polders and the extraction of fresh water plays an ever increasing role in salinization. The creation of polders is considered to be an irreversible process for altering groundwater flows. Salinization caused by extraction of water is considered to be reversible, although recovery is slow (Dufour, 1998; Stuurman and Oude Essink, 2007).

Anthropogenic activity plays a major role in the salinization of the area of Noordbergum (see Figure 1.1), which is called Noardburgum, in the native Frisian language. The area of Noardburgum consists of an aquifer system with stratified layers containing chloride-rich paleo-water, which is disrupted by extraction. Paleo groundwater or fossil groundwater is water that infiltrated millennia ago and has been present in the aquifer ever since (Margat et al., 2006). The Noardburgum well field was closed in 1993, due to the salinization of the groundwater (Rus, 1997). Drinking water company Vitens has been looking for ways to reinstate this well field without the risk of salinization, because of increasing demand for drinking water.

A method is developed to extract groundwater, with reduced the risk of salinization, which is named the Fresh Keeper. The Fresh Keeper extracts groundwater at different depths in the aquifer, thus extracting fresh (top filter) and brackish water (bottom filter) separately. The brackish water is useless for drinking water purposes, and needs to be disposed properly. Reverse Osmosis can be used to treat the brackish water. The concentrate of the brackish water is injected into a different aquifer, and the permeate is used for drinking water purposes after it has been treated accordingly. The brackish water cannot be discharged into surface water, due to environmental regulations. The Fresh Keeper extracts fresh water with reduced risk of salinization due to upconing of brackish water. Upconing is the rise of the fresh-brackish interface towards the well screen (Olsthoorn, 2012). There is, however, still a risk of lateral salinization (van der Valk, 2011).

The Smart Well is a new development based on the Fresh Keeper, introduced by Ate Oosterhof (Vitens). The Smart Well automatically monitors the electrical conductivity (EC) of the brackish water and adapts the extraction of brackish water to the EC. This ensures a stable interface between the brackish and fresh water. The Smart Well injects all brackish water into a different aquifer. No reverse osmosis is used.

1.1. Study Objectives

Many studies have been conducted in the Noardburgum well field in the past. The new pilot of the Smart Well generates a lot of new data. New water quality measurements are conducted in the region of Noardburgum, and new requirements have been established for a potential full-scale well field in Noardburgum. All this new information can be used to evaluate previous studies, and to evaluate the potential full-scale well field.

Figure 1.1: Location of Study area. 1. The Noardburgum well field, 2. The Ritskebos well field, 3. The Garyp well field (Google, 2016)

The main objective of this research is:

Assessment of the uncertainty of model predictions of the Smart Well at Noardburgum

An uncertainty analysis will be done on the model results, to get an idea on how reliable the results actually are. Also, some of the questions from previous research will be revisited and analyzed with the new available information and the new requirements. The following research questions will be considered:

1. Does the Smart Well counteract salinization at Noardburgum?
2. Does the Smart Well lead to an increase of salinization at Ritskebos?
3. How will the Northern Brackish Front react to the Smart Well?

When these questions are answered, a design for a full-scale well field is evaluated. The main questions are:

4. How will the full-scale design perform as compared to a single Smart Well?
5. How sustainable is the Smart Well and a full-scale design?

The full-scale design

The full-scale design of the Noardburgum well field will have an extraction of ± 2.0 million cubic meter of fresh water per year. The brackish extraction may be variable over time. The extraction is adapted to stabilize the interface between fresh and brackish water. For this thesis, it is assumed that all the brackish water is injected into a deeper aquifer. Reverse osmosis will not be used to treat the brackish water.

The full-scale design will consist of 4-5 Smart Wells. The current pilot of the Smart Well can be used in the full-scale design. The pilot of the Fresh Keeper is currently not in operation, but can be used in the full-scale design, provided it will be adapted accordingly to function as a Smart Well. Another 2-3 Smart Wells will be placed within the Noardburgum well field for the full-scale design.

1.2. Outline

This thesis starts with an introduction to the area of Noardburgum in Chapter 2. This chapter starts with the history of the Noardburgum Well field and the geological characteristics of the Noardburgum area, after which the previously conducted studies will be discussed.

In Chapter 3, the model and the data used in the model is presented. Assumptions with regards to the model are also presented in this chapter.

In Chapter 4, the modeling tools and computer programs used during the modeling are presented.

In Chapter 5, the results of the different analyses and models will be presented.

In Chapter 6, the results are discussed and are interpreted. Also, comparisons with previous studies are made.

The conclusions and answers to the research questions of this thesis are given in Chapter 7. Recommendations for further research and other remarks are given in Chapter 8.

2

Introduction to the area of Noardburgum

The history of the Noardburgum area and previously conducted research is discussed, as well as the new full-scale well field design for the Noardburgum well field. Sections 2.2 and 2.3 are based on previous research conducted by IWACO (1978) and IWACO (1979).

2.1. History of the Noardburgum well field

In 1925 the first well was constructed and fully operational. A total of eighteen wells were installed by 1937 to meet the increasing demand. The monitoring network indicated a threat for salinization of the Noardburgum well field. However, the monitoring network gave insufficient information to draw clear conclusions. Therefore, a deep well (202.5 meters below NAP [Normaal Amsterdams Peil]) had been drilled at the Noardburgum well field, as a monitoring well for salinization at several different depths in the ground. Results showed that there is no brackish or salt water present in this deep well. It was concluded that there is no immediate threat for salinization of the groundwater in Noardburgum (Krul, 1940).

In 1955, extraction at the location of Ritskebos started, around 1,300 meters South East of Noardburgum. The water from Ritskebos was transported and treated in Noardburgum. This was the same time the Noordbergum effect was first observed in this area, by the Friesland drinking water company. The Noordbergum effect was the initial increase of the head after a pump was turned on, while one might expect a drawdown (Verruijt, 1969). However, the Noordbergum effect is not relevant for this thesis.

By the year 1978, the total extraction rate of Ritskebos and Noardburgum reached almost 25 million m^3 per year. Both locations showed an increase in chloride levels. Deeper measurements at the location of Noardburgum showed an increase of chloride concentration to above 1,000 mg L^{-1}. Research was conducted in 1978/1979 in order to investigate the salinization of the well fields (IWACO, 1979). It was concluded that there was a serious risk of salinization, if no measures were taken.

Salinization continued and eventually led to the closure of the Noardburgum well field in 1993 (Rus, 1997). After the closure of the Noardburgum well field the salinization of Ritskebos continued. Since 1997 the chloride concentration increased with an average rate of 7 mg L^{-1} per year.

A new well field location named Garyp[1] was opened in the year 2003. The new wells were installed to assure Ritskebos could extract water in a sustainable way without the risk of salinization. Garyp produced 3.0 million m^3 of fresh water per year. However, by the year 2005 the well field of Garyp became saline due to upconing brackish water, which was against all expectations. Thus, the production of Garyp was lowered to 1.5 million m^3 per year. The extracted water from Garyp was transported to the Noardburgum treatment facility for treatment. The historic extractions of the different well fields are shown in Figure 2.1.

[1]WGS84: [53.17709; 5.96451] and RDS: [193,599m; 576,866m]

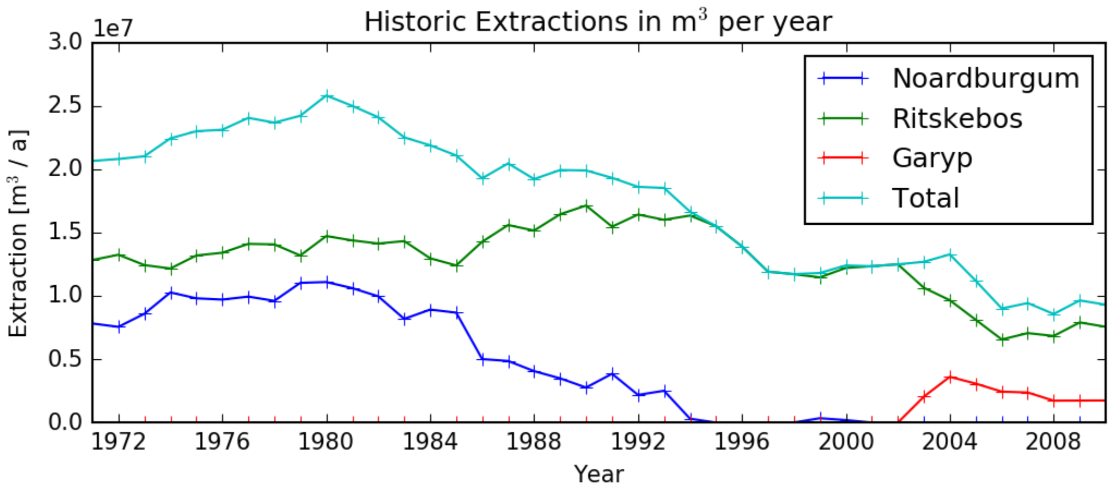

Figure 2.1: Historic extractions of the well fields in the Noardburgum area

Another well field was constructed in the area to compensate for the high chloride concentrations of Ritskebos and Garyp. This well field, Nij Beets, was extracting 3.5 million m^3 fresh water per year. The extracted water from this station was transported and treated at Noardburgum.

Vitens had been searching for an additional source of drinking water in order to assure a sustainable drinking water production. Therefore, research started to extract brackish water at the location of the Noardburgum well field. This system was called the Fresh Keeper. The brackish water was treated by reverse osmosis, since it was not allowed to discharge the brackish water to surface water due to environmental regulations. The permeate was transported to the water treatment plant, and the concentrate was injected into the ground. Injection below the aquitard was deemed to be the best solution (Raat and Kooiman, 2012; Stuyfzand and Raat, 2010). The Fresh Keeper pilot at full-scale was designed to extract 3.0 million m^3 of water per year (Oosterhof and Nederlof, 2007).

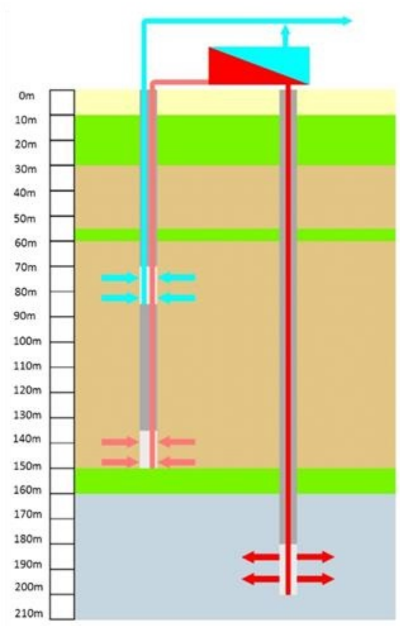

Figure 2.2: Fresh Keeper concept

An injection and an extraction well had been drilled for the Fresh Keeper pilot. The injection well infiltrates the water below an aquitard (160 meter below surface). The extraction well extracts water at two different depths. The first well screen was located at a depth of 65-80 meter below surface; fresh water was extracted here. The second well screen was located at a depth of 130-150 meter below surface, and extracts brackish water. Reverse osmosis was used to treat the brackish water. The permeate was used as drinking water and the concentrate is injected into the aquifer. Both filters of the extraction well extract 50 m^3 water per hour. The recovery of the reverse osmosis is 50 %, which means that 25 m^3 of saline water needs to be injected per hour (Oosterhof and Wolthek, 2008). A representation of the Fresh Keeper concept can be found in Figure 2.2. There was no upconing of brackish water during the operation of the pilot, and the water quality changes were minimal (Oosterhof and Raat, 2010).

Mark van der Valk did his MSc thesis on the Fresh Keeper concept. His research showed a circular well field was best in practice for the full-scale design. There was also no need to extract so much brackish water to prevent salinization. Models showed that an extraction of just 17 m^3 of brackish water per hour is sufficient to prevent upconing (van der Valk, 2011). The pilot was continued in order to investigate the long-term effects of the Fresh Keeper on the aquifer (Wolthek et al., 2013).

Reverse osmosis is expensive and energy consuming. Therefore, the possibility to infiltrate the extracted brackish water directly into the aquifer was proposed. In 2014 a new well was installed at the Noardburgum well field, which infiltrates the extracted brackish water directly. This new pilot was named the Smart Well. It uses the same principle as the Fresh Keeper, but the Smart Well also monitors the electrical conductivity (EC) of the brackish water. The Smart Well can automatically increase or reduce the brackish extraction, depending on the EC of the brackish water. However, to date this automatic extraction has not been successfully tested. The brackish extraction is tested using manual settings. The top of the Smart Well is shown in Figure 2.3. Here, three different pipes are shown at the well. One pipe transports the fresh water to the Noardburgum treatment facility. The other pipes show that the extracted brackish water is directly injected, as the pipes are connected to each other.

Figure 2.3: Top of the Smart Well

2.2. Subsurface characteristics

Drillings have been made to depths of more than 500 meters. A schematization of the geological profile of the subsurface is given in Figure 2.4. The top of the formation of Oosterhout (consisting of shelves, glauconite containing sands and clay) can be found at a depth of 250 meters below surface. Above this formation, a formation called the formation of Maassluis is present, which is considered as the (geo-) hydrological base of this study. The clay layer of the formation of Maassluis is regarded as an impermeable base. Groundwater flow in this clay layer can be neglected. It consists of marine deposits with a thickness of 10 meters mainly containing clay. The formation of Maassluis is covered with a sand layer of fluvial deposits with a thickness of 200 meters (formation of Peize and Waarle). This sand layer is split in half by the Tegelen clay, which can be found at a depth of 150 – 160 meters below surface. The Tegelen clay consists of a compact clay layer. The formation above the formation of Peize and Waalre can be described as less permeable, which is named the Formation of Urk. Directly below the surface a boulder clay layer with low permeability is present.

During the Elsterien (465,000 – 418,000 years ago) Scandinavian land ice penetrated the Northern part of the Netherlands. East of Noardburgum a several hundred meters deep tunnel valley (u-shaped valley) is present, most likely as a result of glacial erosion. This tunnel valley is filled with sand and clay layers. The top part of tunnel-shaped valley is filled with 80 meters of 'Potklei', which is a glaciolacustrine deposit. Potklei is compacted clay with a black or brownish color which can be found in the Northern part of the Netherlands and in East Germany (Ehlers et al., 1984). Friction caused by the glacial erosion is expected to have left a loam layer at sides of the tunnel valley, which is impermeable to horizontal flow. The upper part of the glacial tunnel valley can be seen as impermeable, while the rest of the glacial tunnel valley can be seen as reasonably permeable. This geological formation is more commonly known as the formation of Peelo.

The aquifer in Noardburgum is part of a regional system which is subjected to natural groundwater flow from South East to North West. The area of Noardburgum is higher than the surrounding area. The top layer in the higher area consists of sand. Due to the greater permeability, rain is able to infiltrate the aquifer. Infiltration and the natural groundwater flow from higher grounds in the South-East resulted in a fresh/saline interface North of the area of Noardburgum. Noardburgum is located at the transition area between fresh and salt water. The infiltration of water in the area is estimated to be 118 mm per year. This is 13% of the total extraction in 1978.

In eastern direction, it appears that part of the Tegelen clay is missing, next to the glacial tunnel valley, around 800 meters North East of Ritskebos. This theory is supported by data of the groundwater temperature, hydraulic head and water quality measurements. An estimated 23% of the extraction from Ritskebos

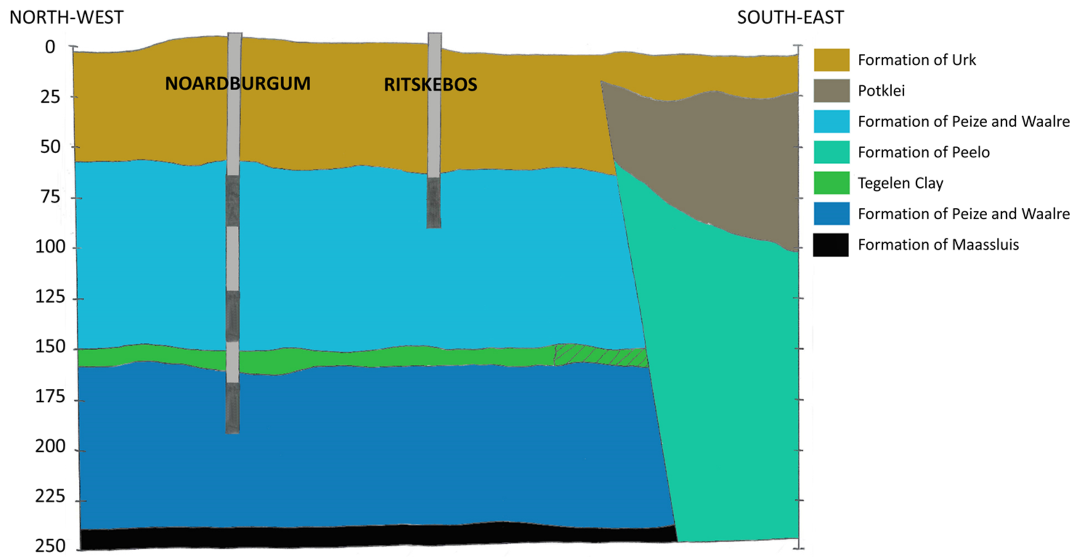

Figure 2.4: Cross-section of the subsurface to a depth of 250 meters

originates from this hole in the Tegelen clay (IWACO, 1979).

Aquifer testing showed that the first aquifer has a transmissivity of 5,200 m^2 d^{-1}. Also, it shows better permeable zones between 65-75 m and 125-145 m below surface (IWACO, 1979). Rus (1997) proposed a transmissivity of 2,500 m^2 d^{-1} for the second aquifer and a hydraulic resistance of the Tegelen clay of 1,300 days, based on aquifer testing and model calibration.

2.3. Water quality analysis

There are four different types of water based on water quality analysis in the area of Noardburgum. The water can be a mixture of the different types. A cross-section of the subsurface, showing the four different water types, is shown in Figure 2.5. This cross-section is based on different water quality measurements[2]. The different types of water identified in the Noardburgum area are:

1. Calcium bicarbonate ($Ca(HCO_3)_2$) type. This water originates from rainfall. This fresh water passes through Calcium-Carbonate-containing minerals. Part of the Calcium-Carbonate is dissolved in the water.
2. Sodium chloride (NaCl) type. This water originates from sea water. This type of water is mainly found in the second aquifer. Deep drillings show that the chloride content of the water is increasing below The Formation van Maassluis. IWACO (1979) concluded that salt transport is taking place due to diffusion from the Formation van Maassluis to the upper layers. Diffusion is extremely slow; therefore, the process of diffusion of salt from the Formation van Maassluis can be neglected when modeling.
3. Calcium chloride ($CaCl_2$) type, this water originates when salt water (NaCl) infiltrates into an aquifer with fresh water, where the soil contains Calcium-rich minerals.
4. Polluted type. This water originates from anthropogenic activity such as agriculture. Polluted water is present in the top layers. Dilution with rainwater gives it an average chloride content of 0.070 g L^{-1}. This source of salinization is small compared to Sodium chloride and Calcium chloride (Rus, 1997).

Water quality analysis shows that the salinization of Noardburgum is caused by lateral attraction of Calcium chloride-rich water from North-Western direction. The salinization of Ritskebos is caused by the attraction of Sodium chloride-rich water from the eastern direction. This water originates from the second aquifer.

[2]Based on the following measurement locations: [06DP0211, 06DP0210, B06D1087, B06D0205, 06DP0214 and 06DP0213]

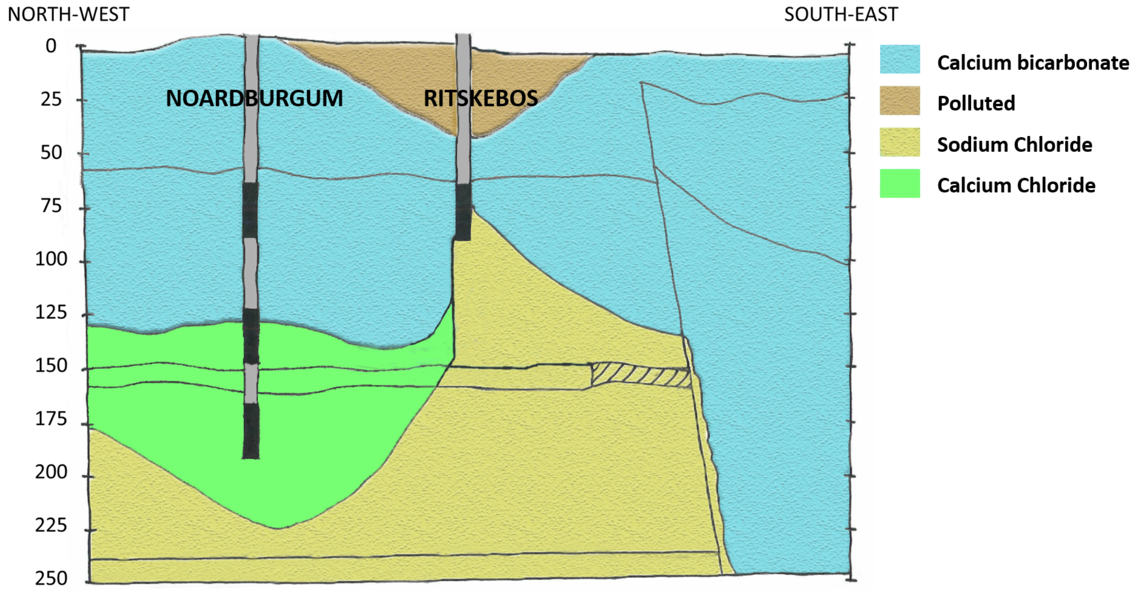

Figure 2.5: Cross-section with the different dominant water types in the subsurface to a depth of 250 meters

This is also an indication that there is an interruption of the Tegelen clay east of Ritskebos. Later research showed, after the closure of the Noardburgum well field, that Calcium chloride-rich water reached the North-West wells of Ritskebos and is causing salinization of the North-West wells (IWACO, 1994; N.V. Waterleiding Friesland, 1990; Rus, 1997).

The brackish water wedge above the Tegelen clay is located at a depth of 135 meters below surface. It is possible to install a well at this depth to extract brackish water and infiltrate it below the Tegelen clay. Research has proven the feasibility of such a well (van der Valk, 2011). It is also possible to reduce the pumping rate of the wells. If less water is extracted, it can stop the salinization of the wells due to upconing. Other measures are the increase of artificial recharge to infiltrate additional fresh water or to infiltrate surface water into the aquifer. However, the surface water needs to be treated before injection. It is doubtful whether this method offers any advantage in comparison with direct treatment of surface water as drinking water source (IWACO, 1990, 1994; Oude Essink, 2001a).

2.4. Overview of previous models

The two main existing models are the Triwaco model IWACO (1994) and the SEAWAT model developed by van der Valk (2011). Additional insight into the different models is presented in Appendix A.

2.4.1. Triwaco model

The Triwaco model is based on the Microfem model develop by Milfac in 1996 and IWACO (1994) (Rus, 1997). The model was made to gain insight into the significant processes in the area and the cause of the salinization of the Noardburgum well field. Also, future predictions for the Noardburgum and Ritskebos well field were made based on streamline analysis.

In 2007 solute transport was added to the Triwaco model. A spatially distributed chloride distribution is made based on water quality measurements (de Graaf et al., 2007). A new future prognosis was made with regards to the salinization of the well field.

In 2014 a sensitivity analysis was conducted and variable density flow is added to the Triwaco model. Also an extra clay layer was added to the second aquifer. The study objective was to determine the regional influence of a full-scale well design of the Noardburgum well field (van der Linde, 2014).

Table 2.1: Location of the Wells for the full-scale design, in RD - coordinates

Name	x coordinate [m]	y coordinate [m]
Current Locations:		
Smart Well	195,703	581,456
Fresh Keeper extraction	195,748	581,550
Fresh Keeper injection	195,774	581,560
Future extraction locations:		
Smart Well 1	195,782	581,076
Smart Well 2	195,740	581,257
Future infiltration locations:		
Smart Well injection	195,760	581,166

The Triwaco model forms the basis for the new flow and transport model that is developed for this thesis. Several changes need to be made to the model in order to make it suitable for MODFLOW.

2.4.2. Models van der Valk (2011)

van der Valk (2011) has made several different models in SEAWAT. These models were mainly used to gain insight into the relevant processes of salinization on large and small-scale (van der Valk, 2011).

- Small-scale model. This model was used to gain insight in local processes surrounding the Fresh Keeper. Also, the effects of the well field configuration on upconing can be determined using this model.
- Cross-sectional model. This model was used to gain insight into the salinization process of the Noardburgum well field. The model was used to simulate the historic salt intrusion (± 10,000 years ago till now). The results of the model were used to make a spatially distributed chloride distribution used in the large-scale model.
- Large-scale model. This model was used to gain insight into the salinization process of the Noardburgum well field.

2.5. The full-scale design

The full-scale design of the Noardburgum well field consists of 4 extraction locations (fresh and brackish) and 3 infiltration locations, and will extract ± 2.5 million m^3 fresh water per year. The current pilot of the Smart Well (extraction and injection) can be used in the full-scale design. The pilot Fresh Keeper well is currently not used, but with some adjustments the Fresh Keeper well can be used in the full-scale design. Two additional extraction locations are chosen within the Noardburgum well field. These two locations will share one infiltration location, due to the high costs of deep drillings. A shared infiltration location should not be a problem for the relatively low volume of injection. The locations of the wells is presented in Table 2.1. The actual locations within the well field can be seen in Figure 2.6.

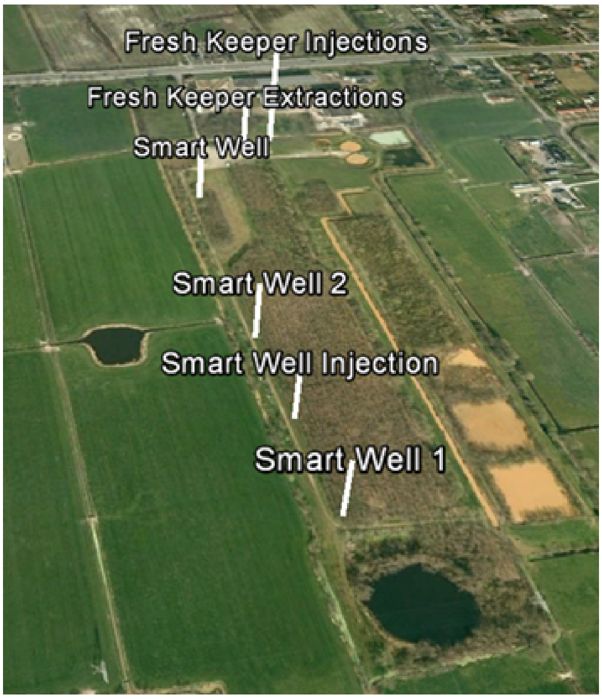

Figure 2.6: Location of the different wells at the Noardburgum well field

3

Flow and transport model

Several different groundwater models have been developed for the area of Noardburgum. The new flow and transport model is constructed in FloPy, and uses the computer software SEAWAT and MODPATH. The previous models are explained in Section 2.4. These models have been studied and analyzed, as presented in Appendix A.

The model of Rus (1997) and de Graaf et al. (2007) is based on field measurements. This model is used as the starting point for the flow and transport model, since this model provides the best match with measurement data from the Noardburgum area. The Triwaco model is based on the finite element method. The Triwaco model input is exported to an Excel file which is read into Python using the Pandas package[1]. The grid is translated to finite differences and minor changes are made to assure the model is compatible with SEAWAT and MODPATH.

3.1. Boundaries of the model

The side boundaries of the model are placed at a large distance from the Noardburgum and Ritskebos well fields, so that the extractions have an negligible effect on the boundary heads. The eastern boundary is different compared to the original Triwaco model. The boundary is place at the glacial tunnel valley in order to reduce the size and the computational time of the model. It is not expected this effects the model results, since the glacial tunnel valley is modeled as impermeable. The boundaries of the original model and the new boundaries are presented in Figure 3.1. Also, a small-scale boundary is presented, which is used for the chloride content analysis.

The starting heads of the model are imported from the Triwaco model. The imported heads are fresh water heads, and need to be adapted to account for density differences. The conversion of the boundary heads is done with the Time-Variant Specified-Head (CHD) package (Harbaugh, 2005).

A General Head Boundary (GHB) is assigned to the top layer of the model. The GHB package can simulate a flux in or out of the aquifer, dependent on the head in the aquifer and the head outside the aquifer. The resistance and corresponding conductance used in the GHB are presented in Figure 3.2a. The resistance of the imported Triwaco model is limited to a maximum of 100,000 days, due to negligible effects of larger resistances.

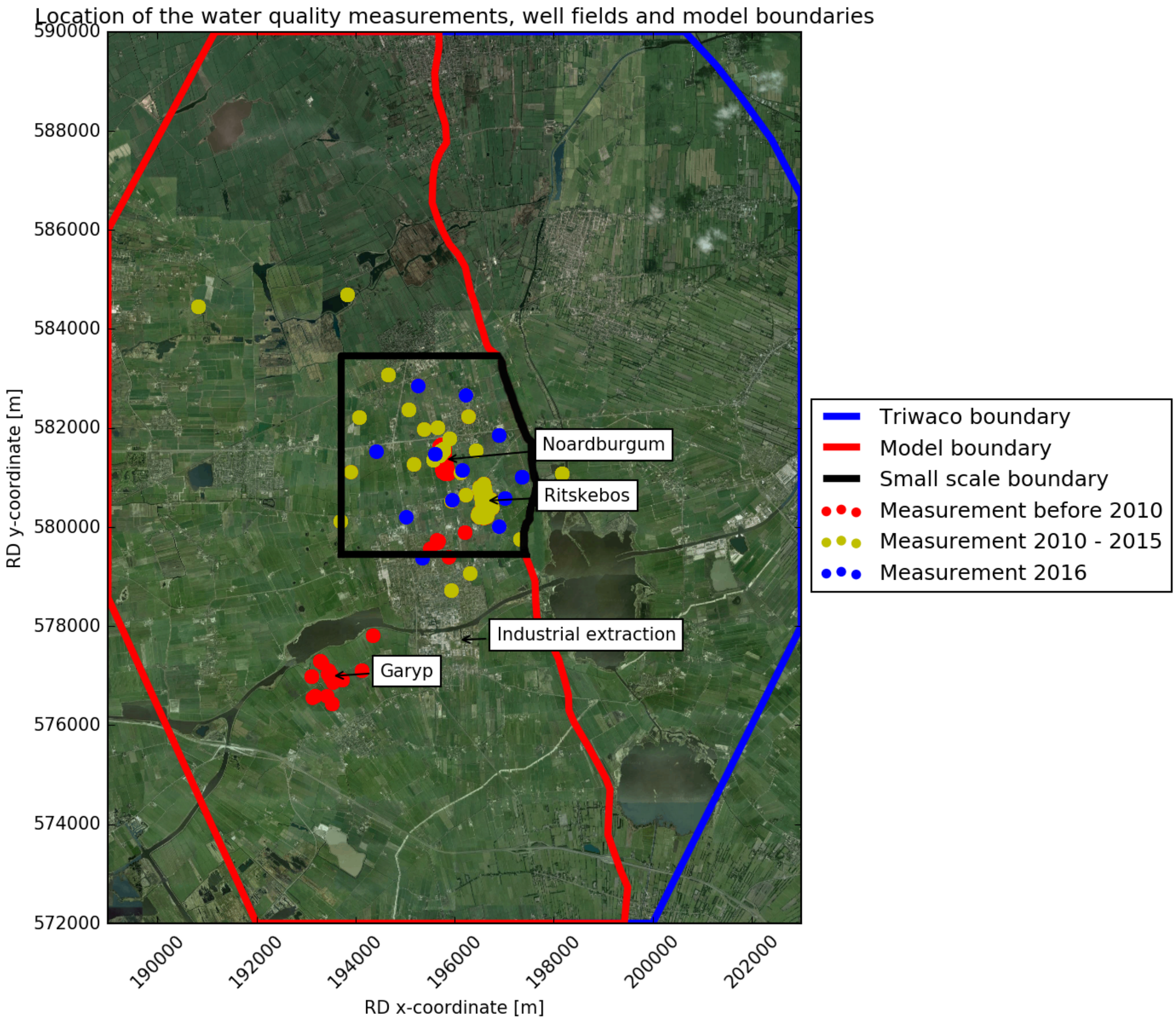

Figure 3.1: The location of the water quality measurement, the location of the boundaries from the Triwaco model and the new model boundaries (large and small-scale)

3.2. Aquifer properties

The different model layers and the corresponding hydraulic conductivity and resistances are presented in Table 3.1. The top and bottom of the layers is uniform over the entire model. The vertical distance between layers is small where chloride transport and density differences are expected to be of importance. The cells have a length and width of 50 meters, which is the best trade-off between accuracy and computational time. The cells of the small-scale model have a length and width of 10 meters. An equidistant grid is preferred in the models, because different cell lengths may lead to numerical instability (Guo and Langevin, 2002).

The resistance of the semi-confining layer is limited to 100,000 days, just as the GHB. It also shows that resistance at the Noardburgum well field and Ritskebos well field is relatively low, which is beneficial for infiltration into the aquifer. The spatially variable resistance is presented in Figure 3.2c.

The resistance of the Tegelen clay is presented in Figure 3.2d. The glacial tunnel valley is presented in dark red, and the hole in the Tegelen clay is shown in dark blue, right beside the glacial tunnel valley.

[1]http://pandas.pydata.org/

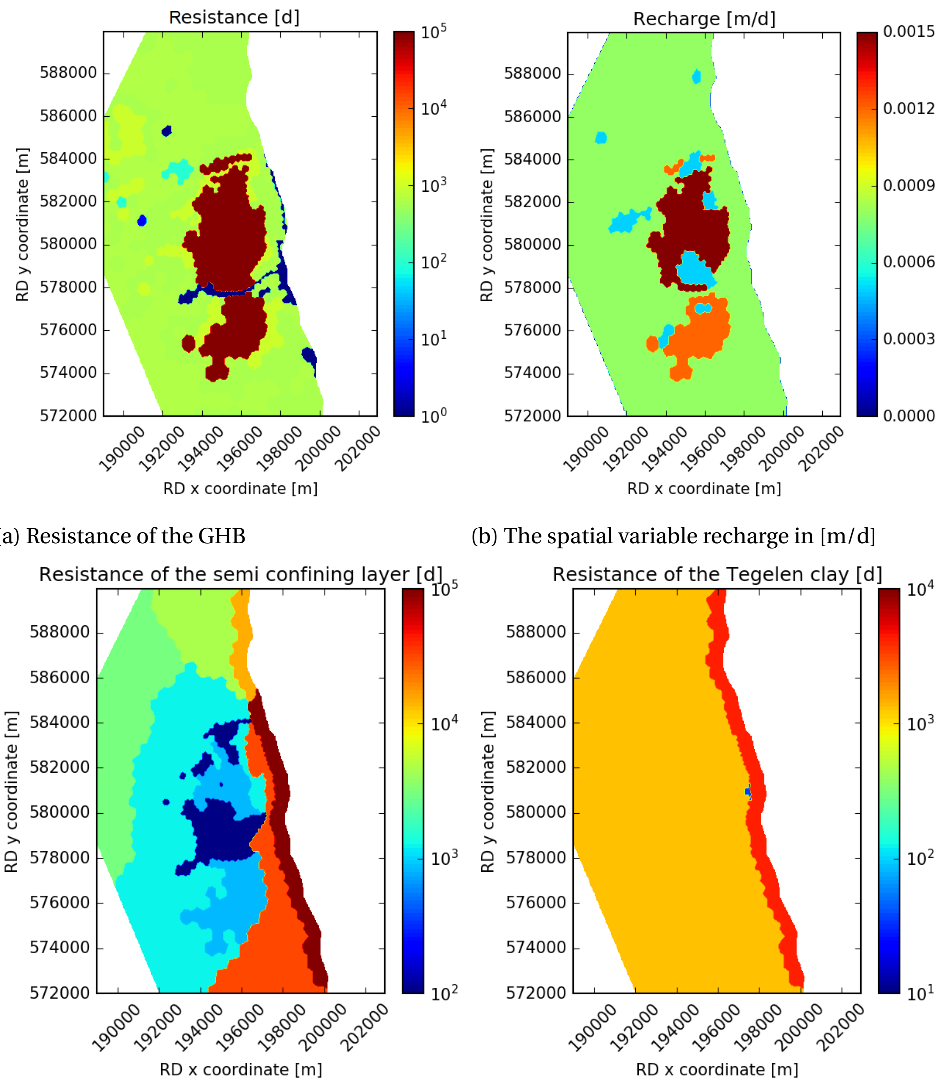

(a) Resistance of the GHB

(b) The spatial variable recharge in [m/d]

(c) Resistance of the semi-confining layer

(d) Resistance of the Tegelen clay

Figure 3.2: Spatially variable model input of the flow and transport model

3.3. Extractions and injections in the model

The Recharge (RCH) package is assigned to the top layer. The RCH package simulates a constant specified flux into the aquifer. Evaporation is included in the imported Triwaco recharge. The spatially variable recharge is given in Figure 3.2b.

The Well (WEL) package is used to simulate extractions and infiltrations in the model due to well activity. The discharge of the different well fields in the Noardburgum area is shown in Figure 2.1. In the period from 2007 till 2010 the extractions are stable. After 2010, the Fresh Keeper started. The average extractions from the period 2007 till 2010 are used during the steady-state modeling. Also, the total extraction of a well field is equally divided over the available extraction wells. The extraction is assumed to be constant along the length of the well filter.

The brackish extraction is assumed to be constant, just as the injection of brackish water. The automatic adjustment of the brackish extraction based on the chloride concentration of the extracted water is not included in the modeling process. A constant chloride concentration of 2.1 g L^{-1} is assumed for the injected water of the brackish water in the 2^{th} aquifer in the model, based on electrical conductivity measurements (see Appendix F).

Table 3.1: Transmissivity and resistance of the different model layers

Name	Layer	Top [m]	Bottom [m]	Hydraulic conductivity [m/d]	Resistance [d]
Phreatic layer	1	0	-10	1	-
Semi-confining layer	2	-10	-35	-	Figure 3.2c
	3	-35	-60	-	Figure 3.2c
First aquifer	4	-60	-75	70	-
	5	-75	-90	70	-
	6	-90	-100	42.5	-
	7	-100	-110	42.5	-
	8	-110	-120	42.5	-
	9	-120	-130	42.5	-
	10	-130	-135	70	-
	11	-135	-140	70	-
	12	-140	-145	70	-
	13	-145	-150	70	-
Tegelen clay	14	-150	-160	-	Figure 3.2d
Second aquifer	15	-160	-165	31.3	-
	16	-165	-170	31.3	-
	17	-170	-175	31.3	-
	18	-175	-185	31.3	-
	19	-185	-196	31.3	-
	20	-196	-204	31.3	-
	21	-204	-223	31.3	-
	22	-223	-240	31.3	-

Near the well fields, extractions of groundwater are taking place for industrial purposes by SCA Hygiene-products Suameer[2] and Sonac Burgum B.V.[3]. The exact extractions are currently not known. It is assumed that the industry is extracting the maximum permitted amount of groundwater (400,000 and 750,000 m^3 per year, respectively). Other extractions in the area are considered to be negligible compared to the well fields (Provincie Fryslân, 2016).

3.3.1. Scenarios

A common misconception is the idea that the water budget of a groundwater system, before anthropogenic activity, can determine the sustainable extraction of a system. This is known as the water budget myth (Alley et al., 1999; Bredehoeft, 2002). Groundwater extractions change the natural flow system and must be accounted for. The water budget changes in response to anthropogenic activity. Four different scenarios are defined. The extractions of the Smart Well are assigned to the Noardburgum well field. The extractions of the well fields for the different scenarios are presented in Table 3.2. The actual extractions over time are shown in Figure 2.1.

1. The first scenario is an over-exploitation scenario. This scenario is based on the extractions from 1970 to 1980.
2. The second scenario is the basic scenario without any additional extractions. This scenario is based on the extractions between 2007 and 2010, when the extractions were constant.
3. The third scenario is the basic scenario and a single Smart Well (the current pilot) in Noardburgum.
4. The fourth scenario is the basic scenario and the full-scale design of the Noardburgum well field.

[2]WGS84: [53.18085; 5.99394] and RDS: [195 563m; 577 301m]
[3]WGS84: [53.22522; 5.99565] and RDS: [195 676m; 577 423m]

Table 3.2: Different scenario for the extractions

	Ritskebos [m^3/d]	Noardburgum [m^3/d]	Noardburgum brackish extraction [m^3/d]	Garyp [m^3/d]	Industrial extraction [m^3/d]
Scenario 1 1970 - 1980	36,480	26,083	-	-	-
Scenario 2 2007 - 2010	20,395	-	-	4,753	3,146
Scenario 3 Smart Well	20,395	1,700	350	4,753	3,146
Scenario 4 Full-scale	20,395	6,800	1,400	4,753	3,146

3.4. Variable-density flow

The Variable-Density Flow (VDF) package is used to simulate the affects of concentration on fluid density. The density of ocean water varies due to variations in temperature, composition and pressure. The equation of state relates the density (ρ) of the water to the concentration of total dissolved solids, (C [M L^{-3}]), temperature (T [T]) and pressure (P [M L^{-1} T^{-2}). The following relation is used: (Langevin et al., 2008; Olsthoorn, 2012)

$$\rho = \rho_0 + \frac{\partial \rho}{\partial C}(C - C_0) + \frac{\partial \rho}{\partial T}(T - T_0) + \frac{\partial \rho}{\partial P}(P - P_0) \tag{3.1}$$

Equation 3.1 can be applied to coastal aquifers where non-uniform density distributions occur, even though it is develop for ocean water density (Oude Essink, 2001b).

In general deeper groundwater tends to be warmer than shallow groundwater. The average groundwater temperature increase is 1.8 °C per 100 meters depth. The temperature increase can be higher in volcanically active areas (Heath, 1983; Holzbecher, 1998). In the equation of state $\partial\rho/\partial T$ is on order of -0.12 kg m^{-3} °C^{-1}, which results in small density differences caused by temperature compared to changes in solute concentration (Fofonoff and Millard, 1983). Therefore, the temperature component in the equation of state is neglected. Also, the pressure difference in the equation of state is neglected due to negligible influence on the density for this given case compared to the influence of solute concentration.

It is assumed that the initial chloride concentration of the water is 0.0 g L^{-1} and that the groundwater has a constant temperature of 12.0 °C, based on temperature measurements. Since only chloride measurements have been conducted, a relation is needed between the solute concentration (C) and the chloride (Cl) content of the groundwater: (Lewis, 1980)

$$C(\texttt{parts per thousand}) \approx 1.80655\ Cl\left(\frac{g}{L}\right) \tag{3.2}$$

Using the UNESCO equation of state calculator[4] and the relation between solute concentration (C) and chloride concentration (Cl) (Equation 3.2), Equation 3.1 can be approximated by the following linear equation:

$$\rho \approx 999.50 + 1.3982\ Cl\left(\frac{g}{L}\right) \tag{3.3}$$

3.5. Head observations

Piezometers are located in the region of the Noardburgum well field. These piezometers continuously measure the water pressure at specified points. Pressure is measured at 174 locations near the well field. Daily measurements are conducted, and during the period of 2007 till 2010 continuous measurements are available at more than 134 locations. The data of these measurements is used for parameter estimation (see Section 4.1). A visual inspection is performed to point out any remaining unreliable piezometers. An example of

[4] http://www.phys.ocean.dal.ca/ kelley/seawater/density.html

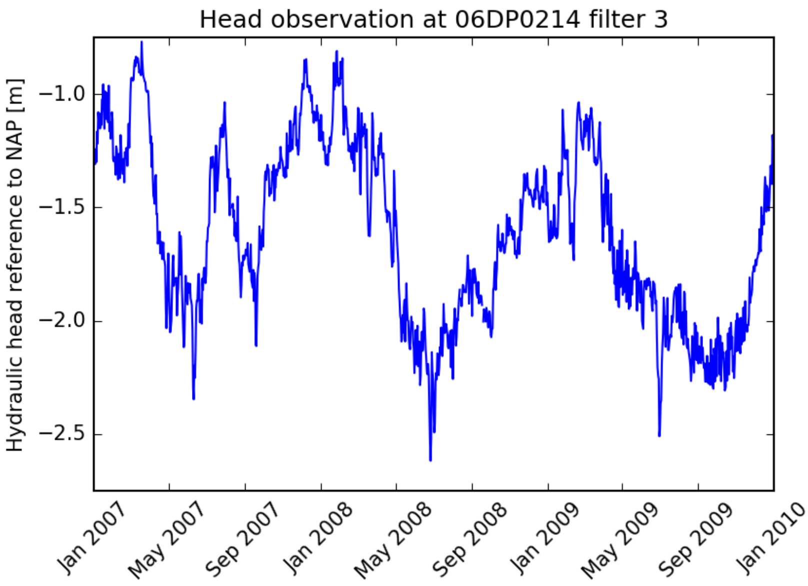

Figure 3.3: Recorded hydraulic head at 06DP0214 filter 3 (168 meters below surface)

the piezometer data is given in Figure 3.3. The data of piezometers has already been corrected for air pressure differences. The piezometers do not measure the electrical conductivity of the groundwater.

The recorded hydraulic head of a piezometer in the Noardburgum well field is presented in Figure 3.3. It can be seen that there is a seasonal pattern. Almost all piezometers show this seasonal pattern. Despite the seasonal pattern, the summer of 2007 (July) shows an increase in hydraulic head, while a decrease in head is expected. This can be explained by the wet summer of 2007. In June, 114 mm of precipitation occurred in Leeuwarden (the 1951 - 2015 average is 65 mm) and in July 181 mm of precipitation is recorded (the 1952 - 2015 average is 87 mm) (KNMI, 2016). The input data of the model is based on yearly averages. Therefore, the average hydraulic head of the piezometer over the entire period is used. Only reliable piezometers with daily measurements throughout the year are included. The variance of the piezometer over the period 2007 - 2010 is used as weighing factor in the calibration. No large differences are observed in the head data between 2007 - 2010 compared to the average of 2000-2015.

3.6. Water quality measurements

Water quality monitoring started in the year 1923, and so far almost 4,000 point measurements have been conducted at 152 unique locations. The location of the measurements and the period the last measurement is conducted are presented in Figure 3.1. The chloride content of the groundwater is always measured when conducting a point measurement. In a few hundred cases the Sodium and Calcium content and the temperature of the groundwater are measured. All measurements are used in the analysis.

Not all measurements are reliable. Some may simply be corrected using the measured electrical conductivity (EC). The uncertainty in these measurements is unknown. For this thesis it is assumed all measurements are correct (after correction for EC) and they are used in the analysis.

During the pilot of the Smart Well, the EC of the fresh and brackish water is measured, as presented in Appendix F. This information is used during the analysis for comparison of the model results.

3.6.1. Initial chloride distributions

It is found that making a new initial chloride distribution only based on the measurements is complicated. The measurements are conducted in three-dimensional space at different times. The locations of the measurements are shown in Figure 3.1, and only the latest measurements (since 2010) are used. The location of the measurements are focused on the area of the Noardburgum and Ritskebos well field. In order to construct an initial condition from measurements the data should be extrapolated throughout the model, as is done in previous studies to construct the initial distribution. Therefore, using previous initial distributions is preferred over constructing a completely new distribution based on measurements.

Several different three-dimensional chloride distributions have been developed in previous studies. These different distributions will be analyzed, compared, and used in the modeling process. The two initial distributions which provide the best match with the conducted measurements are used in further analysis.

de Graaf et al. (2007) developed the first chloride distribution, based on chloride measurements and geoelectric measurements conducted by TNO. This initial chloride distribution is named distribution A.

A new initial chloride distribution is constructed, based on the chloride distribution created by de Graaf et al. (2007). It is assumed this distribution is valid for the year 1985. Using SEAWAT and the calibrated model parameters, an initial distribution for the year 2016 is constructed. This initial chloride distribution is named distribution B.

All initial distributions are shown in Appendix G. Here it can be seen that distribution A and B perform best compared to the measurements. The two initial distributions show similarities at the locations of the measurements, as is shown in Figure G.1b and Figure G.1a. However, differences are visible with regards to the fresh/brackish interface in the first and second aquifer, as is expected since distribution B is created from distribution A.

3.6.2. Chloride transport

Chloride transport is simulated using SEAWAT. The transport of chloride in groundwater can be described by three different mechanisms (Pinder and Celia, 2006):

- Advection is the movement of solute mass due to velocity of the groundwater. The solute mass is moving along at the same velocity as the groundwater.
- Dispersion is the spreading of solute mass over a greater region than would be predicted by the average groundwater velocity (Zheng and Wang, 1999). Dispersion consists of mechanical dispersion and molecular diffusion.
  - Mechanical dispersion is caused by deviations, on micro scale, of the velocity of the groundwater. This can be due to heterogeneities in the aquifer. The mechanical dispersion is a product of the dispersivity times the average groundwater velocity. The longitudinal dispersivity is assumed to be 2 meters. A different dispersivity (0.01 or 10 meters) leads to negligible differences in model results. The transverse dispersivity is one magnitude smaller than the longitudinal dispersivity.
  - Molecular diffusion is driven by concentration gradients. In this study the molecular diffusion is considered to be negligible.

4

Modeling tools

Models are needed to analyze the impact of interventions to a system, such as a full-scale well design in Noardburgum (Savenije, 2009). This chapter presents the tools, assumptions and software used in this thesis. A visualization of the steps of the modeling process applied in this thesis is given in Figure 4.1.

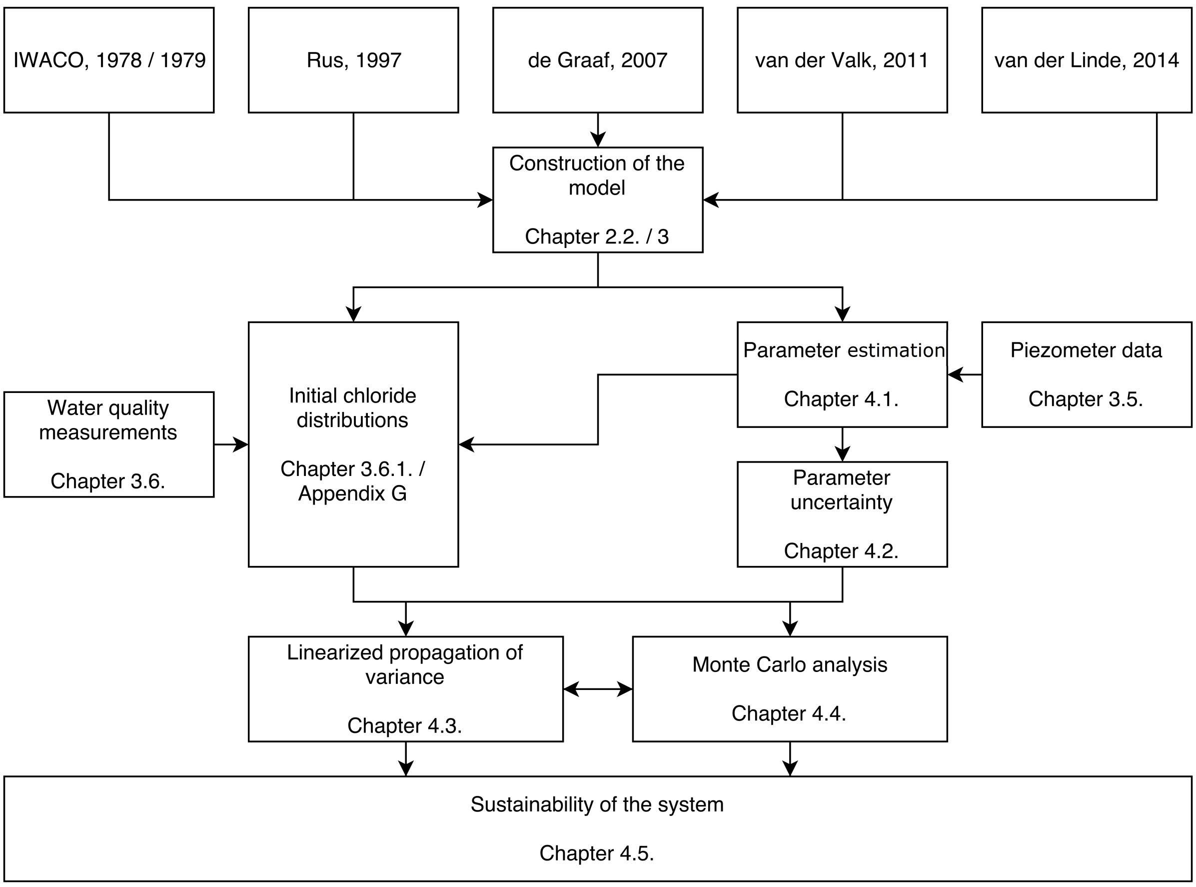

Figure 4.1: Different modeling tools / steps and the corresponding chapters

4.1. Parameter estimation

The (geo-) hydrological reality of a system is complicated. A model consists of equations, procedures and model parameters, and forms a representation of this complex reality (Leijnse and Hassanizadeh, 1994). Estimations of model parameters are made based on observations or prior knowledge. These estimations can be improved using measured values. In model calibration the model input is varied in order to improve the match between the simulated results to the measured values. The estimation of model parameters tends to become meaningless for too many parameters, due to the increasing degrees of freedom (Criminisi et al., 1997; Hill, 1998; Savenije, 2009).

In a groundwater model, observed heads or discharges are used to calibrate a model. Calibration is based on minimizing an objective function which defines the difference in measured observation and simulated results (Fitts, 2002). Calibration is also called historical matching, since the model is adjusted until an adequate match is achieved with the historical data (Bredehoeft and Konikow, 1993). The objective function can be scaled by data uncertainties to account for uncertainty of the measurement. In this thesis the estimated variance of measured heads is used as uncertainty (Newville et al., 2016).

$$F = \sum_{i=1}^{n} \left(\frac{h_i^{meas} - h_i^{model}}{\sigma_i^2} \right)^2 \tag{4.1}$$

Where
F is the objective function,
i is the measurement number,
h_i^{meas} measurement i,
h_i^{model} simulation i,
σ_i^2 is the variance of measurement i

The Levenberg-Marquardt method is applied to minimize the objective function in this thesis. This algorithm locates a local minima of the function, which is not necessarily the global minimum. This makes starting conditions important to the results. Different starting conditions can lead to different results. This calibration algorithm is chosen because it is fast to estimate the uncertainties and correlations of parameters. The LMFIT package is used to perform model parameter calibration (Newville et al., 2016). LMFIT builds on the SciPy package scipy.optimize[1]. One of the main advantages of the LMFIT package is the automatic calculation of many statistical properties of the parameters (e.g. covariance). In the LMFIT package the parameters can be given upper and lower boundaries.

4.1.1. Parameters

Different model parameters are selected to be estimated. Only parameters which are expected to have large influences on model results are selected.

- **Recharge**
  Recharge is defined as precipitation minus evaporation. The recharge enters the model at the top layer. The recharge of the aquifer is spatially variable. The highest recharge rate is in the area of Noardburgum and the lowest recharge rates are found in the polders surrounding Noardburgum. The spatially variable recharge is found in Figure 3.2b. The spatially variable recharge is estimated using a multiplication factor.

- **Semi-confining layer**
  The semi-confining layer is the layer between the phreatic aquifer and the first aquifer. The resistance of the semi-confining layer is spatially variable. the resistance may very by 3 orders of magnitude. Resistances larger than 3,000 days are not included in the calibration process, due to a negligible effect on model results. The estimated resistance is presented as the dark and light blue colors in Figure 3.2c. The spatially variable resistance is estimated using a multiplication factor.

[1] http://docs.scipy.org/doc/scipy/reference/optimize.html

Table 4.1: Parameters, initial values and upper and lower boundaries

Name	Type	Unit	Log-normal distribution	Initial value	Lower boundary	Upper boundary
Recharge	Multiplication factor	[-]	Yes	1	0.01	∞
Semi-confining layer	Multiplication factor	[-]	Yes	1	0.01	∞
First aquifer	Transmissivity	[m^2/d]	Yes	5,200	52	∞
Tegelen clay	Resistance	[d]	Yes	1,300	13	∞
Second aquifer	Transmissivity	[m^2/d]	Yes	2,500	25	∞

- **First aquifer**
  The first aquifer is where the extractions of the different well fields take place. The transmissivity of the aquifer will be estimated.

- **Tegelen clay**
  The Tegelen clay is the aquitard separating the first and second aquifer. The resistance of the Tegelen clay will be estimated. The hole in the Tegelen clay and the impermeable glacial gully are not included in the calibration process. The resistance of the Tegelen clay is presented in Figure 3.2d. The low resistance near the glacial gully is the hole in the Tegelen clay.

- **Second aquifer**
  The second aquifer, also known as the injection aquifer, is where the injections of the Fresh Keeper and Smart Well take place. It is located between the Tegelen clay and the (geo) hydrological base. The transmissivity of the aquifer will be estimated.

Five parameters are selected for the calibration process, which are presented in Table 4.1. Upper and lower boundaries are given for the parameters. All parameters have a log-normal distribution, to assure no negative values can occur. The recharge and semi-confining layer are spatially variable, therefore, a multiplication factor is used for all values instead of assigning a parameter to every cell. This limits the degrees of freedom in the calibration process.

4.2. Uncertainty and confidence intervals

Prior to this study, all models regarding the Noardburgum well field have used the best estimates of the parameters for the modeling process. Instead of estimating the optimal value of the parameter, an interval of plausible values for the parameters can be used. This interval accounts for uncertainty of the estimate. The estimated interval of the parameter can be translated to the predictions arising from the parameters (Dekking et al., 2005; Mood and Graybill, 1963).

4.2.1. Sources of Uncertainty

A few of the most important sources of uncertainty are mentioned: (Cooley et al., 1990)

- Sources of uncertainty in measured head data:
  - Measurement error.
  - Water quality inside the piezometer is unknown. Density differences can cause large differences in freshwater head.
  - Precipitation and evaporation yearly data may not be representative for yearly averages over longer periods.
- Sources of uncertainty in the chloride measurements:
  - Measurement error.

  - Results from point measurements may not be representative for regional values.
  - There are too few measurements to make an accurate estimations of chloride concentration over time.

- Model structural error.

4.2.2. Probability density distributions

In this thesis, two different probability distributions are used:

Normal distribution (Dekking et al., 2005; Mood and Graybill, 1963)

The probability density function $f(x)$ of the normal distribution is given by:

$$f(x) = \frac{1}{\sigma\sqrt{2\pi}} \exp\left(-\frac{(x-\mu)^2}{2\sigma^2}\right) \tag{4.2}$$

Where
σ is the standard deviation,
μ is the expected or mean value,
σ^2 is the variance

The 95 % confidence interval of normally distributed variable is:

$$\theta = \mu \pm 1.96\sigma \tag{4.3}$$

Log-normal distribution

Suppose X is a positive random variable. Y is a random variable defined as Y = log(X). If Y has a normal distribution with mean μ and variance σ^2, than X has a log-normal distribution. The mean $\hat{\mu}$ and variance δ^2 of X is given by: (Olsson, 2005; Zhou and Gao, 1997)

$$\hat{\mu} = \exp\left(\mu + \frac{\sigma^2}{2}\right) \tag{4.4}$$

$$\delta^2 = \exp\left(2\mu + 2\sigma^2\right) - \exp\left(2\mu + \sigma^2\right) \tag{4.5}$$

The 95 % confidence interval of the log-normally distributed variable is: (Olsson, 2005; Zhou and Gao, 1997)

$$\theta = \exp(\mu \pm 1.96\sigma) \tag{4.6}$$

4.3. Linearized propagation of variance

Parameters have uncertainties expressed in variance or standard deviation. These uncertainties have an effect on the reliability of the model results. A quick way to calculate this effect is the linearized propagation of variance. This does not only use the variances of the parameters, but the entire covariance matrix.

Suppose A as a function of B and C, where A is the model result and B and C are parameters. B and C are correlated. The variance of A may be approximated, using the Taylor series method (linearization): (Ku, 1966; Lee and Forthofer, 2005)

$$A = f(B, C) \tag{4.7}$$

$$Var(A) \approx \left(\frac{\partial f}{\partial B}\right)^2 Var(B) + \left(\frac{\partial f}{\partial C}\right)^2 Var(C) + 2\frac{\partial f}{\partial B}\frac{\partial f}{\partial C} Cov(B,C) \tag{4.8}$$

Note that this method is not limited to two parameters. The formula can easily be adapted to account for more than two parameters.

The partial derivative can be estimated with a first order difference quotient. The partial derivatives are the sensitivity coefficients. A higher value for the partial derivative indicates that the outcome is sensitive to changes in that parameter. The partial derivative is approximated by the following equation:

$$\frac{\partial f}{\partial B} \approx \frac{f(B+\Delta B, C) - f(B,C)}{\Delta B} \tag{4.9}$$

Numerical derivatives and the covariance matrix are required input for the linearized propagation of variance. The linearized propagation of variance does not account for non-linearity in the relation between parameters and model results. Monte Carlo simulation can be used to validate the results from the linear propagation of variance (Tellinghuisen, 2001).

4.4. Monte Carlo analysis

A Monte Carlo analysis will be performed to analyze the nonlinear confidence intervals of the model results. The number of runs is determined by the number of parameters. For n parameters, 10^n realizations are needed. Monte Carlo simulation is simple but time-consuming (Kirchner, 2016; Savenije, 2009).

A large set of parameters is generated using the Multivariate Gaussian distribution, a generalization of the normal distribution to higher dimensions (Mood and Graybill, 1963), based on the covariance matrix returned by LMFIT. The multivariate Gaussian distribution makes sure the random set of variables keep their original parameter correlation. The set of parameters is used in the Monte Carlo analysis.

4.5. Sustainability

The American Society of Civil Engineers Task Committee for Sustainability Criteria (ASCE, 1998) proposed the following definition of sustainability with respect to water resources:

> *"Sustainable water resource systems are those designed and managed to fully contribute to the objectives of society, now and in the future, while maintaining their ecological, environmental, and hydrological integrity."*

Based on the definition of sustainability, we can say that a water resource system which satisfies the current and future demands without system degradation can be seen as sustainable. In order to measure sustainability it must be precisely described what we are trying to achieve.

Different indicators are used to connect model output to sustainability (Alley et al., 1999; Gleeson et al., 2012; Pandey et al., 2011; Vrba and Lipponen, 2007). For this thesis three different indicators are selected to measure the sustainability.

- Chloride content of the extracted groundwater.
- Renewability of the groundwater resource.
- Vulnerability of the groundwater resource.

Linear evaluation equations are presented to assess the sustainability of the different indicators. The assessment of the sustainability of the different indicators is combined using weighing factors.

4.5.1. Chloride content of the extracted groundwater

An important indicator for sustainability, for this thesis, is the chloride content of the extracted groundwater. The chloride concentration of the mixed extracted groundwater at the treatment facility in Noardburgum may not exceed 0.15 g L^{-1}. The mixed extracted water in the Noardburgum treatment facility receives water from the Noardburgum Well Field, Ritskebos, Garyp, and Nij Beets. Nij Beets is located 17 kilometers south of Noardburgum, and is not included in the modeling process. It is assumed that the chloride concentration of the extracted groundwater from Nij Beets and Garyp is stable for the coming 50 years.

The definition of sustainability with regards to the chloride content of the extracted groundwater is:

> *"The chloride content of the extracted groundwater is considered to be sustainable if the concentration of the mixed extracted fresh water in the Noardburgum treatment facility does not exceed 0.15 g L^{-1} in the next 50 years."*

The concentration of the extracted groundwater is given a sustainability grade. The following linear evaluation equation is proposed (Equation 4.10). In this evaluation equation a chloride concentration below 0.07 g L^{-1} is a 10 (the best possible grade), a concentration of 0.15 g L^{-1} is a 5.6 (just adequate), and a concentration above 0.25 g L^{-1} equals a 0 (worst possible grade). A minimum concentration of 0.07 g L^{-1} is chosen, since this is the chloride concentration of the groundwater recharge (Rus, 1997).

$$\begin{cases} \text{Grade} = 10 & \text{Cl} \leq 0.07 \\ \text{Grade} = \left(-\frac{\text{Cl}-0.07}{0.18}+1\right)10 & 0.07 < \text{Cl} < 0.25 \\ \text{Grade} = 0 & \text{Cl} \geq 0.25 \end{cases} \tag{4.10}$$

4.5.2. Renewability of the groundwater resource

Groundwater is a renewable resource, therefore, an important criteria for the sustainability is the replenishment of the groundwater by recharge. The origin of the extracted groundwater (Q_p) of a well is divided into four different sources. This is used to calculate the renewability of the groundwater resource.

- **Recharge** (R)
  The recharge, defined as water entering the model through the top layer.
- **Tegelen** (T_s)
  Tegelen, defined as groundwater seeping through the Tegelen clay from the second to the first aquifer.
- **Hole in Tegelen** (T_h)
  The hole in the Tegelen clay is distinguished from the Tegelen clay. All preceding studies showed that the hole in the Tegelen clay is a major contributor to the salinization of Ritskebos. Therefore, it is excluded from the Tegelen clay and analyzed separately.
- **Lateral Flow** (LF)
  Lateral Flow, defined as groundwater originating from side boundaries of the model. No distinction is made between fresh and brackish water.

Initially, when starting the extraction of groundwater, groundwater is removed from storage. Over time the system can come to a new equilibrium.

$$Q_p = R + T_s + T_h + LF \tag{4.11}$$

Using Equation 4.11, the contribution of each source to the total extraction can be calculated. The following definition is used to define the renewability of the groundwater resource (Gleeson et al., 2012):

"The renewability of the groundwater resource is defined by the groundwater footprint (GF). For this thesis the groundwater footprint is the ratio between the extraction of the well field (Q_p) compared to the extraction originating from recharge (R)."

$$GF = \frac{Q_p}{R} \tag{4.12}$$

The following linear evaluation equation is proposed (Equation 4.13) to assess the groundwater footprint. A groundwater footprint of 1 is desired and the best possible result. A groundwater footprint of 3.5 is chosen as the worst possible grade, which is based analysis of the results and the global average groundwater footprint (Gleeson et al., 2012).

$$\begin{cases} \text{Grade} = 10 & \text{GF} = 1 \\ \text{Grade} = \left(-\frac{GF-1}{2.5}+1\right)10 & 1 < \text{GF} < 3.5 \\ \text{Grade} = 0 & \text{GF} \geq 3.5 \end{cases} \tag{4.13}$$

4.5.3. Vulnerability of the groundwater resource

The following definition is used with regards to the vulnerability of the groundwater resource:

"The vulnerability of the groundwater resource is defined as the sensitivity of the groundwater quality to anthropogenic activity. A low vulnerability of the groundwater resource is desired with regards to the sustainability."

The vulnerability of the groundwater resource is split into two different parts. The first part of the vulnerability of the groundwater resource is the contribution from the chloride-rich second aquifer to the extraction, as seen in Equation 4.11. The sustainability evaluation of the contribution of the second aquifer to the extraction consists of the seepage through the Tegelen clay (T_s) added to the flow through the hole in the Tegelen clay (T_h). Obviously, the best case is 0% contribution from the second aquifer, thus equaling a 10. The lowest grade will be based on the maximum expected contribution originating from the second aquifer. The equation used for the sustainability evaluation is presented in Equation 4.14.

$$\begin{cases} \text{Grade} = 10 & T_s + T_h = 0\% \\ \text{Grade} = \left(-\frac{T_s+T_h}{32\%}+1\right)10 & 0\% < T_s + T_h < 32\% \\ \text{Grade} = 0 & T_s + T_h \geq 32\% \end{cases} \tag{4.14}$$

The second part of the vulnerability of the groundwater resource is the movement of the Northern Brackish Front. The location of the Northern Brackish Front, as shown in Figure 4.2, is defined as the coordinates where the chloride concentration exceeds 1 g L^{-1} at a depth of 145 m below surface. Particles are vertically distributed over the depth of the first aquifer at the location of the front using MODPATH. This is done to measure the lateral movement of the front, with respect to the well fields, over a period of 50 years in the different permeable zones of the first aquifer, as described in Section 2.2. The lateral movement of the front is used as an indicator for vulnerability of the groundwater resource. A lateral movement of 2,025 meters towards the well fields is chosen as maximum in the linear evaluation equations.

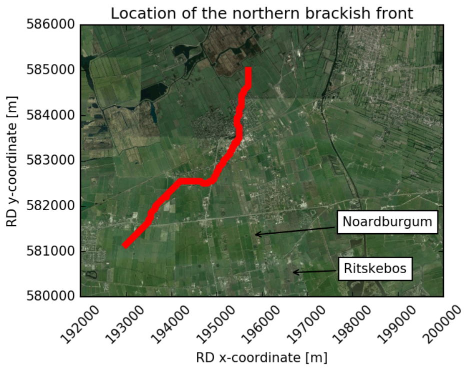

Figure 4.2: Location of the Northern Brackish Front compared to the Noardburgum and Ritskebos well field

Table 4.2: Weighing factors of the indicators for the different well fields for the sustainability grading

	Chloride content	Renewability	Vulnerability	
			Movement of the brackish front	Contribution second aquifer to the extraction
Noardburgum	50 %	$16\frac{1}{3}$ %	$16\frac{1}{3}$ %	$16\frac{1}{3}$ %
Ritskebos	50 %	$16\frac{1}{3}$ %	$16\frac{1}{3}$ %	$16\frac{1}{3}$ %
Garyp	-	50 %	-	50 %
Industrial extraction	-	50 %	-	50 %

$$\begin{cases} \text{Grade} = 10 & \text{Movement} \leq 0 \\ \text{Grade} = \left(-\frac{\text{Movement}}{2{,}025} + 1\right)10 & 0 < \text{Movement} < 2{,}025 \\ \text{Grade} = 0 & \text{Movement} \geq 2{,}025 \end{cases} \tag{4.15}$$

4.5.4. Assigning weighing factors

The total sustainability grade for the different well fields consists of the assigned grades for the indicators times a weighing factor. The weighing factors are based on engineering judgment, and are presented in Table 4.2. The individual grades of the different well fields can be combined to a single grade for each scenario, where the extraction of the well fields (found in Table 3.2) function as the weighing factor. It is assumed that the well field Garyp and the Industrial extraction will have a stable chloride concentration in the groundwater extraction in the coming 50 years.

The movement of the brackish front is found not to be representative for the Garyp well field and the Industrial extraction. The total sustainability grade of Garyp and the Industrial extraction is based on the Renewability (50%) and the fraction of extracted water origination from the second aquifer (50%).

4.6. Computer programs used during modeling

Two different computer programs are used during this thesis, namely SEAWAT and MODPATH. SEAWAT is a combination of MODFLOW and MT3DMS including density effects. All programs are developed by the USGS.[2]

This thesis is conducted using the Programming language Python, version 2.7.11. FloPy is a set of Python scripts to run MODFLOW, MT3DMS, SEAWAT and other MODFLOW related groundwater programs (Bakker et al., 2016). FloPy is an open source project and can be downloaded.[3] FloPy is used to make the new flow and transport model based on the studied models. FloPy version 3.2.5.1265 was used in this thesis.

4.6.1. SEAWAT

SEAWAT is a coupled version of MODFLOW (flow solution) and MT3DMS (Modular 3-Dimensional Transport model Multi Species) designed to simulate three dimensional variable density groundwater flow (Zheng and Wang, 1999). SEAWAT solves transport and flow in an iterative way. SEAWAT, version 4.00.05 (64-bit) is used in this thesis. Information from SEAWAT is obtained from Guo and Langevin (2002), Langevin and Guo (2006) and Langevin et al. (2008).

[2] http://water.usgs.gov/ogw/seawat/
[3] https://github.com/modflowpy/flopy

Several packages were developed to simulate hydrological stresses to a groundwater system. These packages add terms to an external source to represent sinks or sources. The packages used while modeling are described in Appendix B. Information from the packages is obtained from Harbaugh (2005).

4.6.2. MODPATH

MODPATH is particle tracking software designed to use the output files of MODFLOW and SEAWAT. MODPATH, version 6.0.01 (64-bit) is used in this thesis. The 32-bit version of MODPATH version 6.0.01 resulted in errors. MODPATH releases particles and tracks them throughout the model. The particles have the same velocity and direction as the groundwater. MODPATH calculates the flow path and it keeps track of the travel time. Information about MODPATH is obtained from Pollock (1989, 2012).

The script in the FloPy version used in this thesis does not present the entire MODPATH outcome. Therefore, the script is adapted to present the desired outcome. The modpathfile.py get_data function is changed to:

```
idx = self._data['particleid'] == partid
self._ta = self._data[idx]
if final:
    ra = np.rec.fromarrays((self._ta['i0'], self._ta['j0'], self._ta['k0'],
                            self._ta['finaltime'], self._ta['i'],
                            self._ta['j'], self._ta['k'],
                            self._ta['particleid'], self._ta['x0'],
                            self._ta['y0'], self._ta['x'], self._ta['y']),
                            dtype=self.outdtype)
else:
    ra = np.rec.fromarrays((self._ta['x0'], self._ta['y0'], self._ta['z0'],
                            self._ta['initialtime'], self._ta['k0'],
                            self._ta['particleid']), dtype=self.outdtype)
return ra
```

5

Results of the flow and transport model

The analysis and results of the flow and transport model are presented in this chapter. The results of the parameter estimation are presented first. Then the model results are presented, which makes use of the estimated parameter set. The results of the linearized propagation of variance for chloride transport are presented next, after which the Monte Carlo analysis results are shown. The outcome of the Monte Carlo analysis and the linearized propagation of variance are compared, and finally, the sustainability grades for the different scenarios and well fields are presented.

5.1. Optimal output of the model

A steady-state model calibration is performed using the methods presented in section 4.1 and 4.2. The objective function, Equation 4.1, is minimized using 134 piezometers. The two different initial chloride distributions are analyzed and compared. Lastly, the velocity and direction of the groundwater flow is presented using the estimated parameter values calculated in the calibration process.

5.1.1. Calibration results

Most of the piezometers are located in the phreatic aquifer. This is to monitor and evaluate compensation to farmers for drought, caused by drawdown of the water-table due to pumping activity. The optimal values from the calibration and the corresponding confidence intervals are given in Table 5.1. The 95% confidence interval is constructed using the methods explained in Section 4.2. The results of this calibration are obtained using the initial chloride distribution B to account for differences in head due to density differences.

The optimal parameters for the second aquifer and the Tegelen clay are considered to be unrealistic, due to an improbable optimal value or an unusually high variance. There are just 10 measurement locations in the second aquifer, and the water quality inside the piezometer is unknown. Since the calibration results of these parameters are rejected, new values based on literature are used, as is presented in Table 5.2. The covariance of the resistance of Tegelen clay and the transmissivity of the second aquifer is set to be uncorrelated to the other parameters. The resistance of the Tegelen clay has a strong correlation with the transmissivity of the first aquifer, and transmissivity of the second aquifer has a very weak correlation with all the other parameters. Since the resistance of Tegelen clay has a strong correlation with the transmissivity of the first aquifer, the calibration should have been executed again with the optimal selected values for the Tegelen clay and the second aquifer. A new calibration is expected to lead to different optimal values due to parameter correlation.

Analysis shows minor differences in model results with the parameter values from Table 5.2 compared to Table 5.1. The optimal values before adjustment show a slightly higher contribution from the second aquifer, as is expected due to the low resistance of the Tegelen clay. The parameters from Table 5.2 are used in further analysis.

Table 5.1: Optimal values of the parameters

Name	Parameter number	Type	Unit	Optimal value	95% confidence interval
Recharge	1	Multiplication factor	[-]	0.678	1.062 0.433
Semi-confining layer	2	Multiplication factor	[-]	0.478	1.538 0.149
First aquifer	3	Transmissivity	[m^2/d]	2,586	6,410 1,043
Tegelen clay	4	Resistance	[d]	95	2,874 3
Second aquifer	5	Transmissivity	[m^2/d]	23,761	5.69^{15} 0

Table 5.2: Adjusted optimal values of the parameters, no additional calibration is conducted with the fixed optimal values

Name	Parameter number	Type	Unit	Optimal value	95% confidence interval
Recharge	1	Multiplication factor	[-]	0.678	1.062 0.433
Semi-confining layer	2	Multiplication factor	[-]	0.478	1.538 0.149
First aquifer	3	Transmissivity	[m^2/d]	2,586	6,410 1,043
Tegelen clay	4	Resistance	[d]	1,300	2,600 650
Second aquifer	5	Transmissivity	[m^2/d]	2,500	5,000 1,250

5.1.2. Piezometer analysis

The piezometer data is compared with the heads in the different aquifers using the estimated parameters. The largest differences between measured and modeled head are found in the phreatic aquifer, as is presented in Figure 5.1. The dots are scaled to the difference between observed and measured head, where the dot in the legend represents a difference of 1.0 meters. A black dot indicates the modeled head is higher than the observed a head. A white dot indicates the observed head is higher than the measured head. The average difference between modeled and observed head is -0.18 meter, and absolute average difference is 0.55 meters.

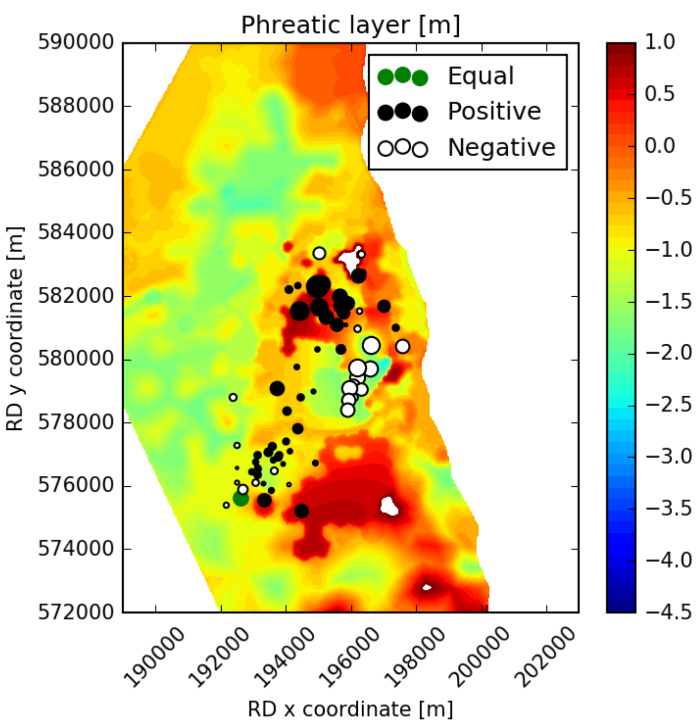

Figure 5.1: Measured head compared with modeled heads in the phreatic aquifer for the period 2007-2010

5.1.3. Streamline analysis

The direction and speed of the groundwater in the model are analyzed, in order to understand the salinization process. Results show that currently, and in

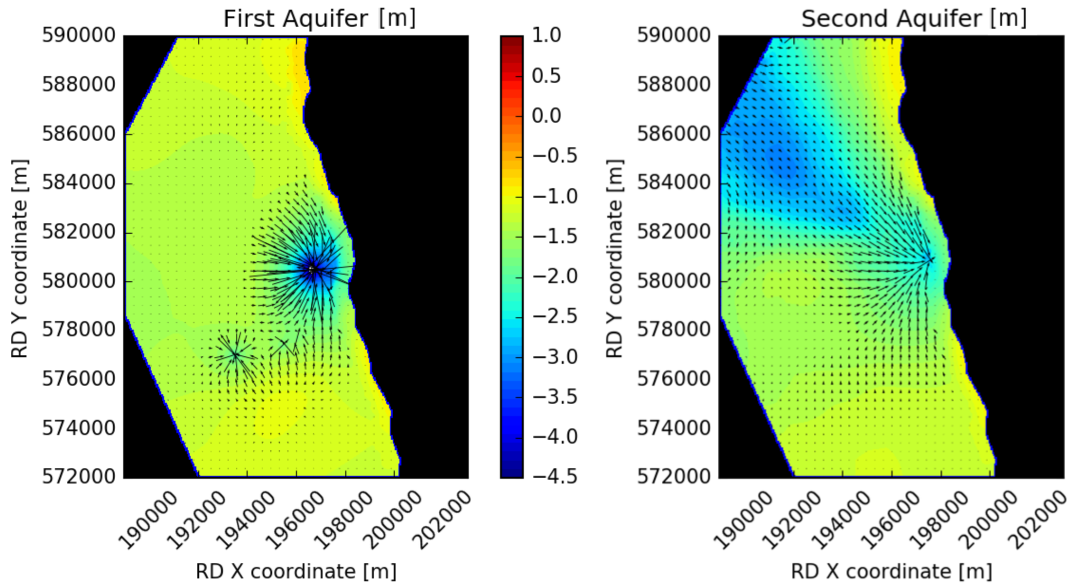

Figure 5.2: Specific discharge vector plot with head contours. The extractions locations can be seen in the first aquifer. The second aquifer shows the location of the hole in the Tegelen clay

all other scenarios, almost all groundwater in the second aquifer is flowing towards the hole in the Tegelen clay, as can be seen on the right side of Figure 5.2. This figure represent the vectorized specific discharge plot on top of a contour plot of the point water heads for the first and second aquifer, using the 2007 - 2010 extractions for the well fields. The vectors show the direction and the magnitude of the specific discharge. Note that the length of the vectors in the first aquifer can not be compared with the second aquifer. The magnitude of the vector is determined based on the specific discharge in the specified layer.

This result indicates the injected brackish water at the Noardburgum well field is also flowing towards the hole in the Tegelen clay. Water seeping through the hole in the Tegelen clay from the second to the first aquifer flows towards the Ritskebos well field. The left part of Figure 5.2 shows that all water from the hole in the Tegelen clay ends up in Ritskebos. Also, it is shown that for all scenarios the brackish front located North West of Noardburgum flows towards the Noardburgum and Ritskebos well field.

5.2. Linearized propagation of variance

The linearized propagation of variance is used for the uncertainty analysis of the model output for the small and large-scale model (see Figure 3.1). The small-scale model is focused on the chloride content of the extracted groundwater over a period of 50 years. The large-scale model is used to evaluate the renewability and vulnerability of the groundwater resource.

5.2.1. Small-scale analysis

This analysis is conducted for the small-scale model. It is focused on the Noardburgum and the Ritskebos well field, where all recent water quality measurements took place (see Figure 3.1). The analysis considers the extracted concentration of groundwater at the Noardburgum well field, the Ritskebos well field and the concentration of the water leaking through the hole in the Tegelen clay. This analysis is conducted for the two different initial chloride distributions, which have the best match with the measurements.

The results of the concentration after 50 years are shown in Table 5.3. Here, the expected value of the chloride concentration with the corresponding 95% confidence intervals originating from parameter uncertainty are presented. It is possible that negative concentrations are part of the confidence intervals. The sensitivity coefficients, calculated with Equation 4.9, are presented in Appendix E. The concentration is presented in the

Table 5.3: Results from the linearized propagation of variance for chloride content after 50 years, using two different initial distributions, in [g L^{-1}]
Here, NB = Noardburgum, RB = Ritskebos, and Hole stand for hole in the Tegelen clay

	Location:	Scenario 1 1970 - 1980	Scenario 2 2007 - 2010	Scenario 3 Single Smart Well	Scenario 4 Full-scale design
Distribution A	NB	$0.202\,^{0.421}_{-0.017}$	-	$0.067\,^{0.076}_{0.059}$	$0.088\,^{0.132}_{0.044}$
	RB	$0.257\,^{0.558}_{-0.045}$	$0.103\,^{0.158}_{0.048}$	$0.112\,^{0.177}_{0.047}$	$0.137\,^{0.255}_{0.020}$
	Hole	$2.250\,^{2.984}_{1.515}$	$1.134\,^{1.970}_{0.298}$	$1.206\,^{2.048}_{0.365}$	$1.435\,^{2.282}_{0.588}$
Distribution B	NB	$0.204\,^{0.443}_{-0.035}$	-	$0.070\,^{0.078}_{0.062}$	$0.091\,^{0.146}_{0.037}$
	RB	$0.289\,^{0.588}_{-0.010}$	$0.132\,^{0.234}_{0.030}$	$0.146\,^{0.264}_{0.028}$	$0.183\,^{0.342}_{0.024}$
	Hole	$2.452\,^{3.103}_{1.800}$	$1.887\,^{2.733}_{1.042}$	$1.944\,^{2.743}_{1.146}$	$2.112\,^{2.758}_{1.466}$

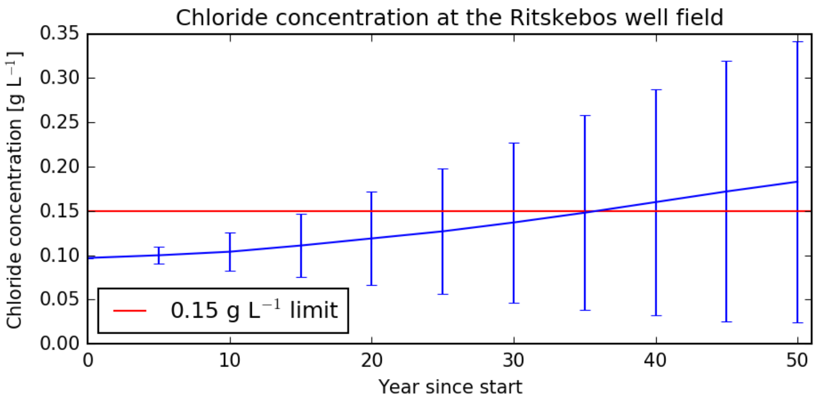

Figure 5.3: Chloride concentration and corresponding confidence intervals over time of the fresh water extraction at Ritskebos for the full-scale scenario using distribution B

following manner: expected concentration $^{\text{95\% confidence interval maximum concentration}}_{\text{95\% confidence interval minimum concentration}}$. The results from Table 5.3 are given for the different well fields:

- **Noardburgum [NB]**
  Results show that scenario 1, the high-extraction scenario, has the highest overall chloride concentration. Both distributions show that the expected chloride concentration is well above the 0.15 g L^{-1} limit scenario 1. No extraction is taking place in scenario 2 (the 2007 - 2010 scenario). The single Smart Well and the full-scale scenario stay below the 0.15 g L^{-1} limit.

- **Ritskebos [RB]**
  Both distributions show there is a high probability that Ritskebos will suffer from salinization in the high-extraction scenario (scenario 1). Furthermore, the different initial distributions show that there is an increase in chloride concentration with the development of the Noardburgum well field.

- **Hole in Tegelen clay [Hole]**
  Both distributions show that scenario 1 has the highest chloride concentration of the different scenarios. Without extraction at Noardburgum (scenario 2), the lowest chloride concentration is observed.

The probability of exceedance of the 0.15 g L^{-1} limit can be calculated for the Noardburgum and Ritskebos well field, for the different scenarios and initial distributions. Also, the probability of exceedance of the chloride limit for the Noardburgum treatment facility is calculated. This is based on the mixed water of the

Table 5.4: Probability 0.15 g L^{-1} chloride limit will be exceeded for the different scenarios and initial distributions
Here, NB = Noardburgum, RB = Ritskebos and NBTF = Noardburgum treatment facility

	Distribution A			Distribution B		
	NB	RB	NBTF	NB	RB	NBTF
Scenario 1 - 1970 - 1980	68%	76%	83%	67%	82%	86%
Scenario 2 - 2007 - 2010	-	5%	5%	-	36%	36%
Scenario 3 - Smart Well	0%	13%	9%	0%	47%	43%
Scenario 4 - Full-scale	0%	42%	31%	2%	66%	55%

Noardburgum and Ritskebos well field. The results of this calculation are given in Table 5.4. It can be seen that there is a high probability both well fields will suffer from salinization in the high-extraction scenario (scenario 1). There is a low probability the Noardburgum well field will suffer from salinization in the full-scale scenario, contrary to the Ritskebos well field. The expected increase and confidence boundaries of the Ritskebos well field over a 50 year period is presented in Figure F.

The measurements of the electrical conductivity of the Smart Well shows that the fresh water well remains fresh, as present. These measurements are conducted over a period of 3 non consecutive months. Initially the brackish water has a chloride concentration of ± 2.1 g L^{-1} (calculated by using the electrical conductivity, see Appendix F). Over this period it decreases to 1.2 g L^{-1} and seems to reach an equilibrium over time of ± 1.2 g L^{-1}.

5.2.2. Large-scale analysis

The results from the linearized propagation of variance large-scale analysis are shown in Table 5.5. The results show the different sources of the extracted water and are presented as the percentage of contribution to the total extraction (100 %) at the specified station. Negative contribution and contributions larger than 100 % can be seen in Table 5.5. The results are presented, with the expected value and the 95% confidence interval, in the following manner: Expected contribution$^{\text{95\% confidence interval maximum contribution}}_{\text{95\% confidence interval minimum contribution}}$. Also, the movement of the brackish front is presented with the corresponding confidence interval.

Results show there is an influence from the Smart Well on the expected contribution from the different sources, and an even greater influence from the full-scale design. The results indicate that the development of the Noardburgum area has an influence on the Ritskebos well field and the movement of the brackish front. The results from Table 5.5 are given for the different well fields:

- **Noardburgum [NB]**
  Differences in the expected contribution between the different scenarios with regards to the origin of the extracted groundwater is seen for the Noardburgum station, but also the corresponding confidence intervals. The first scenario, which is considered as over-exploitation due to the high extractions, show large contributions from sources with high chloride concentration. Also, in the full-scale design the brackish extraction [NBQB] seems to mainly attract groundwater from sources with a high chloride concentration, which is the purpose of the brackish extraction.

- **Ritskebos [RB]**
  Model results show that only the well field of Ritskebos is extracting water originating from the second aquifer through the hole in the Tegelen clay. It can be seen that the development of the Noardburgum area influences the expected contribution of the hole in the Tegelen clay and the seepage through the Tegelen clay at the Ritskebos extraction.

- **Garyp [GR]**
  The effects of the Noardburgum Well field seem limited in the different scenarios. The extraction from

Table 5.5: Results from the linearized propagation of variance, presenting the contribution to the total extraction originating from the different sources, and the lateral movement of the brackish front
Here, RB = Ritskebos, NB = Noardburgum, NBQB = Noardburgum brackish extraction, GR = Garyp, and IN = Industrial extraction

	Location:	Scenario 1 1970 - 1980	Scenario 2 2007 2010	Scenario 3 Single Smart Well	Scenario 4 Full-scale design
Contribution from recharge	RB	$39.1\%^{57.5\%}_{20.6\%}$	$62.9\%^{93.5\%}_{32.2\%}$	$57.9\%^{83.4\%}_{32.3\%}$	$49.6\%^{76.0\%}_{23.2\%}$
	NB	$49.5\%^{71.1\%}_{27.8\%}$	-	$98.4\%^{127.5\%}_{69.3\%}$	$86.3\%^{120.3\%}_{52.2\%}$
	NBQB	-	-	$77.6\%^{274.9\%}_{-119.7\%}$	$0.9\%^{38.1\%}_{-36.2\%}$
	GR	-	$31.9\%^{64.4\%}_{-0.6\%}$	$32.1\%^{52.7\%}_{11.5\%}$	$32.5\%^{48.3\%}_{16.6\%}$
	IN	-	$77.6\%^{104\%}_{51.2\%}$	$77.9\%^{141.5\%}_{14.3\%}$	$80.5\%^{126.3\%}_{34.7\%}$
Contribution from Tegelen	RB	$20.9\%^{30.9\%}_{10.9\%}$	$13.4\%^{25.8\%}_{1.0\%}$	$16.6\%^{32.7\%}_{0.5\%}$	$23.4\%^{44.1\%}_{2.6\%}$
	NB	$13.6\%^{23.0\%}_{4.2\%}$	-	$0.0\%^{0.0\%}_{0.0\%}$	$1.8\%^{4.2\%}_{-0.6\%}$
	NBQB	-	-	$6.9\%^{26.7\%}_{-13.0\%}$	$48.2\%^{75.0\%}_{21.4\%}$
	GR	-	$7.9\%^{21.7\%}_{-6.0\%}$	$7.7\%^{22.3\%}_{-6.9\%}$	$7.1\%^{18.4\%}_{-4.2\%}$
	IN	-	$2.7\%^{6.8\%}_{-1.4\%}$	$2.4\%^{6.9\%}_{-2.2\%}$	$1.5\%^{10.5\%}_{-7.6\%}$
Contribution from hole	RB	$10.6\%^{19.9\%}_{1.2\%}$	$6.9\%^{13.4\%}_{0.3\%}$	$7.3\%^{14.1\%}_{0.5\%}$	$8.7\%^{16.2\%}_{1.3\%}$
	NB	$0.0\%^{0.0\%}_{0.0\%}$	-	$0.0\%^{0.0\%}_{0.0\%}$	$0.0\%^{0.0\%}_{0.0\%}$
	NBQB	-	-	$0.0\%^{0.0\%}_{0.0\%}$	$0.0\%^{0.0\%}_{0.0\%}$
	GR	-	$0.0\%^{0.0\%}_{0.0\%}$	$0.0\%^{0.0\%}_{0.0\%}$	$0.0\%^{0.0\%}_{0.0\%}$
	IN	-	$0.0\%^{0.0\%}_{0.0\%}$	$0.0\%^{0.0\%}_{0.0\%}$	$0.0\%^{0.0\%}_{0.0\%}$
Contribution from boundaries	RB	$29.5\%^{40.8\%}_{18.1\%}$	$16.9\%^{34.1\%}_{-0.3\%}$	$18.2\%^{26.6\%}_{9.9\%}$	$18.3\%^{37.5\%}_{-0.9\%}$
	NB	$36.9\%^{59.2\%}_{14.7\%}$	-	$1.6\%^{30.7\%}_{-27.5\%}$	$11.9\%^{44.3\%}_{-20.4\%}$
	NBQB	-	-	$15.6\%^{203.0\%}_{-171.9\%}$	$50.8\%^{80.2\%}_{21.5\%}$
	GR	-	$60.2\%^{102.1\%}_{18.3\%}$	$60.2\%^{82.5\%}_{37.9\%}$	$60.4\%^{71.9\%}_{49.0\%}$
	IN	-	$19.7\%^{43.2\%}_{-3.8\%}$	$19.7\%^{83.9\%}_{-44.5\%}$	$18.0\%^{65.2\%}_{-29.1\%}$
Movement of the brackish front [m]	Top layer [60 – 90 m]	$1,912^{3,157}_{667}$	120^{586}_{-346}	238^{783}_{-306}	$627^{1,372}_{-119}$
	Middle layer [90 – 130 m]	$1,714^{2,292}_{1,135}$	117^{471}_{-237}	214^{618}_{-190}	$515^{1,067}_{-37}$
	Bottom layer [130 – 150 m]	$2,030^{2,264}_{1,797}$	151^{685}_{-382}	298^{981}_{-385}	$817^{1,704}_{-71}$

Table 5.6: Results from the Monte Carlo analysis, presenting the contribution to the total extraction originating from the different sources, and the lateral movement of the brackish front
Here, RB = Ritskebos, NB = Noardburgum, NBQB = Noardburgum brackish extraction, GR = Garyp, and IN = Industrial extraction

	Location:	Scenario 1 1970 - 1980	Scenario 2 2007 - 2010	Scenario 3 Single Smart Well	Scenario 4 Full-scale design
Contribution from recharge	RB	$38.5\%\,^{50.2\%}_{26.1\%}$	$61.8\%\,^{77.4\%}_{43.0\%}$	$57.2\%\,^{74.6\%}_{38.6\%}$	$48.6\%\,^{67.2\%}_{32.8\%}$
	NB	$49.1\%\,^{59.5\%}_{38.9\%}$	-	$98.4\%\,^{100.0\%}_{91.7\%}$	$85.2\%\,^{97.3\%}_{69.7\%}$
	NBQB	-	-	$70.3\%\,^{95.9\%}_{0.0\%}$	$1.8\%\,^{50.1\%}_{0.0\%}$
	GR	-	$32.8\%\,^{54.0\%}_{23.0\%}$	$32.9\%\,^{52.0\%}_{23.1\%}$	$33.3\%\,^{47.0\%}_{23.3\%}$
	IN	-	$77.3\%\,^{95.7\%}_{52.2\%}$	$77.7\%\,^{95.4\%}_{53.2\%}$	$80.2\%\,^{93.3\%}_{56.5\%}$
Contribution from Tegelen	RB	$20.5\%\,^{28.1\%}_{13.6\%}$	$12.5\%\,^{21.1\%}_{5.7\%}$	$15.6\%\,^{25.2\%}_{7.4\%}$	$22.3\%\,^{33.5\%}_{11.9\%}$
	NB	$12.7\%\,^{21.7\%}_{7.3\%}$	-	$0.0\%\,^{0.0\%}_{0.0\%}$	$1.6\%\,^{4.1\%}_{0.4\%}$
	NBQB	-	-	$7.2\%\,^{15.9\%}_{3.7\%}$	$45.7\%\,^{63.2\%}_{27.9\%}$
	GR	-	$7.7\%\,^{17.4\%}_{2.5\%}$	$7.5\%\,^{16.9\%}_{2.5\%}$	$7.0\%\,^{15.2\%}_{2.6\%}$
	IN	-	$2.2\%\,^{4.3\%}_{0.4\%}$	$2.0\%\,^{4.0\%}_{0.4\%}$	$1.3\%\,^{3.3\%}_{0.4\%}$
Contribution from hole	RB	$10.1\%\,^{17.2\%}_{4.6\%}$	$6.5\%\,^{10.9\%}_{3.0\%}$	$7.0\%\,^{11.7\%}_{3.2\%}$	$8.4\%\,^{13.9\%}_{4.0\%}$
	NB	$0.0\%\,^{0.0\%}_{0.0\%}$	-	$0.0\%\,^{0.0\%}_{0.0\%}$	$0.0\%\,^{0.0\%}_{0.0\%}$
	NBQB	-	-	$0.0\%\,^{0.0\%}_{0.0\%}$	$0.0\%\,^{0.0\%}_{0.0\%}$
	GR	-	$0.0\%\,^{0.0\%}_{0.0\%}$	$0.0\%\,^{0.0\%}_{0.0\%}$	$0.0\%\,^{0.0\%}_{0.0\%}$
	IN	-	$0.0\%\,^{0.0\%}_{0.0\%}$	$0.0\%\,^{0.0\%}_{0.0\%}$	$0.0\%\,^{0.0\%}_{0.0\%}$
Contribution from boundaries	RB	$30.3\%\,^{38.0\%}_{23.5\%}$	$18.4\%\,^{29.1\%}_{11.2\%}$	$19.4\%\,^{30.3\%}_{11.3\%}$	$19.2\%\,^{31.3\%}_{11.8\%}$
	NB	$36.7\%\,^{50.1\%}_{29.0\%}$	-	$1.6\%\,^{7.6\%}_{0.0\%}$	$12.8\%\,^{27.3\%}_{1.6\%}$
	NBQB	-	-	$21.7\%\,^{88.8\%}_{0.0\%}$	$47.4\%\,^{64.4\%}_{18.5\%}$
	GR	-	$58.8\%\,^{68.2\%}_{37.0\%}$	$59.0\%\,^{68.3\%}_{40.0\%}$	$59.1\%\,^{69.1\%}_{45.5\%}$
	IN	-	$20.2\%\,^{43.7\%}_{3.4\%}$	$20.1\%\,^{43.5\%}_{3.6\%}$	$18.2\%\,^{41.2\%}_{5.8\%}$
Movement of the brackish front [m]	Top layer [60 – 90 m]	$1{,}906\,^{2{,}160}_{1{,}337}$	$109\,^{420}_{-198}$	$225\,^{420}_{-106}$	$606\,^{1{,}027}_{163}$
	Middle layer [90 – 130 m]	$1{,}706\,^{1{,}908}_{1{,}190}$	109^{325}_{-138}	$204\,^{443}_{-56}$	$502\,^{792}_{182}$
	Bottom layer [130 – 150 m]	$2{,}025\,^{2{,}320}_{1{,}552}$	$140\,^{517}_{-123}$	$276\,^{743}_{-48}$	$786\,^{1{,}253}_{218}$

recharge is considerably less than the other stations. The main origin of the extracted water is the contribution from the boundaries.

- **Industrial extraction [IN]**
  Almost all the extracted water originates from recharge. The contribution from water originating from the second aquifer in the form of seepage through the Tegelen clay is almost negligible. It shows that the development of the Noardburgum area has a limited influence on the Industrial extraction.

5.3. Monte Carlo analysis

Monte Carlo analysis is computationally intensive, compared to the linearized propagation of variance, and in order to get good parameter sampling for the five parameters 10^5 model runs are needed. The computational time is ± 12 minutes per model run. It will take around 2.28 years to get all the results. Therefore, it is decided to only do 10^4 model runs on four different Python consoles. This reduced the computational time to an acceptable 3 weeks. A Monte Carlo analysis for the small-scale model will take approximately 41 weeks (for 10^4 model runs). Therefore, no Monte Carlo analysis is conducted for the small-scale model with regards to the chloride transport

The parameter set, created with the multivariate Gaussian distribution, is used in the Monte Carlo analysis. The results are used to construct a probability density function. From this function the expected outcome (the 50^{th} percentile) and the 95 % confidence boundaries (2.5 and 97.5 percentile) are determined. The results of the Monte Carlo analysis are presented in Table 5.6.

By comparing Table 5.5 and Table 5.6 it can be seen that the expected value and confidence interval are quite similar. Large differences are observed when low extractions occur (NBQB) or when the contribution from a certain source is high (± 100%). In contrast to the linearized propagation of variance the minimum contribution is 0.0% and the maximum contribution is 100.0%.

Correlation Coefficients

A correlation matrix is constructed with the entire outcome from the Monte Carlo analysis. The matrices for all the scenarios are presented in Appendix C. Similar behavior is observed between the correlation coefficients of the different well fields and the origin of the extracted water. The different scenarios have a strong correlation with each other. When analyzing Appendix C it can be seen that the parameter recharge has a strong correlation with all sources of the extraction, except for the Garyp station. The movement of the brackish front has a strong correlation with the parameters recharge and transmissivity of the first aquifer.

5.4. Sustainability evaluation

A single grade cannot represent the uncertainties arising from the parameters. Therefore, the expected grade is presented with the corresponding 95 % confidence interval grades as minimum and maximum grade. It will be presented as: Expected grade $^{\text{95\% confidence interval maximum grade}}_{\text{95\% confidence interval minimum grade}}$.

5.4.1. Chloride content of the extracted groundwater

The results of the linearized propagation of variance analysis, Table 5.3, is used for the evaluation of the chloride content of the extracted groundwater. The results of the brackish extraction of the Smart Wells are not used in the evaluation. The results of the evaluation is presented in Table 5.7. Equation 4.10 is used to calculate the grades. Note that if the sustainability grade is below a 5.6, the limit of 0.15 g L^{-1} chloride is exceeded. Also, a total sustainability grade is presented. This grade is based on the results of distribution A and B.

5.4.2. Renewability of the groundwater resource

The evaluation of the renewability of the groundwater resource is based on the Monte Carlo analysis. The brackish extraction of the Noardburgum well field is not included in the sustainability evaluation of the renewability of the groundwater. Garyp and the Industrial extraction are included in the evaluation. The evaluation is based on Equation 4.13. The results are presented in Table 5.8.

5.4.3. Vulnerability of the groundwater resource

The evaluation of the vulnerability is based on the Monte Carlo analysis. The movement of the top and middle layer are strongly correlated to the movement of bottom layer (see Appendix C). The bottom layer is chosen to be the reference point in Equation 4.15, since brackish water is mainly present in this layer.

5.4.4. Total sustainability grade

The total sustainability grade consists of the previously assigned grades times a weighing factor, presented in Table 4.2. The extraction of the different well fields, found in Table 3.2, is used as weighing factor for the total sustainability grade for the different scenarios. .

The sustainability grades for the different well fields for the different scenarios is presented in Table 5.10, where also the total sustainability grade is presented. It can be seen that the scenario with the high extractions (scenario 1) has the overall lowest scores. The low extraction scenario (scenario 2) has the highest expected outcome of the sustainability.

Table 5.7: Sustainability grades, with corresponding confidence intervals, of the chloride concentration of the extracted groundwater for the different initial distributions
Here, NB = Noardburgum, and RB = Ritskebos

	Distribution A		Distribution B		Total	
	NB	RB	NB	RB	NB	RB
Scenario 1	$2.7^{10.0}_{0.0}$	$0.0^{10.0}_{0.0}$	$2.6^{10.0}_{0.0}$	$0.0^{10.0}_{0.0}$	$2.6^{10.0}_{0.0}$	$0.0^{10.0}_{0.0}$
Scenario 2	-	$8.2^{10.0}_{5.1}$	-	$6.6^{10.0}_{0.9}$	-	$7.4^{10.0}_{3.0}$
Scenerio 3	$10.0^{10.0}_{9.7}$	$7.7^{10.0}_{4.0}$	$10.0^{10.0}_{9.5}$	$5.8^{10.0}_{0.0}$	$10.0^{10.0}_{9.6}$	$6.7^{10.0}_{2.0}$
Scenario 4	$9.0^{10.0}_{6.6}$	$6.3^{10.0}_{0.0}$	$8.8^{10.0}_{5.8}$	$3.7^{10.0}_{0.0}$	$8.9^{10.0}_{6.2}$	$5.0^{10.0}_{0.0}$

Table 5.8: Sustainability grades, with corresponding confidence intervals, of the renewability of the groundwater resources

	Noardburgum	Ritskebos	Garyp	Industry
Scenario 1	$6.1\,^{7.5}_{0.0}$	$3.9\,^{6.3}_{0.0}$	-	-
Scenario 2	-	$7.7\,^{7.7}_{5.0}$	$1.8\,^{6.6}_{0.0}$	$8.8\,^{9.8}_{6.3}$
Scenario 3	$9.9\,^{10.0}_{9.6}$	$7.2\,^{8.8}_{3.9}$	$1.9\,^{6.3}_{0.0}$	$8.9\,^{9.8}_{6.3}$
Scenario 4	$9.3\,^{9.9}_{8.3}$	$6.0\,^{8.2}_{2.2}$	$2.0\,^{5.5}_{0.0}$	$9.0\,^{9.7}_{6.9}$

Table 5.9: Sustainability grades, with corresponding confidence intervals, of the vulnerability of the groundwater resource

	Noardburgum	Ritskebos	Garyp	Industry	Movement of the brackish front
Scenario 1	$5.9\,^{7.6}_{3.0}$	$0.2\,^{4.1}_{0.0}$	-	-	$0.0\,^{2.5}_{0.0}$
Scenario 2	-	$3.9\,^{7.2}_{0.0}$	$7.6\,^{9.2}_{4.5}$	$9.3\,^{9.9}_{8.7}$	$9.3\,^{10.0}_{7.4}$
Scenario 3	$10.0\,^{10.0}_{10.0}$	$2.7\,^{6.6}_{0.0}$	$7.7\,^{9.2}_{4.7}$	$9.4\,^{9.9}_{8.8}$	$8.6\,^{10.0}_{6.3}$
Scenario 4	$9.5\,^{9.9}_{8.7}$	$0.4\,^{4.9}_{0.0}$	$7.8\,^{9.2}_{5.3}$	$9.6\,^{9.9}_{9.0}$	$6.1\,^{8.9}_{3.8}$

Table 5.10: The combined sustainability grades, with corresponding confidence intervals, for the different scenarios and the different well fields

	Noardburgum	Ritskebos	Garyp	Industry	Total Sustainability Grade
Scenario 1 1970 - 1980	$3.3\,^{7.9}_{0.5}$	$0.7\,^{7.1}_{0.0}$	-	-	$1.8\,^{7.5}_{0.2}$
Scenario 2 2007 - 2010	-	$7.2\,^{9.4}_{3.6}$	$4.7\,^{7.9}_{2.3}$	$9.1\,^{9.9}_{7.5}$	$7.0\,^{9.2}_{3.8}$
Scenario 3 Smart Well	$9.8\,^{10.0}_{9.1}$	$6.5\,^{9.2}_{2.7}$	$4.8\,^{7.8}_{2.4}$	$9.1\,^{9.8}_{7.6}$	$6.7\,^{9.1}_{3.5}$
Scenario 4 Full-scale	$8.6\,^{9.8}_{6.6}$	$4.5\,^{8.7}_{1.0}$	$4.9\,^{7.3}_{2.6}$	$9.3\,^{9.8}_{7.9}$	$5.8\,^{8.8}_{2.9}$

6

Discussion of the flow and transport model

The model parameters and input will be discussed first. Next, the linearized propagation of variance and the Monte Carlo analysis will be discussed. Lastly, the sustainability indicators and the sustainability of the different scenarios are discussed.

6.1. Model parameters and input

The model is optimized using the piezometer measurements conducted in the area from 2007-2010. During this period the extractions of the different well fields were more or less constant and are still representative for the current situation. During this period there is no extraction at the Noardburgum well field. From 2010 onwards the Fresh Keeper pilot at the Noardburgum well field is expected to influence groundwater heads.

6.1.1. Steady-state simulations

The system is assumed to be in steady-state. A steady-state situation never occurs in reality (Sonnenborg et al., 2003). Parameters related tot the storage characteristics of the system are not included in the steady-state model. The flow and transport model is based on yearly averages and is used to study long-term effects of the different well fields. Seasonal differences, as shown in Figure 3.3, can not be reproduced using the steady-state model.

6.1.2. Parameter estimation

In the calibration a multiplication factor is used for the recharge and semi-confining layer, due to the spatial variability of the parameters, but also to limit the degrees of freedom in the calibration process. Alternatively, only certain values could be varied instead of a multiplication factor. This approach is not expected to affect the conclusions.

Calibration results

The optimal values from the calibration were presented in Table 5.1. It can be seen that some parameters give a wide confidence interval or unrealistic optimal value. In some cases the piezometers do not contain enough information for effective calibration. This may be related to too few measurement locations. The confidence intervals of the expected parameters can be reduced by reducing the variance. More measurements (e.g. piezometer measurements, aquifer tests, deep observation drillings or discharge measurements to construct a water balance for the top system) are needed to reduce the variance of the different parameters.

Table 5.2 is used as values for the different parameters, but it would have been better if a new calibration would have been conducted with fixed values for parameters of the resistance of the Tegelen clay and transmissivity of the second aquifer (parameter 4 and 5). The expected values and corresponding confidence intervals from Table 5.2 are in line with previous studies (de Graaf et al., 2007; IWACO, 1979; Rus, 1997; van der Valk, 2011).

Interpretation of the calibration results

In the area of Noardburgum the heads in the phreatic aquifer are above ground surface, which is not realistic. A General Head Boundary is assigned to the phreatic aquifer, but is negligible in the Noardburgum area due to the high resistance (see Figure 3.2c). Many piezometers are located in the phreatic aquifer near Noardburgum, and this may influence the calibration results. The head above ground surface is not observed in the Triwaco model, most likely because the extraction at the Noardburgum and Ritskebos well field was much higher during the period simulated by the Triwaco model.

6.1.3. Chloride distribution

There are measurement errors in the chloride measurements. Most of the errors are easily detectable when using common sense or comparing them to electrical conductivity (EC). However, measurement of EC did not start until 2010. Therefore, it is not known if measurements before 2010 contain errors. Two locations are chosen to discuss the measurements, namely 06DP0040 and 06DP0294.

06DP0040 - Located within the Noardburgum well field

There was no well activity at the Noardburgum well field until 2010. The measurements of the chloride concentration over time at three different depths are presented in Figure 6.1. Note that the points at 137 meter and 168 meter below surface are separated by the Tegelen clay, which was observed at the drilling of this borehole. The measurements show strange decreases and increases of the chloride concentration. This phenomenon can be related to measurement error, although it is also observed at four other locations (06DP0208, 06DP0212, 06DP0215 and 06DP0294). It may be an indication of a more complex process. The months June and July in the year 2005 have a large amount of precipitation compared to the long-term average. The measurements for the chloride concentration of the groundwater in 2005 are conducted after these months. It is possible that the additional precipitation introduced seepage from the first to the second aquifer. This vertical flux can be responsible for a sudden decrease in chloride concentration if the fresh/brackish interface is located just above the measurement depth. However, during the summers of 2007 and 2008 even larger precipitation sums were measured (KNMI, 2016). Measurements were also conducted during these summers, and none of the measurements show a sudden decrease or increase of chloride concentration. Therefore, it can not be concluded that the precipitation is the definite explanation for this anomaly. Based on current knowledge this anomaly cannot be explained.

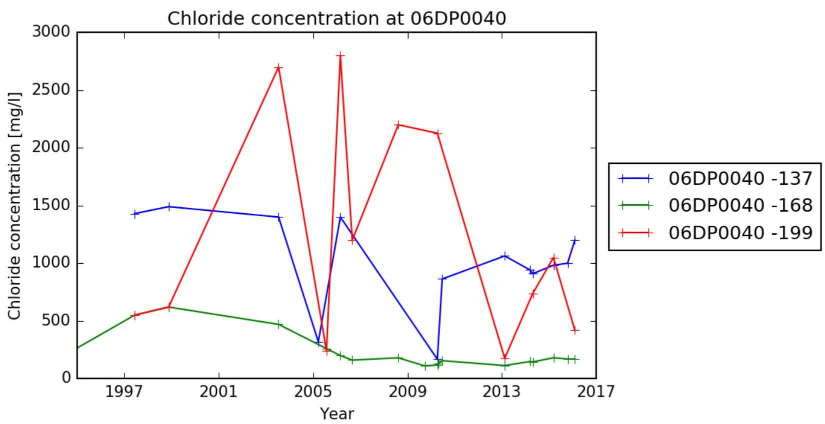

Figure 6.1: Chloride concentration at 06DP0040 at different depths

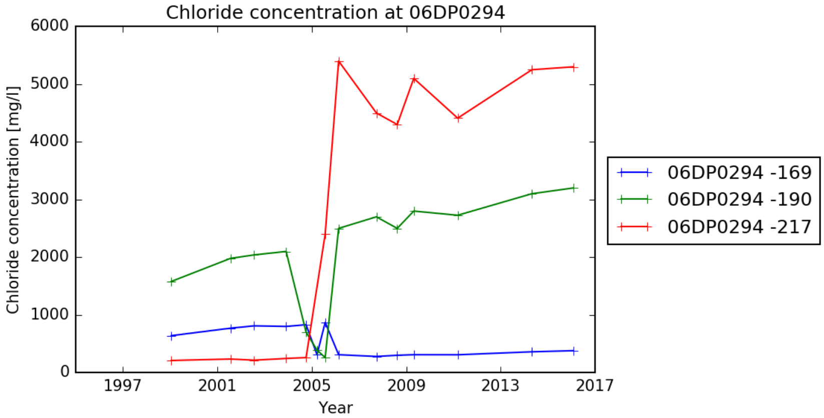

Figure 6.2: Chloride concentration at 06DP0294 at different depths

06DP0294 - Located near the hole in the Tegelen clay

The measurements of the chloride concentration over time at three different depths is shown in Figure 6.2. At a depth of 217 meters a clear increase of chloride concentration is observed. A possible explanation is that the sharp front between brackish and fresh water reached this location in the year 2004 by means of lateral movement. However, this cannot explain the sharp decrease of chloride concentration at a depth of -190 meters. Three measurements at 190 meters below surface indicate this sharp decrease around the same time as the measurements conducted at 06DP0040. It is not plausible to assume all three measurements have errors. The possible interpretation of this anomaly is the vertical movement of the groundwater.

This raises another question. Why is the chloride concentration at 217 meter below surface lower than at 190 and 169 meter below surface? And also, why is there an increase in chloride concentration while the other measurements show a decrease? A few drillings in the Noardburgum area suggest a second clay layer is located at a depth of around 200 meters below surface. It is possible that this clay layer is present at a depth of 200 meters, between the different measurement depths. This could be the reason why the water at a depth of 217 meters remained fresh. The vertical movement of the groundwater, the possible cause for the decrease of chloride concentration at 169 and 190 meter below surface, provides seepage of brackish water through the clay layer. This subsequently gives a rise of chloride concentration at 217 meter below surface.

6.2. Linearized propagation of variance and Monte Carlo analysis

The results from the linearized propagation of variance method are similar to the results of the Monte Carlo analysis. The largest differences occur in cases of a low extraction at the well field, or when the contribution from a source of the extracted groundwater is high. In the Monte Carlo analysis the contribution of a source is limited between 0% and 100%. Due to the uncertainty which is presented in the form of the parameter standard deviation in the linearized propagation of variance, the contribution of a source (or the chloride concentration) can become negative or the contribution to the extraction can become more than 100%, which is impossible. This is the result of the linearization at a specific point and the assumption that the outcome is normally distributed. It cannot account for any non-linearity in the model results. This is one of the main draw backs of the linearized propagation of variance.

Interpretation of the Results

The question arises on how the results should be interpreted from Table 5.3 and Table 5.6. It can be seen that the 95% confidence intervals between the different scenarios are overlapping. Considering these confidence intervals, are there significant see differences between the different scenarios?

The Monte Carlo analysis indicates a strong positive correlation between the different scenarios. Thus, differences are observed between the different scenarios, as is presented in Table 5.6. The total contribution to the extraction origination from recharge decreases with higher extractions, while the contribution to the extraction origination from leakage through the Tegelen clay increases. This increases the vulnerability of the system, thus affecting the sustainability in a negative manner.

6.3. Sustainability Indicators

The sustainability is quantified with three different indicators. These indicators are based on their presumed effect on the sustainability of the system.

6.3.1. Chloride transport

Chloride transport is modeled with SEAWAT. The model for chloride transport is focused on the area of Noardburgum, Ritskebos and the hole in the Tegelen clay, as is presented in Figure 3.1. This is done because almost all (recent) chloride measurements have been conducted there. It is expected no additional information is gained from modeling a larger area.

Noardburgum

There is a low probability that the water will become saline, due to the brackish extraction. Upconing is the major contributor to the salinization of the Noardburgum wells, but the brackish extraction prevents salinization due to upconing. The highest chloride concentrations are found in the lowest parts of the first aquifer. The brackish extraction is able to capture this groundwater and prevent the salinization of the fresh well. The brackish extraction mainly originates from sources with a high chloride concentration, which is the main purpose of the brackish extraction. Note that during this analysis the brackish extraction is kept at a constant rate of 350 $m^3\ d^{-1}$. When in operation and fully functional, the Smart Well will be able to adjust the extraction based on the chloride concentration of the brackish water.

Ritskebos

Both initial chloride distributions and every scenario indicates that Ritskebos may suffer from salinization. The high-extraction scenario (scenario 1) shows the highest probability (76-82%). The basic scenario (scenario 2) shows the lowest probability (5-36%). Distribution B shows a higher probability of salinization for the Ritskebos station compared to distribution A. This is expected, since the distribution B is created from 31 years of chloride transport modeling based on distribution A.

The exact extraction of Ritskebos is known, but the individual extractions per well are unknown. It is assumed that all wells extract the same amount of water. There is a well in the North East (closest to the hole in the Tegelen clay) which shows a chloride concentration of 0.9 g L^{-1}. This is also shown in the model results. The wells in the North East show the highest chloride concentration while other wells remain under the 0.15 g L^{-1} limit (even after 50 years). Using variable discharges over the wells, to relief the North East wells, will delay the salinization of Ritskebos for a short period. The source of the salinization is the seepage of water through the Tegelen clay and the leakage of water through the hole in the Tegelen clay.

During the streamline analysis it is found that all water flowing through the hole in the Tegelen clay ends up in Ritskebos. It also shows that all injected water in the second aquifer at the Noardburgum well field flows towards the hole in the Tegelen clay. The expected increase of the chloride concentration of the hole in the Tegelen clay is a threat for the sustainability of the Ritskebos well field.

6.3.2. Renewability of the groundwater resource

IWACO (1979) concluded 13% of the extraction of Noardburgum and Ritskebos originates from water infiltrating through the top layer. This study shows an expected 44% of the extraction of Noardburgum and Ritskebos originating from infiltration through the top layer, based on the high-extraction scenario (see Table 5.6). A reason for this difference is that IWACO (1979) underestimated the amount of infiltration (0.32 mm d^{-1}) and looked at an area which is not representative for the entire capture zone of the well fields. Rus (1997) estimated the recharge to be 1.5 mm d^{-1} in the area of Noardburgum, based on new data.

New information with regards to the phreatic aquifer (e.g. discharge measurements to construct a water balance of the surface water system) can be used to compare the simulated infiltration with the calculated infiltration. This can improve the understanding of the phreatic aquifer and the recharge to the phreatic aquifer.

6.4. Sustainability of the different scenarios

The sustainability assessment indicates whether the indicator has a positive or negative influence on the sustainability. An evaluation equation is chosen for the assessment, where a 0 is the worst possible grade and not sustainable, and a 10 is the best possible grade and considered to be fully sustainable.

The weighing factors used for the different indicators are based on how important an indicator is for the sustainability. Using weighing factors to assess the sustainability of the indicators may lead to biased results (Pandey et al., 2011). Different weighing factors may lead to different results, but it is not expected it will lead to different conclusions about the sustainability of the system. The well field sustainability grades and the total sustainability grades are presented in Table 5.10.

6.4.1. Sustainability of the high-extraction scenario

It is assumed this high-extraction scenario is unsustainable, and this can also be seen in the results. Every indicator shows a high probability that the scenario will be unsustainable, and will most likely lead to closure of the Noardburgum and Ritskebos station due to salinization of the groundwater. Also, a large increase in chloride concentration is observed at the hole in the Tegelen clay. This can be interpreted that the salinization will continue. This is not the desired outcome for sustainability, and as anticipated, this scenario has the overall lowest score in the evaluation of the sustainability.

6.4.2. Sustainability of the 2007 - 2010 situation

This scenario has the highest expected sustainability grades. This is expected, since the total extractions are lowest in this scenario. Even though this scenario has the highest sustainability grades, there is still a low probability that salinization will occur within 50 years at Ritskebos. This scenario is considered to be the most sustainable scenario, however, there are indications of serious threats to the long-term sustainability of the system.

6.4.3. Sustainability of the Smart Well and the full-scale design

The results of these scenarios show a very low probability (0-2%) that salinization will occur at the Noardburgum well field. This is related to the brackish extraction, since it prevents the salinization of the fresh wells. Almost all extraction of the fresh wells originates from the recharge. Seepage from the Tegelen clay and lateral transport of brackish water are captured by the brackish well. The extraction of the brackish well can be increased if salinization due to upconing is a threat to the fresh wells.

All injected brackish water at Noardburgum will end up at the Ritskebos well field or at the brackish extraction of Noardburgum. Thus, the Smart Well prevents the salinization of Noardburgum, but shifts the problem to the Ritskebos well field. This results in an increased probability of salinization at Ritskebos. There is a moderate probability (31-55%) that the 0.15 g L^{-1} chloride concentration limit will be exceeded at the Noardburgum treatment facility in the full-scale scenario. Note that the chloride concentration of the extracted water of Garyp and Nij Beets are not included in this calculation. The extracted water from Garyp is saline, according to Vitens.

7
Conclusions

The research objective and corresponding sub-questions from Section 1.1 are discussed in the following.

Assessment of the uncertainty of model predictions of the Smart Well at Noardburgum

Based on the model results, it can be concluded that there are two major sources of uncertainty.

The initial chloride concentration distribution
The initial distributions show some large differences with the observed chloride concentration, as is shown in Appendix G. Also, the measurements of the chloride concentration show unexplained variations through time, as is shown in Section 6.1.3.

The modeled phreatic layer
Not enough information is known about the phreatic layer. More measurement, e.g. discharge measurements to construct a water balance of the surface water system, are needed to reduce the uncertainty.

The uncertainty of the phreatic layer and the initial chloride distribution are not included in the modeling process. The uncertainty of several parameters is used to evaluate the uncertainty in the model results. The uncertainty of the model results can be decreased by more information on the different parameters, and more accurate measurements. The results show that there is uncertainty in the model results, which can make the difference whether the system is sustainable or not. Also, additional information on the chloride distribution or the phreatic aquifer may lead to different results and conclusions.

1. Does the Smart Well counteract salinization at Noardburgum?

The results indicate a negligible probability that salinization will occur within 50 years at the Noardburgum well field for a single Smart Well. In reality the brackish extraction will be adjusted to assure salinization will not occur. This feedback from the chloride concentration of the brackish extraction has not been implemented into the model. The brackish water extraction prevents the upconing of brackish water, and intercepts the lateral transport of brackish water and captures the seepage from the second to the first aquifer. Thus, the brackish water extraction does exactly what it is supposed to do: prevent the salinization of the Noardburgum well field.

2. Does the Smart Well lead to an increase of salinization at Ritskebos?

All results show that the Smart Well and the full-scale design lead to an increased probability of exceedance of the 0.15 g L^{-1} chloride concentration limit at Ritskebos. Both initial chloride distributions indicate a moderate to high probability (42-66 %) of salinization at Ritskebos in the full-scale scenario. Salinization of the

Ritskebos well field originates from seepage through the Tegelen clay and flow through the hole in the Tegelen clay. The expected increase, calculated with the linearized propagation of variance, of the chloride concentration of the extraction at Ritskebos is 1.0 (± 2.4) mg L^{-1} per year for a single Smart Well at Noardburgum, and 1.7 (± 3.2) mg L^{-1} per year in case of the full-scale scenario. Without extractions at the Noardburgum well field the expected increase is 0.7 (± 2.0) mg L^{-1} per year. The scenario based on 1970-1980 extractions, shows an increase of the chloride concentration at Ritskebos of 3.8 (± 6.0) mg L^{-1} per year.

3. How will the Northern Brackish Front react to the Smart Well?

The interface between the brackish and fresh water, defined as the Northern Brackish Front, is drawn closer to the Noardburgum and the Ritskebos Well field, due to the Smart Well. Higher extractions at Noardburgum and Ritskebos lead to larger displacement of the front towards the well fields. This is in line with previous research. The expected movement of the brackish front, over a period of 50 years, in the high-extraction scenario is 2,025 meters with a 95% confidence interval of 1,552 - 2,320 meters. The basic scenario without Noardburgum activity shows an expected movement of 140 meters with a 95% confidence interval of -123 - 517 meters. The full-scale scenario shows an expected movement of 786 meters with a 95% confidence interval of 218 - 1,253 meters.

4. How will the full-scale design perform as compared to a single Smart Well?

The full-scale design, with 4 smart wells, will enhance the salinization at Ritskebos, compared to a scenario without the full-scale design. Most of the extracted water of the full-scale design originates from infiltration into the phreatic aquifer (85.2% with a 95% confidence interval of 69.7%-97.3%). In case of a single Smart Well almost all extracted water originates from infiltration into the phreatic aquifer (98.4% with a 95% confidence interval of 91.7%-100%).

5. How sustainable is the Smart Well and a full-scale design?

The sustainability is assessed with a Monte Carlo analysis and the linearized propagation of variance approach. It is concluded that the linearized propagation of variance is a reasonable estimation for model results and uncertainty in this model.

The Smart Well and the full-scale design can be seen as sustainable for the Noardburgum Well field. There is a 0-2% probability that the chloride concentration limit will be exceeded, which can be prevented by changing the brackish extraction. The full-scale design of Noardburgum increases the probability of the exceedance of the 0.15 g L^{-1} chloride concentration limit at Ritskebos (42-66%) compared to the basic scenario (5-36%).

The expected sustainability grade of the full-scale scenario is between a 2.9 and 8.8, with an expected 5.8 (Table 5.10). There is a high probability (almost 50 %) the full-scale scenario may not be sustainable. There are serious threats to the long-term sustainability of the Ritskebos station, and therefore the full-scale scenario.

8

Recommendations

In this chapter, several recommendations are given for the model and for further research.

A possibility to reduce the uncertainty of the phreatic aquifer is through a local water balance of the area, based on precipitation, evaporation and discharge in or out of an area through open water. Through a water balance it is possible to determine the seepage or infiltration into the aquifer. These results can be used to limited recharge or seepage rates from the model with actual data. This is not done in this thesis due to data availability. It is expected the phreatic aquifer is not modeled accurately enough to make good predictions for the phreatic aquifer. New data should improve the accuracy. Also, the model cannot account for seasonal differences in the top system, since the model is based on yearly averages.

The results of the thesis show there is a 42-66% probability that salinization will occur at the Ritskebos well field in case of the full-scale well design. It is advised to compare the model results with the actual measurements of the mixed water from the Ritskebos well field. Only the concentration per well is known, but the extraction rates of the the individual wells are unknown.

The 'smart' part (automatic adjustment of the brackish extraction) of the Smart Well has not been implemented into the model (or the field). This feedback can be implemented using short time steps. After each time step the concentration of the brackish extraction is determined. The brackish extraction will be adjusted in the next time step based on the current concentration of the brackish extraction. The infiltration will be adapted accordingly. Implementing the automatic adjustment can provide insight into the brackish extraction per Smart Well, and possibly reduce the amount of brackish extraction (see Appendix F).

Different locations are selected to monitor the salinization process during the chloride transport modeling. All locations show an increase in chloride concentration. Additional monitoring is advised near the area of the hole in Tegelen clay. This will provide additional information into the salinization process and can serve as an early warning system for high chloride concentrations of the groundwater.

It can be considered to install a brackish extraction well at the Ritskebos well field or at the hole in the Tegelen clay to counteract the salinization, since it is found that the vulnerability of the groundwater resource at Ritskebos is high. It is not wise to infiltrate this extraction at the same location, due to circulation and the short travel time of the brackish water to the Ritskebos extraction. Other infiltration locations need to be investigated, or investigation should focus on other means of disposal of the brackish water.

Another consideration for the full-scale design can be to reintroduce the reverse osmosis. It is deemed too expensive for a single Smart Well. However, it can provide many benefits for the full-scale design; additional fresh water can be produced and less water needs to be infiltrated which can be beneficial to counteract salinization at Ritskebos. A costs-benefit analysis can provide additional insight whether this is feasible.

Another possibility is to use a different well configuration for the full-scale design of the Noardburgum well field. The current configuration assumes all wells will be placed within the Noardburgum well field. It is possible to install an infiltration well outside of the Noardburgum well field. This infiltration well can be installed at a large distance from the hole in the Tegelen clay. This can be an effective measure against the recirculation of the brackish water at the Noardburgum well field and the salinization of the Ritskebos well field.

8.1. Estimation of the parameters

Currently, the model does not give realistic heads in the phreatic aquifer in the area of Noardburgum. This is related to the top boundary. More realistic top boundary conditions need to be imposed. This will have an effect on the renewability of the groundwater resource, but also on the parameters, and their confidence intervals.

8.2. Chloride distribution

The uncertainty related to the chloride distribution and the chloride measurements is not used in the thesis. It is assumed that there is no uncertainty in the initial distributions. The problem with regards to the possible errors in the chloride measurements is known at Vitens, and they are currently trying to locate the errors in the measurements.

It is advised to construct a new chloride distribution to further analyze the effects of the initial distribution. A new initial distribution based on the highest values of the measurements can be considered. This way a worst case scenario can be constructed for the chloride concentration of the extraction.

8.3. Garyp and Nij Beets

For this thesis it is assumed that the well field of Garyp and Nij Beets will have a stable chloride concentration in the coming 50 years. This assumption still needs to be tested. The same methods, used in this thesis, can be used to analyze the station of Garyp and Nij Beets to asses the sustainability. It is also advised to redo the sustainability analysis for the Garyp well field. It is located close to the boundaries of the model, which may influence the results. Chloride transport simulation is advised for the Garyp well field, since according to Vitens the well station is already salinized.

Bibliography

W.M. Alley, T.E. Reilly, and O.L. Franke. *Sustainability of ground-water resources*, volume 1186. US Geological Survey, Denver, 1999.

ASCE. *Sustainability criteria for water resource systems / prepared by the Task Committee on Sustainability Criteria, Water Resources Planning and Management Division, American Society of Civil Engineers and the working group of UNESCO/IHP IV Project M-4.3* . American Society of Civil Engineers, 1998.

M. Bakker, V. Post, C.D. Langevin, J.D. Hughes, J.T. White, J.J. Starn, and M.N. Fienen. Scripting MODFLOW Model Development Using Python and FloPy. *Groundwater*, pages 1–7, 2016. doi: 10.1111/gwat.12413.

W.L. Berendrecht, J.J.J.C. Snepvangers, B. Minnema, and P.T.M. Vermeulen. Mipwa: A methodology for interactive planning for water management. In *MODSIM07 International Congress on Modelling and Simulation "Land, Water and Environmental Management : Integrated Systems for Sustainability", Christchurch, 10-13 December 2007*, pages 330–334. Modelling and Simulation Society of Australia and New Zealand, 2007.

J.D. Bredehoeft. The Water Budget Myth Revisited: Why Hydrogeologists Model. *Ground Water*, 40(4):340–345, 2002. doi: 10.1111/j.1745-6584.2002.tb02511.x.

J.D. Bredehoeft and L.F. Konikow. Ground-water models: validate or invalidate. *Ground Water*, 31(2):178–179, 1993. doi: 10.1111/j.1745-6584.1993.tb01808.x.

R.L. Cooley, R.L. Naff, and O.L. Franke. *Regression modeling of ground-water flow.* US Government Printing Office, 1990.

A. Criminisi, T. Tucciarelli, and G.P. Karatzas. A methodology to determine optimal Transmissivity measurement locations in groundwater quality management models with scarce field information. *Water Resources Research*, 33(6):1265–1274, 1997. doi: 10.1029/97WR00300.

G.J. De Glee. Over grondwaterstroomingen bij wateronttrekking door middel van putten. Report, Doctoral dissertation, TU Delft, Delft University of Technology, Delft, 1930.

C. de Graaf, A. Niemeijer, and W.J. Zaadnoordijk. Verziltingsprognose pompstation Noardburgum. Report, Royal Haskoning, 2007.

F.M. Dekking, C. Kraaikamp, H.P. Lopuhaä, and L.E. Meester. *A modern introduction to probability and statistics: Understanding why and how.* Springer, London, 2005.

F.C. Dufour. *Grondwater in Nederland. Onzichtbaar water waarop wij lopen.* TNO, Delft, 1998.

J. Ehlers, K.D. Meyer, and H.J. Stephan. The pre-weichselian glaciations of North-West Europe. *Quaternary Science Reviews*, 3(1):1 – 40, 1984. doi: 10.1016/0277-3791(84)90003-9.

C.R. Fitts. *Groundwater science.* Academic Press, Amsterdam, 2002.

N.P. Fofonoff and R.C. Millard. *Algorithms for computation of fundamental properties of seawater.* UNESCO Technical Papers in Marine Science 44, Paris, 1983.

T. Gleeson, Y. Wada, M.F.P. Bierkens, and L.P.H. van Beek. Water balance of global aquifers revealed by groundwater footprint. *Nature*, 488(7410):197–200, 2012. doi: 10.1038/nature11295.

Google. Location of Study area, 5 23 2016. URL https://www.google.nl/maps/@53.2005252,5.9010855,24393m/data=!3m1!1e3.

W. Guo and C.D. Langevin. *User's guide to SEAWAT: a computer program for simulation of three-dimensional variable-density ground-water flow.* U.S.Geological Survey, 2002.

K.J. Halford and R.T. Hanson. *User guide for the drawdown-limited, multi-node well (MNW) package for the US Geological Survey's modular three-dimensional finite-difference ground-water flow model, versions MODFLOW-96 and MODFLOW-2000.* U.S.Geological Survey, Sacramento, 2002.

M.S. Hantush. Analysis of data from pumping tests in leaky aquifers. *Eos, Transactions American Geophysical Union*, 37(6):702–714, 1956. doi: 10.1029/TR037i006p00702.

A.W. Harbaugh. MODFLOW-2005, the US Geological Survey modular ground-water model: The ground-water flow process. Report, US Depertment of the Interior, US Geological Survey, 2005.

R.C. Heath. *Basic ground-water hydrology.* U.S.Geological Survey, 1983.

K. Hemker and V. Post. MLU for Windows: Well flow modeling in multilayer aquifer systems. *www.microfem.com*, 2014.

M.C. Hill. *Methods and guidelines for effective model calibration.* US Geological Survey, Denver, 1998.

E.O. Holzbecher. *Modeling density-driven flow in porous media.* Springer-Verlag Berlin Heidelberg New York, Berlin, 1998.

IWACO. Vooronderzoek inzake putverziltingsverschijnselen op het pompstation Noordbergum. Report, IWACO B.V., 1978.

IWACO. Geohydrologisch onderzoek inzake de verzilting van het pompstation jhr. E.C. Storm van 's Gravezande en mogelijke maatregelen ter bijsturing van het verziltingsproces. Report, IWACO B.V., 1979.

IWACO. Haalbaarheidsstudie bijsturingsmaatregelen verzilting pompstation "Storm" te Noardburgum. Report, IWACO B.V., 1990.

IWACO. Grondwatermodelstudie Noordbergum. Report, IWACO B.V., 1994.

J. Kirchner. Data Analysis Toolkit 5: Uncertainty Analysis and Error Propagation, 4 21 2016. URL `http://seismo.berkeley.edu/~kirchner/eps_120/Toolkits/Toolkit_05.pdf`.

KNMI. Daggegevens van het weer in Nederland, 5 23 2016. URL `https://www.knmi.nl/nederland-nu/klimatologie/daggegevens`.

L.F. Konikow and G.Z. Hornberger. Modeling Effects of Multinode Wells on Solute Transport. *Ground Water*, 44(5):648–660, 2006. doi: 10.1111/j.1745-6584.2006.00231.x.

W.F.J.M. Krul. De geo-hydrlogische gesteldheid van de waterwinplaats bij Noordbergum. Report, Rijksinstituut voor drinkwatervoorziening, 1940.

G.P. Kruseman and N.A. de Ridder. *Analysis and evaluation of pumping test data.* International Institute for Land Reclamation and Improvement, Wageningen, 1979.

H.H. Ku. Notes on the use of propagation of error formulas. *Journal of Research of the National Bureau of Standards.Section C: Engineering and Instrumentation*, 70C(4):263–273, 1966. doi: 10.6028/jres.070C.025.

C.D. Langevin and W. Guo. MODFLOW/MT3DMS–Based Simulation of Variable-Density Ground Water Flow and Transport. *Ground Water*, 44(3):339–351, 2006. doi: 10.1111/j.1745-6584.2005.00156.x.

C.D. Langevin, D.T. Thorne Jr, A.M. Dausman, M.C. Sukop, and W. Guo. *SEAWAT Version 4: a computer program for simulation of multi-species solute and heat transport.* U.S.Geological Survey, Reston, 2008.

E.S. Lee and R.N. Forthofer. *Analyzing complex survey data*, volume 71. Sage Publications, Thousand Oaks, 2005.

A. Leijnse and S.M. Hassanizadeh. Model definition and model validation. *Advances in Water Resources*, 17 (3):197–200, 1994. doi: 10.1016/0309-1708(94)90041-8.

E. Lewis. The practical salinity scale 1978 and its antecedents. *Oceanic Engineering, IEEE Journal of*, 5(1):3–8, 1980. doi: 10.1109/JOE.1980.1145448.

C. Maas and E.J.M. Veling. Een snelle benadering van de formule van hantush. *Stromingen : vakblad voor hydrologen*, 16(1):59–69, 2010.

J. Margat, S. Foster, and A. Droubi. Concept and importance of non-renewable resources. *Non-renewable groundwater resources: A guidebook on socially-sustainable management for water-policy makers*, 10:13–24, 2006.

A.M. Mood and F.A. Graybill. *Introduction to the theory of statistics*. McGraw-Hill, New York, 1963.

M. Newville, T. J. Stensitzki, D.B. Allen, and A. Ingargiola. *Non-linear least-squares minimization and curve-fitting for Python*. Massachusetts Institute of Technology, 2016.

N.V. Waterleiding Friesland. Rapport inzake de vergunningaanvraag in het kader van de grondwaterwet voor het inrichten van een selectief zoutwateronttrekkingssysteem op de winplaats Noardburgum. Report, N.V. Waterleiding Friesland, 1990.

U. Olsson. Confidence intervals for the mean of a log-normal distribution. *Journal of Statistics Education*, 6 (1):6–, 2005.

T.N. Olsthoorn. *CIE4420 Fresh and salt water*. TU Delft, Delft, 2012.

A.T. Oosterhof and M.M. Nederlof. Demonstratieproject brakwater; beschrijving voorgenomen activiteiten. Report, Vitens, 2007.

A.T. Oosterhof and K.J. Raat. Keep it Fresh! Field test results of the fresh keeper concept including disposal of the RO membrane concentrate by deep well injection. Report, Vitens and KWR, 2010.

A.T. Oosterhof and N. Wolthek. Demonstratieproject brakwater; Opslagplan membraanconcentraat in kader van de mijnbouwwet. Report, Vitens, 2008.

G.H.P Oude Essink. Improving fresh groundwater supply—problems and solutions. *Ocean and Coastal Management*, 44(5–6):429–449, 2001a. doi: 10.1016/S0964-5691(01)00057-6.

G.H.P. Oude Essink. *Density dependent groundwater flow: salt water intrusion and heat transport*. IHE, 2001b.

V.P. Pandey, S. Shrestha, S.K. Chapagain, and F. Kazama. A framework for measuring groundwater sustainability. *Environmental Science and Policy*, 14(4):396 – 407, 2011. doi: http://dx.doi.org/10.1016/j.envsci.2011.03.008.

G.F. Pinder and M.A. Celia. *Subsurface hydrology*. John Wiley and Sons, Hoboken, 2006.

D.W. Pollock. *Documentation of computer programs to compute and display pathlines using results from the U.S.Geological Survey modular three-dimensional finite-difference ground-water flow model*. US Geological Survey, 1989.

D.W. Pollock. *User guide for MODPATH version 6: a particle tracking model for MODFLOW*. US Geological Survey, 2012.

Provincie Fryslân. Grondwateronttrekkingenkaart, 1 25 2016. URL `http://www.fryslan.frl/3183/grondwateronttrekkingenkaart/`.

K.J. Raat and J.K. Kooiman. Brak grondwater: niet mijden, maar gebruiken! Report, KWR, 2012.

J.S. Rus. Modelonderzoek verzilting Noordbergum. Report, IWACO B.V., 1997.

H.H.G. Savenije. *CT4431 - Hydrological Modelling*. TU Delft, Delft, 2009.

T.O. Sonnenborg, B.S. Christensen, P. Nyegaard, H.J. Henriksen, and J.C. Refsgaard. Transient modeling of regional groundwater flow using parameter estimates from steady-state automatic calibration. *Journal of Hydrology*, 273(1–4):188 – 204, 2003. doi: 10.1016/S0022-1694(02)00389-X.

R. Stuurman and G.H.P. Oude Essink. Naar een uniforme landelijke inrichting van het KRW-grondwatermeetnet Zoet-Zout. Report, TNO, 2007.

P.J. Stuyfzand and K.J Raat. Benefits and hurdles of using brackish groundwater as a drinking water source in the Netherlands. *Hydrogeology Journal*, 18(1):117–130, 2010. doi: 10.1007/s10040-009-0527-y.

J. Tellinghuisen. Statistical Error Propagation. *The Journal of Physical Chemistry A*, 105(15):3917–3921, 2001. doi: 10.1021/jp003484u.

S. van der Linde. A modelling study for the TKI - project "keep it Fresh". Report, KWR, 2014.

M.J.H. van der Valk. A fresh-keeper for Noard Burgum; The future for a salinated well field? Report, TU Delft, 2011.

A. Verruijt. Elastic Storage of Aquifers. Flow Through Porous Media. *Academic Press, New York, N.Y.*, pages 331–376, 1969.

J.R. Von Asmuth. *Groundwater System Identification through Time Series Analysis*. TU Delft, Delft University of Technology, 2012.

J. Vrba and A. Lipponen. *Groundwater resources sustainability indicators*, volume IHP-VI series on groundwater 14. UNESCO, 2007. doi: IHP/2007/GW-14.

I. Weir. Spearman's correlation, 12 16 2011. URL `http://www.statstutor.ac.uk/resources/uploaded/spearmans.pdf`.

N. Wolthek, K.J. Raat, J.A. de Ruijter, and A.T. Oosterhof. Desalination of brackish groundwater and concentrate disposal by deep well injection. *Desalination and water treatment*, 51(4-6):1131–1136, 2013. doi: 10.1080/19443994.2012.694205.

C. Zheng and P.P. Wang. *MT3DMS: a modular three-dimensional multispecies transport model for simulation of advection, dispersion, and chemical reactions of contaminants in groundwater systems; documentation and user's guide*. University of Alabama, Alabama, 1999.

X.H. Zhou and S.U.J.U.A.N. Gao. Confidence intervals for the log-normal mean. *Statistics in medicine*, 16(7): 783–790, 1997. doi: 10.1002/(SICI)1097-0258(19970415)16:7<783::AID-SIM488>3.0.CO;2-2.

A

Reproducing preceding models

The previous models created by van der Valk (2011) and van der Linde (2014) are analyzed and presented in this Appendix.

A.1. Previous models

The most important aspects of the previous models are presented below.

The small-scale simulations (model 1) made by van der Valk (2011) is a useful model. It demonstrates the effect of the Fresh Keeper, and how it prevents upconing. The scenarios provide insight to how the chloride distribution is influenced by different well field configurations on a small-scale. The best well configurations seems to be a circular design of six wells, were the brackish well extracts 17 m^3 per hour. The small-scale simulations do not take lateral salinization into account. Also, the importance of density differences of the groundwater is shown. Not including density differences leads to different results.

The cross-sectional model (model 2), made by van der Valk (2011), gives insight into the cause of the salinization in Noardburgum. The model shows that there is salt intrusion from the sea over the last 10,000 years, which over time reaches the location of Noardburgum 20 kilometers inland. There is no orthogonal spread in the model, this is most likely the reason it is overestimating the chloride concentration in the second aquifer.

The large-scale model (model 3), made by van der Valk (2011), provides insight into the salinization of the area. One of the most important conclusions of the model is that this area needs to include density differences when modeling. When this is not included the model incorrectly shows that the entire area will remain fresh.

The large-scale model (model 4) made by Siebren focused on how the Fresh Keeper will influence the regional (geo-) hydrology. Sensitivity analysis showed that: (van der Linde, 2014)

- The resistance of the Tegelen clay does not have a significant influence on the model results.
- The injection depth of the brackish water has a negligible effect on the salinization of Ritskebos.
- The Fresh Keeper leads to minimal increase in flow velocity in the deepest part of the aquifer (which is most saline).
- It is concluded that the Fresh Keeper does not lead to significant salinization at the Ritskebos well field.

A.1.1. (van der Valk, 2011), Model 1, Small-scale simulations

The extraction of fresh and brackish groundwater in the extraction aquifer is kept at a rate of 50 m^3 per hour. Reverse osmosis is used to desalinize the brackish water. The recovery is initially kept at 50 %, meaning the permeate and concentrate are produced at a rate of 25 m^3 per hour. At a later stadium of the pilot the recovery is increased to 75%, resulting into 35 m^3 per hour permeate and 15 m^3 per hour of concentrate. Increasing the recovery leads to higher chloride concentration in the concentrate, but this proved not to be a problem for the Reverse osmosis installation as for the injection well.

The grid is limited to a size of 600 times 600 meters. This is because the variance of the chloride concentration is likely to be limited to this plot due to the small time scale (1+ year). The horizontal grid of the model is made by systematically increasing the cells around the well from 5 meter interval to 50 meters. The vertical grid is manually constructed based on density and layers of interest.

The subsurface is described by information gained from drilling in the area. The transmissivity of the first aquifer is 5,200 $m^2\ d^{-1}$, which is determined by aquifer tests. To derive the conductivity for each layer the relation with the mean grain size diameter is used (gained from the drilling). The same method is used to derive the conductivity in the injection aquifer.

The initial chloride concentration is a homogeneous distribution, based on samples taken at the pilot location. The concentrations are fixed at the boundaries of the model. The top and bottom layer are considered as no flow boundaries. The vertical boundaries at the sides of the model are modeled as constant head boundaries with a correction for density differences. Also natural flow of the groundwater is included in the boundaries. Furthermore, the drawdown effects of the well are included in the vertical boundaries, as is calculated with de Glee formula (see Equation H.1).

Results

This model has been made to describe the local situation of the fresh-keeper. A total of 10 cases have been made in order to understand and describe the local situation surrounding the wells. The model has been split into two parts, the extraction aquifer and the injection aquifer. The aquifers are separated by an aquitard, but leakage through the aquitard is considered negligible on the timescale and size of model 1.

A total of five full case scenarios were modeled. In each scenario the wells were placed differently in order to evaluate the extraction of brackish water. It is found that a circular well field with equal distance between the wells resulted in the lowest brackish water extraction, see Figure A.1a. The main advantage of such a system is that brackish water can be extracted where needed.

Sensitivity testing shows that density difference is important for modeling the Fresh Keeper, if not used it can lead to large differences. Also, the assumption that the aquitard has no leakage is tested. Negligible differences were found when leakage is present in the aquitard.

The concentration of the water in the fresh water well is displayed in Figure A.1b. Here an increase can be seen in the case without brackish water extraction. At the last time step of the model (400 days after starting extracting) the water has reached a concentration of 100 mg L^{-1}. Considering that Vitens is maintaining a maximum concentration of 0.15 g L^{-1} for the production of drinking water, it does not take long before the fresh water well becomes too saline for fresh water extraction. Upconing of brackish water eventually led to salinization of the fresh water well. The upconing of brackish water caused the closure of the well field in Noardburgum in 1993 (Rus, 1997).

A.1.2. (van der Valk, 2011), Model 2: Cross-sectional model

The second model is made to create an initial condition for the large 3d model (model 3), but also to gain insight into the historic intrusion. It turned out to be difficult to create an initial condition for the chloride distribution from measurements. Therefore, Mark van der Valk made a model which describes the historic salt intrusion into the groundwater in Friesland. The model starts at a time the underground is assumed to be completely fresh (± 8,000 years ago). This can be assumed because the sea level is 25 meters lower

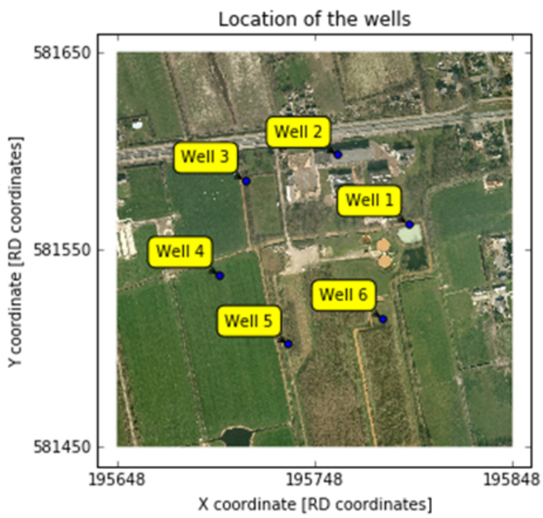

(a) Circular design of the well field

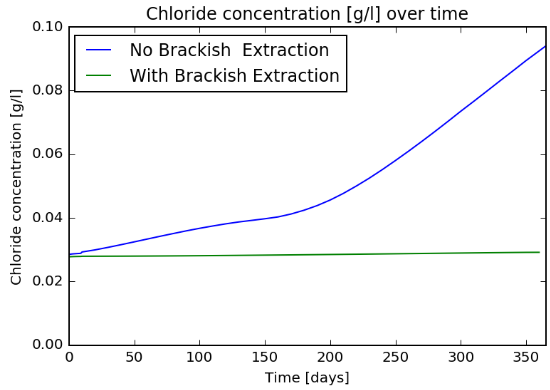

(b) Concentration of the extracted fresh water with and without brackish extraction

Figure A.1: Design of the well field and the effect on the chloride concentration of the extracted fresh water

than it is today. With this knowledge, and the Ghyben – Herzberg relation, the assumption can be made that groundwater under Friesland is completely fresh. The model is a cross-section with a length of 60 kilometer. The model starts in the North Sea (kilometer km North from Noardburgum) and ends 20 kilometer south of Noardburgum. The horizontal grid is spaced 250 meters apart at locations of interest; otherwise a spacing of 500 meters of 1 kilometer is used. The vertical grid is 10 meters apart to include the effect of density differences.

The schematization of the subsurface is obtained from data by REGIS (Regionaal Geohydrlogisch Informatie Systeem). Also, MIPWA (Methodiekontwikkeling voor Interactieve Planvorming ten behoeve van Waterbeheer) is used to get a more detailed description of the top layers (Berendrecht et al., 2007).

It is assumed there is no leakage in the model. Therefore, the bottom layer and the North boundary are no flow boundaries. The Southern boundary is a constant flow boundary. The head gradient is assumed equal to the surface gradient. The top boundary is variable in time due to land rise and subsidence. The surface drains the groundwater and determines the head gradient in the aquifers. The top boundary is therefore modeled as drainage.

Furthermore, no wells are present in this model, since there were no extractions of importance to influence the chloride distribution in the modeled period. Noardburgum is located at the 40,000 meters mark in the cross-section. The chloride concentration at two different times is presented in Figure A.2.

A.1.3. (van der Valk, 2011), Model 3: Large-scale simulation of Noardburgum

This model evaluates the period of 1930 till 2050 AD. The initial chloride distribution is obtained from Model 2. The subsurface of the model is a copy of Model 2 and expanded in orthogonal direction. The section from 35 till 46 km in Model 2 from the shore is copied into Model 3. Extra detail is added in vertical direction, like the hole in the Tegelen clay near the Peelo Gully. The total grid has a size of 11km by 6.75 kilometer.

The grid consists of horizontal cells of 250 by 250 meters. The vertical spacing is 10 meters. The model will not give a good representation of the chloride distribution near the wells, but it does give a representation of the entire lateral chloride transport. The top boundary has been modeled with drains, just like Model 2. The side boundaries are modeled as no flow boundaries, since the natural groundwater flow is found to be parallel to side boundaries. The North and South boundaries are given by an environmental head, equal to the head from Model 2 at time 1900 AD, which is adaptable over depth for density differences.

Analysis of the model shows that the salt plume is slowly moving towards Ritskebos following historic ex-

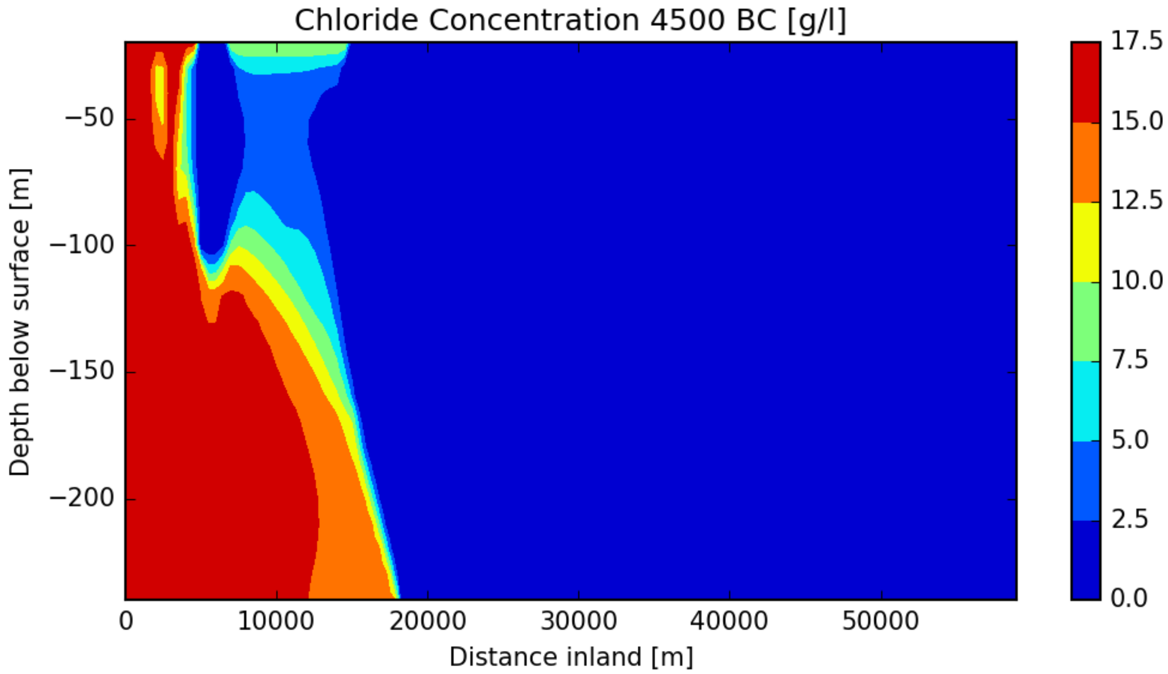

(a) Cross-section present chloride concentration [g L^{-1}] 4500 BC

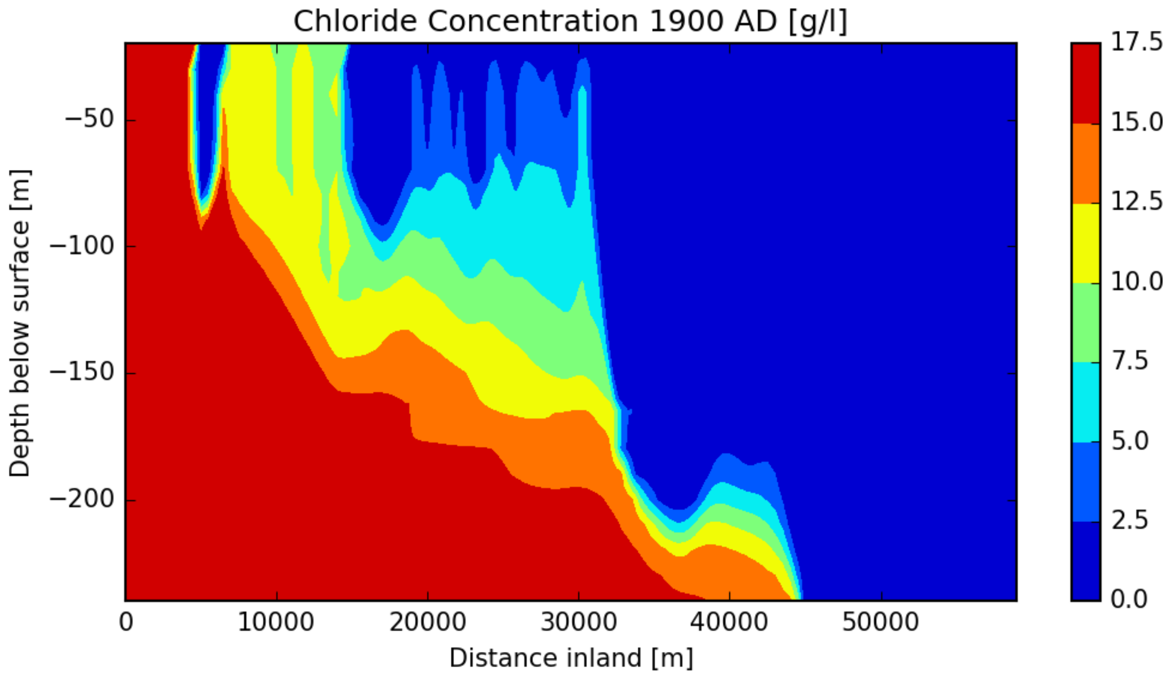

(b) Cross-section present chloride concentration [g L^{-1}] 1900 AD

Figure A.2: Cross-sections present chloride distribution at two different times tractions. Further analysis shows that the injection well of the Fresh Keeper is injecting fresh water with a chloride concentration of 0.0 g L^{-1}. The brackish water extraction well is extracting water with a chloride concentration > 0.0 g L^{-1}. This means the injection well should also inject water with a chloride concentration that is larger than 0.0 g L^{-1}.

A.1.4. (van der Linde, 2014), Model 4, Keep it Fresh!

Previous models developed by Royal Haskoning focused on the first extraction aquifer. Siebren reused this model for the first aquifer and added the second injection aquifer. His model is to evaluate the effect of full-scale implementation of the Freshkeeper on the regional geohydrology and if it will lead to an increased salinization at Ritskebos.

The grid consists of squares which are 50 by 50 meters. The total grid is 4,750 by 5,000 meters. The northern boundary is chosen as the 6,000 mg L^{-1} chloride concentration isohaline. Other boundaries are located at streamline isohalines derived from contour maps. Head boundaries are imposed at all sides, and General Head Boundaries are imposed at the top layer.

All the wells in the model have a specific discharge. Each layer in which the well is present has the same discharge. The discharge is not varying over the well screen. At the injection well the water is given a chloride concentration of 1,500 mg L^{-1}. This concentration is constant in all the time steps.

Numerical instability occurred along the Northern boundary. This created high chloride values. For this reason the results from the model after 25-30 years are rejected. The effects of the Fresh Keeper can be seen in the 2th aquifer, relatively lower chloride levels are observed near the injection well. Considering that the water in the injection well has a chloride concentration of 1,500 mg L^{-1} this observation makes sense. Analysis shows that there is brackish water transported through the hole in the Tegelen clay and is flowing towards Ritskebos.

B

MODFLOW Packages used for boundary conditions

Several packages are developed to simulate hydrological stresses to a groundwater system. These packages add terms to the flow equation to represent sinks or sources. The basic process and mathematical description of the packages is described. Only the hydrological stresses which will be used during modeling are described. Information from the packages has been obtained from manual for MODFLOW – 2005 (Harbaugh, 2005).

These sources and sinks are presented as an external process, thus additional terms are required to the flow equation to the receiving cell. These processes can be depended on head in cell i,j,k but independent to other heads. MODFLOW accounts for such processes by the following expression:

$$a_{i,j,k,n} = p_{i,j,k,n}\, h_{i,j,k} + q_{i,j,k,n} \tag{B.1}$$

Where

$a_{i,j,k,n}$	Is the flow volume from the nth external source to cell i,j,k ($L^3\ T^{-1}$),
$h_{i,j,k}$	Is the head in cell i,j,k (L),
$q_{i,j,k,n}$	Is a constant ($L^3\ T^{-1}$),
$p_{i,j,k,n}$	Is a constant ($L^2\ T^{-1}$)

B.1. Recharge Package (RCH)

The Recharge Package is used to simulate the percolation of precipitation into the groundwater system. The recharge is given as a flux for each cell in the top layer. This flux is multiplied by the top area of the cell to give the recharge flow rate for each cell. The recharge to a cell is independent to the head in the receiving cell.

B.2. Well Package (WEL)

The Well Package is used to simulate extraction or infiltration of water in the aquifer system. The rate of extraction or infiltration is constant during a time period. The rate is giving as fluid volume per unit of time. The extraction or infiltration rate needs to be specified per cell. The extraction or infiltration is independent to the heads in the aquifer.

B.3. Multi Node Package (MNW)

The Multi Node Package (MNW) is used to simulate wells that extend beyond a single cell in the aquifer (Halford and Hanson, 2002). MNW can provide preferential pathways to flow and solute transport along the length of the filter, thus it can simulate pathways between aquifers with a confining layer, but also in a single aquifer (Konikow and Hornberger, 2006). The WEL Package is not able to simulate such a preferential pathway for both solute transport and flow. The MNW Package has not been used since it is currently not fully supported by FloPy. MNW is independent to heads in the aquifer.

B.4. General Head Boundary (GHB)

The General Head Boundary (GHB) is used to simulate flow into or out of a cell from an external source. A constant head is assigned to the external source. The boundary conductance represents the resistance to flow between the boundary and aquifer. The boundary conductance times the difference in head between the external source and the head determines the amount of flow into or out of the cell. In this thesis the GHB is used to simulated ditches. The ditches are able to discharge water out of a system, but also able to add water to as system. This is dependent on the head in the aquifer.

$$CB = \frac{A}{R} \tag{B.2}$$

Where
CB Is the boundary conductance ($L^2\ T^{-1}$),
A The area of the cell (L^2),
R Is the resistance (T),

$$Q_{GHB} = CB\ (HB - h_{i,j,k}) \tag{B.3}$$

Where
Q_{GHB} Is the flow volume into or out of the cell ($L^3\ T^{-1}$),
HB Is the head in the external source (L),

B.5. Time-Variant Specified Head Package(CHD)

The CHD Package can account for changes in head along a boundary over a period of time. The CHD package can vary the heads of the boundary for each stress period, instead of using the same boundary head for every stress period. The CHD package is independent to the heads in the aquifer. Using an additional option the boundary head can be corrected for density differences when using SEAWAT.

B.6. Drain Package (DRN)

The Drain Package is used to simulate the effect of a drain. This means the drain is active when the head in the cell is above the drain elevation. The drain will remove water from the aquifer as long as the head in the cell is above the drain elevation. The drain conductance is depended the size and density of the openings in the drain. In this thesis the Drain Package is used to simulate ditches. The ditches are only able to discharge water out of the system.

$$\begin{cases} h_{i,j,k} > HD, & Q_d = CD\,(h_{i,j,k} - HD) \\ h_{i,j,k} \leq HD, & Q_d = 0 \end{cases} \tag{B.4}$$

Where

Q_d	Is the flow volume into or out of the cell ($L^3\ T^{-1}$),
CD	Is the drain conductance ($L^2\ T^{-1}$),
HD	Is the drain elevation (L),

B.7. Evapotranspiration Package (EVT)

The Evapotranspiration (ET) Package is used to simulate evaporation. When the groundwater table is close to the land surface, ET can occur. A maximum value needs to be assigned for the ET. When the head in the cell is above the surface elevation, the maximum ET occurs. When the head in the cell is below surface level, the ET decreases linearly until extinction depth is reached. ET is no longer possible when the head in the cell is below the extinction depth.

$$\begin{cases} h_{i,j,k} > SURF, & Q_{ET} = Q_{ETM} \\ (SURF - EXDP) \leq h_{i,j,k} \leq SURF, & Q_{ET} = Q_{ETM}\,\frac{h_{i,j,k} - (SURF - EXDP)}{EXDP} \\ h_{i,j,k} < SURF, & Q_{ET} = 0 \end{cases} \tag{B.5}$$

Where

Q_{ET}	Is the rate of water going out of the aquifer due to ET ($L\ T^{-1}$),
Q_{ETM}	Is the maximum value of Q_{ET} ($L\ T^{-1}$),
$SURF$	Is the ET surface level where maximum ET occurs (L),
$EXDP$	Is the extinction depth (L)

C

Correlation matrices of the Monte Carlo analysis

The different correlation matrices of the Monte Carlo analysis are presented in this Appendix. A reminder of how the absolute value of the correlation coefficient is interpreted and a recapitulation of the different parameters: (Weir, 2011)

0.00 - 0.19 → very weak
0.20 - 0.39 → weak
0.40 - 0.59 → moderate
0.60 - 0.79 → strong
0.80 - 1.00 → very strong

Recharge [Parameter 1]
Semi-confining layer [Parameter 2]
Aquifer 1 [Parameter 3]
Tegelen clay [Parameter 4]
Aquifer 2 [Parameter 5]
Movement of the brackish front is subdivided into the different permeable zones in the first aquifer.

The correlation coefficients of the model output can be calculated using the outcome of the Monte Carlo analysis. The correlation between the parameters resulting from the calibration process is the same as the correlation between the parameters from the parameter set of the Multivariate Gaussian Distribution, as expected. The different scenarios show similar correlation between model output and the parameters. Also, similarities are found between the different scenarios and model output. Only the high-extraction scenario show slight differences. This could be related to the high-extraction and the corresponding changes to the groundwater flows and the origin of the extracted groundwater.

The correlation coefficient is used to determine the relation between the model output. If different results of the model results have a high correlation, it is not wise to use both in the sustainability evaluation. This may lead to incorrect results. It is expected there will be a correlation between the different origins of the groundwater (see equation 4.11).

All scenarios indicate that there is a strong correlation between the extraction from recharge and the extraction from the boundaries. When the parameter recharge is low, compared to the original value, the extraction from recharge is low. This results in a high-extraction from the boundaries. It is decided to not use the extraction from the boundaries in the sustainability evaluation, due to the strong correlation with the recharge.

Table C.1: Monte Carlo analysis correlation matrix for Scenario 1970 - 1980 (part 1)

Scenario 1 1970 - 1980		Parameters					Contribution from boundaries					Contribution from recharge				
		1	2	3	4	5	RB	NB	NBQB	GR	IN	RB	NB	NBQB	GR	IN
Parameters	1	1.00	-0.86	0.03	-0.00	0.00	-0.78	0.09	-	-	-	0.71	-0.06	-	-	-
	2	-0.86	1.00	-0.02	0.00	0.01	0.61	-0.27	-	-	-	-0.52	0.36	-	-	-
	3	0.03	-0.02	1.00	0.01	0.00	0.21	0.82	-	-	-	0.50	-0.56	-	-	-
	4	-0.00	0.00	0.01	1.00	0.00	0.14	0.11	-	-	-	-0.07	-0.07	-	-	-
	5	0.00	0.01	0.00	0.00	1.00	-0.41	-0.18	-	-	-	-0.44	-0.38	-	-	-
Contribution from boundaries	RB	-0.78	0.61	0.21	0.14	-0.41	1.00	0.35	-	-	-	-0.33	-0.08	-	-	-
	NB	0.09	-0.27	0.82	0.11	-0.18	0.35	1.00	-	-	-	0.43	-0.75	-	-	-
	NBQB	-	-	-	-	-	-	-	-	-	-	-	-	-	-	-
	GR	-	-	-	-	-	-	-	-	-	-	-	-	-	-	-
	IN	-	-	-	-	-	-	-	-	-	-	-	-	-	-	-
Contribution from recharge	RB	0.71	-0.52	0.50	-0.07	-0.44	-0.33	0.43	-	-	-	1.00	0.02	-	-	-
	NB	-0.06	0.36	-0.56	-0.07	-0.38	-0.08	-0.75	-	-	-	0.02	1.00	-	-	-
	NBQB	-	-	-	-	-	-	-	-	-	-	-	-	-	-	-
	GR	-	-	-	-	-	-	-	-	-	-	-	-	-	-	-
	IN	-	-	-	-	-	-	-	-	-	-	-	-	-	-	-
Contribution from Tegelen	RB	-0.32	0.19	-0.58	0.45	0.55	-0.05	-0.48	-	-	-	-0.82	-0.04	-	-	-
	NB	-0.05	-0.10	-0.43	-0.06	0.80	-0.41	-0.42	-	-	-	-0.65	-0.28	-	-	-
	NBQB	-	-	-	-	-	-	-	-	-	-	-	-	-	-	-
	GR	-	-	-	-	-	-	-	-	-	-	-	-	-	-	-
	IN	-	-	-	-	-	-	-	-	-	-	-	-	-	-	-
Contribution from hole	RB	-0.07	0.06	-0.50	-0.54	0.65	-0.45	-0.62	-	-	-	-0.54	0.09	-	-	-
Movement brackish front	Top	-0.19	0.11	0.85	-0.18	-0.32	0.38	0.70	-	-	-	0.43	-0.34	-	-	-
	Middle	-0.30	0.27	0.72	-0.17	-0.50	0.50	0.56	-	-	-	0.41	-0.09	-	-	-
	Bottom	-0.17	0.13	0.80	-0.22	-0.36	0.38	0.64	-	-	-	0.43	-0.27	-	-	-

Table C.2: Monte Carlo analysis correlation matrix for Scenario 1970 - 1980 (part 2)

Scenario 1		Contribution from Tegelen					Contribution from hole	Movement brackish front		
1970 - 1980		RB	NB	NBQB	GR	IN	RB	Top	Middle	Bottom
Parameters	1	-0.32	-0.05	-	-	-	-0.07	-0.19	-0.30	-0.17
	2	0.19	-0.10	-	-	-	0.06	0.11	0.27	0.13
	3	-0.58	-0.43	-	-	-	-0.50	0.85	0.72	0.80
	4	0.45	-0.06	-	-	-	-0.54	-0.18	-0.17	-0.22
	5	0.55	0.80	-	-	-	0.65	-0.32	-0.50	-0.36
Contribution from boundaries	RB	-0.05	-0.41	-	-	-	-0.45	0.38	0.50	0.38
	NB	-0.48	-0.42	-	-	-	-0.62	0.70	0.56	0.64
	NBQB	-	-	-	-	-	-	-	-	-
	GR	-	-	-	-	-	-	-	-	-
	IN	-	-	-	-	-	-	-	-	-
Contribution from recharge	RB	-0.82	-0.65	-	-	-	-0.54	0.43	0.41	0.43
	NB	-0.04	-0.28	-	-	-	0.09	-0.34	-0.09	-0.27
	NBQB	-	-	-	-	-	-	-	-	-
	GR	-	-	-	-	-	-	-	-	-
	IN	-	-	-	-	-	-	-	-	-
Contribution from Tegelen	RB	1.00	0.76	-	-	-	0.43	-0.65	-0.67	-0.68
	NB	0.76	1.00	-	-	-	0.79	-0.55	-0.71	-0.57
	NBQB	-	-	-	-	-	-	-	-	-
	GR	-	-	-	-	-	-	-	-	-
	IN	-	-	-	-	-	-	-	-	-
Contribution from hole	RB	0.43	0.79	-	-	-	1.00	-0.47	-0.54	-0.44
Movement brackish front	Top	-0.65	-0.55	-	-	-	-0.47	1.00	0.95	0.96
	Middle	-0.67	-0.71	-	-	-	-0.54	0.95	1.00	0.91
	Bottom	-0.68	-0.57	-	-	-	-0.44	0.96 5	0.91	1.00

Table C.3: Monte Carlo analysis correlation matrix for Scenario 2007 - 2010 (part 1)

Scenario 2 2007 - 2010		Parameters					Contribution from boundaries					Contribution from recharge				
		1	2	3	4	5	RB	NB	NBQB	GR	IN	RB	NB	NBQB	GR	IN
Parameters	1	1.00	-0.86	0.03	-0.00	0.00	-0.85	-	-	-0.75	-0.98	0.83	-	-	0.66	0.98
	2	-0.86	1.00	-0.02	0.00	0.01	0.71	-	-	0.47	0.85	-0.68	-	-	-0.35	-0.84
	3	0.03	-0.02	1.00	0.01	0.00	-0.19	-	-	0.12	-0.15	0.47	-	-	0.25	0.15
	4	-0.00	0.00	0.01	1.00	0.00	0.15	-	-	-0.15	0.00	-0.14	-	-	-0.16	-0.02
	5	0.00	0.01	0.00	0.00	1.00	-0.02	-	-	-0.07	0.02	-0.26	-	-	-0.02	-0.03
Contribution from boundaries	RB	-0.85	0.71	-0.19	0.15	-0.02	1.00	-	-	0.53	0.87	-0.85	-	-	-0.61	-0.86
	NB	-	-	-	-	-	-	-	-	-	-	-	-	-	-	-
	NBQB	-	-	-	-	-	-	-	-	-	-	-	-	-	-	-
	GR	-0.75	0.47	0.12	-0.15	-0.07	0.53	-	-	1.00	0.65	-0.49	-	-	-0.86	-0.66
	IN	-0.98	0.85	-0.15	0.00	0.02	0.87	-	-	0.65	1.00	-0.87	-	-	-0.61	-1.00
Contribution from recharge	RB	0.83	-0.68	0.47	-0.14	-0.26	-0.85	-	-	-0.49	-0.87	1.00	-	-	0.68	0.88
	NB	-	-	-	-	-	-	-	-	-	-	-	-	-	-	-
	NBQB	-	-	-	-	-	-	-	-	-	-	-	-	-	-	-
	GR	0.66	-0.35	0.25	-0.16	-0.02	-0.61	-	-	-0.86	-0.61	0.68	-	-	1.00	0.64
	IN	0.98	-0.84	0.15	-0.02	-0.03	-0.86	-	-	-0.66	-1.00	0.88	-	-	0.64	1.00
Contribution from Tegelen	RB	-0.70	0.57	-0.49	0.35	0.26	0.62	-	-	0.39	0.75	-0.90	-	-	-0.64	-0.77
	NB	-	-	-	-	-	-	-	-	-	-	-	-	-	-	-
	NBQB	-	-	-	-	-	-	-	-	-	-	-	-	-	-	-
	GR	0.09	-0.18	-0.71	0.59	0.17	0.20	-	-	-0.18	-0.00	-0.40	-	-	-0.35	-0.02
	IN	-0.69	0.39	-0.12	0.25	0.19	0.50	-	-	0.66	0.65	-0.68	-	-	-0.75	-0.70
Contribution from hole	RB	-0.22	0.18	-0.62	-0.43	0.60	0.16	-	-	0.12	0.29	-0.54	-	-	-0.24	-0.30
Movement brackish front	Top	-0.87	0.71	0.35	-0.04	-0.24	0.70	-	-	0.82	0.78	-0.48	-	-	-0.58	-0.78
	Middle	-0.85	0.70	0.38	-0.03	-0.27	0.66	-	-	0.82	0.76	-0.44	-	-	-0.57	-0.76
	Bottom	-0.80	0.66	0.45	-0.08	-0.23	0.68	-	-	0.78	0.71	-0.39	-	-	-0.50	-0.71

Table C.4: Monte Carlo analysis correlation matrix for Scenario 2007 - 2010 (part 2)

Scenario 2		Contribution from Tegelen					Contribution from hole	Movement brackish front		
2007 - 2010		RB	NB	NBQB	GR	IN	RB	Top	Middle	Bottom
Parameters	1	-0.70	-	-	0.09	-0.69	-0.22	-0.87	-0.85	-0.80
	2	0.57	-	-	-0.18	0.39	0.18	0.71	0.70	0.66
	3	-0.49	-	-	-0.71	-0.12	-0.62	0.35	0.38	0.45
	4	0.35	-	-	0.59	0.25	-0.43	-0.04	-0.03	-0.08
	5	0.26	-	-	0.17	0.19	0.60	-0.24	-0.27	-0.23
Contribution from boundaries	RB	0.62	-	-	0.20	0.50	0.16	0.70	0.66	0.68
	NB	-	-	-	-	-	-	-	-	-
	NBQB	-	-	-	-	-	-	-	-	-
	GR	0.39	-	-	-0.18	0.66	0.12	0.82	0.82	0.78
	IN	0.75	-	-	-0.00	0.65	0.29	0.78	0.76	0.71
Contribution from recharge	RB	-0.90	-	-	-0.40	-0.68	-0.54	-0.48	-0.44	-0.39
	NB	-	-	-	-	-	-	-	-	-
	NBQB	-	-	-	-	-	-	-	-	-
	GR	-0.64	-	-	-0.35	-0.75	-0.24	-0.58	-0.57	-0.50
	IN	-0.77	-	-	-0.02	-0.70	-0.30	-0.78	-0.76	-0.71
Contribution from Tegelen	RB	1.00	-	-	0.51	0.75	0.48	0.32	0.30	0.19
	NB	-	-	-	-	-	-	-	-	-
	NBQB	-	-	-	-	-	-	-	-	-
	GR	0.51	-	-	1.00	0.25	0.25	-0.38	-0.40	-0.45
	IN	0.75	-	-	0.25	1.00	0.28	0.53	0.52	0.45
Contribution from hole	RB	0.48	-	-	0.25	0.28	1.00	-0.17	-0.21	-0.23
Movement brackish front	Top	0.32	-	-	-0.38	0.53	-0.17	1.00	1.00	0.98
	Middle	0.30	-	-	-0.40	0.52	-0.21	1.00	1.00	0.98
	Bottom	0.19	-	-	-0.45	0.45	-0.23	0.98	0.98	1.00

Table C.5: Monte Carlo analysis correlation matrix for Scenario Smart Well (part 1)

Scenario 3 Smart Well		Parameters					Contribution from boundaries					Contribution from recharge				
		1	2	3	4	5	RB	NB	NBQB	GR	IN	RB	NB	NBQB	GR	IN
Parameters	1	1.00	-0.86	0.03	-0.00	0.00	-0.86	-0.75	-0.87	-0.71	-0.97	0.84	0.75	0.88	0.62	0.97
	2	-0.86	1.00	-0.02	0.00	0.01	0.72	0.53	0.72	0.42	0.84	-0.69	-0.53	-0.73	-0.29	-0.83
	3	0.03	-0.02	1.00	0.01	0.00	-0.07	0.10	0.16	0.15	-0.19	0.46	-0.09	-0.15	0.23	0.18
	4	-0.00	0.00	0.01	1.00	0.00	0.11	-0.09	-0.08	-0.16	0.01	-0.14	0.08	0.08	-0.16	-0.02
	5	0.00	0.01	0.00	0.00	1.00	-0.07	0.06	-0.09	-0.08	0.04	-0.26	-0.06	0.05	-0.02	-0.05
Contribution from boundaries	RB	-0.86	0.72	-0.07	0.11	-0.07	1.00	0.71	0.86	0.58	0.85	-0.79	-0.71	-0.87	-0.60	-0.84
	NB	-0.75	0.53	0.10	-0.09	0.06	0.71	1.00	0.69	0.54	0.70	-0.61	-1.00	-0.71	-0.43	-0.71
	NBQB	-0.87	0.72	0.16	-0.08	-0.09	0.86	0.69	1.00	0.61	0.82	-0.64	-0.69	-1.00	-0.44	-0.82
	GR	-0.71	0.42	0.15	-0.16	-0.08	0.58	0.54	0.61	1.00	0.59	-0.49	-0.53	-0.62	-0.85	-0.61
	IN	-0.97	0.84	-0.19	0.01	0.04	0.85	0.70	0.82	0.59	1.00	-0.90	-0.70	-0.84	-0.57	-1.00
Contribution from recharge	RB	0.84	-0.69	0.46	-0.14	-0.26	-0.79	-0.61	-0.64	-0.49	-0.90	1.00	0.61	0.67	0.67	0.90
	NB	0.75	-0.53	-0.09	0.08	-0.06	-0.71	-1.00	-0.69	-0.53	-0.70	0.61	1.00	0.71	0.43	0.71
	NBQB	0.88	-0.73	-0.15	0.08	0.05	-0.87	-0.71	-1.00	-0.62	-0.84	0.67	0.71	1.00	0.46	0.84
	GR	0.62	-0.29	0.23	-0.16	-0.02	-0.60	-0.43	-0.44	-0.85	-0.57	0.67	0.43	0.46	1.00	0.60
	IN	0.97	-0.83	0.18	-0.02	-0.05	-0.84	-0.71	-0.82	-0.61	-1.00	0.90	0.71	0.84	0.60	1.00
Contribution from Tegelen	RB	-0.64	0.52	-0.55	0.37	0.29	0.49	0.38	0.35	0.31	0.73	-0.89	-0.38	-0.38	-0.60	-0.74
	NB	-0.05	0.05	-0.25	0.12	0.09	0.20	0.03	0.00	-0.04	0.13	-0.22	-0.04	-0.02	-0.12	-0.12
	NBQB	-0.72	0.60	-0.00	0.01	0.37	0.65	0.64	0.62	0.48	0.72	-0.71	-0.64	-0.68	-0.48	-0.74
	GR	0.11	-0.20	-0.70	0.59	0.18	0.07	-0.15	-0.27	-0.19	0.02	-0.38	0.14	0.25	-0.35	-0.02
	IN	-0.67	0.36	0.04	0.15	0.20	0.46	0.55	0.52	0.69	0.61	-0.60	-0.55	-0.55	-0.70	-0.66
Contribution from hole	RB	-0.21	0.17	-0.59	-0.46	0.61	0.05	0.16	0.03	0.10	0.31	-0.52	-0.16	-0.07	-0.20	-0.31
Movement brackish front	Top	-0.82	0.68	0.44	-0.08	-0.26	0.74	0.67	0.84	0.78	0.69	-0.41	-0.67	-0.84	-0.49	-0.70
	Middle	-0.79	0.66	0.47	-0.07	-0.29	0.69	0.61	0.81	0.78	0.65	-0.36	-0.61	-0.80	-0.48	-0.66
	Bottom	-0.74	0.61	0.54	-0.15	-0.23	0.69	0.63	0.82	0.74	0.60	-0.31	-0.63	-0.82	-0.41	-0.61

Table C.6: Monte Carlo analysis correlation matrix for Scenario Smart Well (part 2)

Scenario 1 1970 - 1980		Contribution from Tegelen					Contribution from hole	Movement brackish front		
		RB	NB	NBQB	GR	IN	RB	Top	Middle	Bottom
Parameters	1	-0.64	-0.05	-0.72	0.11	-0.67	-0.21	-0.82	-0.79	-0.74
	2	0.52	0.05	0.60	-0.20	0.36	0.17	0.68	0.66	0.61
	3	-0.55	-0.25	-0.00	-0.70	0.04	-0.59	0.44	0.47	0.54
	4	0.37	0.12	0.01	0.59	0.15	-0.46	-0.08	-0.07	-0.15
	5	0.29	0.09	0.37	0.18	0.20	0.61	-0.26	-0.29	-0.23
Contribution from boundaries	RB	0.49	0.20	0.65	0.07	0.46	0.05	0.74	0.69	0.69
	NB	0.38	0.03	0.64	-0.15	0.55	0.16	0.67	0.61	0.63
	NBQB	0.35	0.00	0.62	-0.27	0.52	0.03	0.84	0.81	0.82
	GR	0.31	-0.04	0.48	-0.19	0.69	0.10	0.78	0.78	0.74
	IN	0.73	0.13	0.72	0.02	0.61	0.31	0.69	0.65	0.60
Contribution from recharge	RB	-0.89	-0.22	-0.71	-0.38	-0.60	-0.52	-0.41	-0.36	-0.31
	NB	-0.38	-0.04	-0.64	0.14	-0.55	-0.16	-0.67	-0.61	-0.63
	NBQB	-0.38	-0.02	-0.68	0.25	-0.55	-0.07	-0.84	-0.80	-0.82
	GR	-0.60	-0.12	-0.48	-0.35	-0.70	-0.20	-0.49	-0.48	-0.41
	IN	-0.74	-0.12	-0.74	-0.02	-0.66	-0.31	-0.70	-0.66	-0.61
Contribution from Tegelen	RB	1.00	0.18	0.54	0.57	0.59	0.48	0.15	0.12	0.01
	NB	0.18	1.00	0.12	0.30	-0.07	0.07	-0.11	-0.12	-0.11
	NBQB	0.54	0.12	1.00	0.04	0.69	0.37	0.51	0.46	0.49
	GR	0.57	0.30	0.04	1.00	0.09	0.21	-0.48	-0.50	-0.57
	IN	0.59	-0.07	0.69	0.09	1.00	0.23	0.55	0.53	0.49
Contribution from hole	RB	0.48	0.07	0.37	0.21	0.23	1.00	-0.22	-0.27	-0.25
Movement brackish front	Top	0.15	-0.11	0.51	-0.48	0.55	-0.22	1.00	1.00	0.98
	Middle	0.12	-0.12	0.46	-0.50	0.53	-0.27	1.00	1.00	0.98
	Bottom	0.01	-0.11	0.49	-0.57	0.49	-0.25	0.98	0.98	1.00

Table C.7: Monte Carlo analysis correlation matrix for Scenario full-scale (part 1)

Scenario 4 full-scale		Parameters					Contribution from boundaries					Contribution from recharge				
		1	2	3	4	5	RB	NB	NBQB	GR	IN	RB	NB	NBQB	GR	IN
Parameters	1	1.00	-0.86	0.03	-0.00	0.00	-0.78	-0.93	-0.39	-0.56	-0.89	0.84	0.94	0.80	0.44	0.91
	2	-0.86	1.00	-0.02	0.00	0.01	0.66	0.69	0.33	0.21	0.76	-0.69	-0.70	-0.64	-0.05	-0.76
	3	0.03	-0.02	1.00	0.01	0.00	0.22	0.16	0.25	0.26	-0.37	0.44	-0.07	-0.06	0.12	0.33
	4	-0.00	0.00	0.01	1.00	0.00	0.03	0.00	-0.14	-0.18	0.04	-0.12	-0.04	0.02	-0.16	-0.03
	5	0.00	0.01	0.00	0.00	1.00	-0.24	-0.02	-0.39	-0.08	0.14	-0.27	-0.02	0.06	-0.05	-0.16
Contribution from boundaries	RB	-0.78	0.66	0.22	0.03	-0.24	1.00	0.86	0.54	0.56	0.54	-0.57	-0.83	-0.64	-0.40	-0.56
	NB	-0.93	0.69	0.16	0.00	-0.02	0.86	1.00	0.40	0.69	0.76	-0.74	-0.99	-0.74	-0.55	-0.79
	NBQB	-0.39	0.33	0.25	-0.14	-0.39	0.54	0.40	1.00	0.65	0.09	-0.13	-0.36	-0.77	-0.43	-0.10
	GR	-0.56	0.21	0.26	-0.18	-0.08	0.56	0.69	0.65	1.00	0.29	-0.37	-0.66	-0.78	-0.83	-0.34
	IN	-0.89	0.76	-0.37	0.04	0.14	0.54	0.76	0.09	0.29	1.00	-0.92	-0.81	-0.57	-0.36	-1.00
Contribution from recharge	RB	0.84	-0.69	0.44	-0.12	-0.27	-0.57	-0.74	-0.13	-0.37	-0.92	1.00	0.80	0.63	0.53	0.92
	NB	0.94	-0.70	-0.07	-0.04	-0.02	-0.83	-0.99	-0.36	-0.66	-0.81	0.80	1.00	0.74	0.57	0.84
	NBQB	0.80	-0.64	-0.06	0.02	0.06	-0.64	-0.74	-0.77	-0.78	-0.57	0.63	0.74	1.00	0.65	0.60
	GR	0.44	-0.05	0.12	-0.16	-0.05	-0.40	-0.55	-0.43	-0.83	-0.36	0.53	0.57	0.65	1.00	0.39
	IN	0.91	-0.76	0.33	-0.03	-0.16	-0.56	-0.79	-0.10	-0.34	-1.00	0.92	0.84	0.60	0.39	1.00
Contribution from Tegelen	RB	-0.52	0.40	-0.64	0.40	0.34	0.08	0.36	-0.15	0.07	0.75	-0.83	-0.45	-0.37	-0.43	-0.74
	NB	-0.48	0.37	-0.61	0.32	0.33	0.13	0.35	-0.17	0.03	0.73	-0.78	-0.46	-0.30	-0.38	-0.72
	NBQB	-0.78	0.61	-0.20	0.13	0.36	0.36	0.68	0.01	0.44	0.79	-0.83	-0.73	-0.65	-0.51	-0.81
	GR	0.17	-0.28	-0.65	0.58	0.23	-0.25	-0.21	-0.34	-0.23	0.13	-0.31	0.13	0.17	-0.35	-0.11
	IN	-0.48	0.21	0.40	-0.15	0.23	0.39	0.58	0.17	0.67	0.25	-0.28	-0.56	-0.50	-0.49	-0.33
Contribution from hole	RB	-0.17	0.14	-0.52	-0.53	0.62	-0.22	0.04	-0.27	0.01	0.39	-0.45	-0.09	-0.08	-0.08	-0.40
Movement brackish front	Top	-0.70	0.57	0.59	-0.16	-0.28	0.77	0.77	0.61	0.70	0.33	-0.24	-0.71	-0.68	-0.29	-0.38
	Middle	-0.61	0.51	0.65	-0.16	-0.36	0.73	0.69	0.64	0.66	0.21	-0.12	-0.61	-0.63	-0.24	-0.25
	Bottom	-0.63	0.52	0.65	-0.23	-0.26	0.70	0.71	0.60	0.69	0.25	-0.16	-0.64	-0.65	-0.25	-0.29

Table C.8: Monte Carlo analysis correlation matrix for Scenario full-scale (part 2)

Scenario 4 full-scale		Contribution from Tegelen					Contribution from hole	Movement brackish front		
		RB	NB	NBQB	GR	IN	RB	Top	Middle	Bottom
Parameters	1	-0.52	-0.48	-0.78	0.17	-0.48	-0.17	-0.70	-0.61	-0.63
	2	0.40	0.37	0.61	-0.28	0.21	0.14	0.57	0.51	0.52
	3	-0.64	-0.61	-0.20	-0.65	0.40	-0.52	0.59	0.65	0.65
	4	0.40	0.32	0.13	0.58	-0.15	-0.53	-0.16	-0.16	-0.23
	5	0.34	0.33	0.36	0.23	0.23	0.62	-0.28	-0.36	-0.26
Contribution from boundaries	RB	0.08	0.13	0.36	-0.25	0.39	-0.22	0.77	0.73	0.70
	NB	0.36	0.35	0.68	-0.21	0.58	0.04	0.77	0.69	0.71
	NBQB	-0.15	-0.17	0.01	-0.34	0.17	-0.27	0.61	0.64	0.60
	GR	0.07	0.03	0.44	-0.23	0.67	0.01	0.70	0.66	0.69
	IN	0.75	0.73	0.79	0.13	0.25	0.39	0.33	0.21	0.25
Contribution from recharge	RB	-0.83	-0.78	-0.83	-0.31	-0.28	-0.45	-0.24	-0.12	-0.16
	NB	-0.45	-0.46	-0.73	0.13	-0.56	-0.09	-0.71	-0.61	-0.64
	NBQB	-0.37	-0.30	-0.65	0.17	-0.50	-0.08	-0.68	-0.63	-0.65
	GR	-0.43	-0.38	-0.51	-0.35	-0.49	-0.08	-0.29	-0.24	-0.25
	IN	-0.74	-0.72	-0.81	-0.11	-0.33	-0.40	-0.38	-0.25	-0.29
Contribution from Tegelen	RB	1.00	0.89	0.75	0.64	0.03	0.43	-0.19	-0.30	-0.27
	NB	0.89	1.00	0.67	0.62	0.05	0.42	-0.20	-0.31	-0.28
	NBQB	0.75	0.67	1.00	0.14	0.57	0.45	0.34	0.23	0.30
	GR	0.64	0.62	0.14	1.00	-0.28	0.12	-0.67	-0.71	-0.73
	IN	0.03	0.05	0.57	-0.28	1.00	0.15	0.63	0.57	0.63
Contribution from hole	RB	0.43	0.42	0.45	0.12	0.15	1.00	-0.27	-0.37	-0.26
Movement brackish front	Top	-0.19	-0.20	0.34	-0.67	0.63	-0.27	1.00	0.99	0.99
	Middle	-0.30	-0.31	0.23	-0.71	0.57	-0.37	0.99	1.00	0.99
	Bottom	-0.27	-0.28	0.30	-0.73	0.63	-0.26	0.99	0.99	1.00

D

Alternative top system: DRN instead of GHB

Unfortunately, during the modeling process a mistake has been made. A mistake is made with regards to the phreatic aquifer and the recharge of the phreatic aquifer. When importing the model input from Triwaco the drain resistance is mistakingly interpreted as the drain conductance. Also, the drains in the Triwaco Model are able to add water to the aquifer. Thus, the drain package is incorrectly used. The General Head Boundary (GHB) should have been used in the model. This mistake has been made when construction the flow and transport model (± January 2016) and had not been found until halfway through June 2016.

The Drain package is replaced by the General Head Boundary. Using the General Head Boundary, water can be added and taken away from the aquifer instead of just taking water away (the purpose of the Drain package, see Appendix B). The Drain resistance from the Triwaco parameter input is used to calculated the conductance for the General Head Boundary.

The consequence of using the Drain package is that no water is added to the aquifer. Also, the resistance is used as conductance. The result of this misinterpretation is that areas with a high resistance have a high conductance, which when interpreted correctly, should have resulted into a low conductance. The conductance determines the resistance to flow. Therefore, the entire analysis is repeated. The complete analysis with the Drain package had already been conducted.

The entire methodology for this analysis is presented in the main report, and execution of the analysis is preformed similar to the analysis when using the General Head Boundary.

D.1. Parameter estimation

The optimal values from the calibration and the corresponding confidence interval boundaries are given in Table D.1. The calibration results from the parameters semi-confining layer, Tegelen clay and second aquifer are not considered to be reliable. The optimal values and variance from the calibration results will be changed to prior knowledge or measurements results (see Table D.2). The corresponding covariance and correlations of the changed parameters will be set to zero (uncorrelated). The adjusted parameters are used in further analysis.

Table D.1: Optimal values of the Parameters

Name	Parameter number	Unit	Factor	Optimal Value	95% Confidence Interval
Recharge	1	$[-]$	Yes	0.888	$^{1.442}_{0.547}$
Semi-confining Layer	2	$[-]$	Yes	0.333	$^{2.940}_{0.038}$
First Aquifer	3	$[m^2/d]$	No	5,566	$^{15,344}_{2,019}$
Tegelen clay	4	$[d]$	No	722	$^{180,702}_{3}$
Second Aquifer	5	$[m^2/d]$	No	23,448	$^{7,572,290}_{73}$

Table D.2: Adjusted values of the Parameters

Name	Parameter number	Unit	Factor	Optimal Value	95% Confidence Interval
Recharge	1	$[-]$	Yes	0.888	$^{1.442}_{0.547}$
Semi-confining Layer	2	$[-]$	Yes	0.333	$^{2.940}_{0.038}$
First Aquifer	3	$[m^2/d]$	No	5,566	$^{15,344}_{2,019}$
Tegelen clay	4	$[d]$	No	1,300	$^{2,600}_{650}$
Second Aquifer	5	$[m^2/d]$	No	2,500	$^{5,000}_{1,250}$

D.2. Linearized propagation of variance

Chloride analysis

This analysis is conducted for the four different initial chloride distributions. The results are shown in Table D.4, where the mean value of the chloride concentration with the corresponding uncertainty intervals origination from parameter uncertainty is presented: Mean value $^{\text{95\% confidence interval maximum value}}_{\text{95\% confidence interval minimum value}}$.

van der Valk (2011) tried to match his model to observed chloride concentration at Ritskebos. He tried to achieve this by posing a constant concentration at the hole in Tegelen clay. Also, he assumed the hole in Tegelen clay is along the entire length of the glacial tunnel valley. Directly below this imposed constant concentration at the hole in the Tegelen clay the chloride concentration of the groundwater is assumed to be near 10 g L^{-1}. This is the deduction why the distribution from Mark shows an unrealistic expected concentration and small confidence width at the Hole in the Tegelen clay, compared to the other distributions.

- **Noardburgum [NB]**
  Results show that scenario 1 is the unsustainable scenario with regards to chloride concentration. The highest chloride concentrations are observed in scenario 1. The different initial distribution show there is an high probability the 0.15 g/L will be exceeded in scenario 1. The initial distribution A and B show that the full-scale design of Noardburgum will have no problems with salinization. It is also expected that the brackish extraction can be increased if problems with salinization occur, thus it is not expected that salinization will occur in Noardburgum.

- **Ritskebos [RB]**
  The different distributions show there is a high probility that Ritskebos will suffer from salization in scenario 1. furthermore, All initial distributions show that there is a clear increase in chloride concen-

tration with the development of the Noardburgum well field. However, the initial distributions A and B indicate that the chloride concentration will be below the 0.15 g L^{-1}.

- **Hole in Tegelen clay [Hole]**
  Large differences are observed between the different initial distributions. All distributions show that scenario 1 has the highest chloride concentration of the scenarios. Without extraction at Noardburgum the lowest chloride concentration is observed. All distributions show (except Mark) the concentration at the hole in the Tegelen clay is subjected to high uncertainty.

Renewability and vulnerability

The results from the linearized propagation of variance analysis are shown in Table D.5. The results show the different sources of the extracted water and are presented as the percentage of contribution to the total extraction (100%) at the specified station. The results immediately show the drawback of the linearized propagation of variance . The drawback is most obvious with the NBQB (Noardburgum brackish extraction). The linearization cannot account for non linearity, and it approximates the partial derivative in a single point. Thus, it can lead to negative values, or values larger than the extraction, which cannot be true. The results are presented with the mean value and the 95% confidence interval boundaries in the following manner: Mean value $^{\text{95\% confidence interval maximum value}}_{\text{95\% confidence interval minimum value}}$.

- **Noardburgum [NB]**
  The results presented in Table 5.5 indicate differences between the different scenarios with regards to the origin of the extracted groundwater. The first scenario, which is considered unsustainable due to high extractions, shows large contributions from sources with high chloride concentration. Also, in the full-scale design the brackish extraction [NBQB] seems to mainly attract from sources with a high chloride concentration, which is the main purpose of the brackish extraction.

  Results do show there is a influence from the Smart Well, and an even greater influence from the full-scale design. The results indicate that the development of the Noardburgum area has an influence on the Ritskebos well field. The influence on the Garyp well field and the Industrial extraction is rather limited. It does show that the full-scale design has an influence on the movement of the brackish front.

- **Ritskebos [RB]**
  Model results shows that only the well field of Ritskebos is receiving water from the second aquifer through the hole in the Tegelen clay. It can be seen that the development of the Noardburgum area influences the contribution of the hole in the Tegelen clay at the Ritskebos extraction.

- **Garyp [GR]**
  The effects of the Noardburgum Well field seems limited in the different scenarios. The extraction from recharge is significantly less than the other stations. The main origin of the extracted water is the Extraction from the boundaries.

- **Industry [IN]**
  Almost all the extracted water originates from recharge. The contribution from water originating from the second aquifer in the form of seepage through the Tegelen clay is almost negligible. It shows that the development of the Noardburgum area has no significant influence on the industrial extraction.

D.3. Monte Carlo analysis

The parameter set created with the multivariate gaussian distribution is used in the Monte Carlo analysis. The model results is used to construct a probability density function. From this function the expected outcome (the 50^{th} percentile) and the confidence intervals (2.5 and 97.5 percentile) are determined. The results of the Monte Carlo analysis are shown in Table D.6.

By comparing Table D.5 and Table D.6 it can be seen the expected value and uncertainty are quite similar. The linearized propagation of variance appears to be a good estimation for model results and uncertainty.

Table D.3: Probability 0.15 g L^{-1} chloride limit will be exceeded

	Distribution B		Distribution A		Siebren		Mark	
	NB	RB	NB	RB	NB	RB	NB	RB
Scenario 1	50%	64%	52%	42%	53%	95%	68%	100%
Scenario 2	-	0%	-	0%	-	93%	-	100%
Scenario 3	0%	0%	0%	0%	16%	94%	0%	100%
Scenario 4	0%	2%	0%	0%	49%	96%	91%	100%

Table D.4: Results from the linearized propagation of variance for chloride content in [g L^{-1}]

	Location:	Scenario 1 1970 - 1980	Scenario 2 2007 - 2010	Scenario 3 Single Smart Well	Scenario 4 Full-scale design
Distribution B	NB	$0.1499^{0.2176}_{0.0822}$	$0.0687^{0.0695}_{0.0679}$	$0.0700^{0.0711}_{0.0688}$	$0.0793^{0.0905}_{0.0680}$
	RB	$0.1700^{0.2783}_{0.0617}$	$0.0972^{0.1202}_{0.0743}$	$0.1047^{0.1324}_{0.0770}$	$0.1138^{0.1476}_{0.0801}$
	Hole	$2.2098^{2.6234}_{1.7961}$	$1.5103^{1.9687}_{1.0519}$	$1.5756^{2.0314}_{1.1198}$	$1.7588^{2.1941}_{1.3236}$
Distribution A	NB	$0.1512^{0.2099}_{0.0925}$	$0.0642^{0.0674}_{0.0609}$	$0.0671^{0.0701}_{0.0641}$	$0.0771^{0.0870}_{0.0673}$
	RB	$0.1394^{0.2394}_{0.0395}$	$0.0869^{0.0968}_{0.0770}$	$0.0917^{0.1034}_{0.0801}$	$0.0921^{0.1084}_{0.0757}$
	Hole	$1.7031^{2.5335}_{0.8726}$	$0.7418^{1.1659}_{0.3176}$	$0.7998^{1.2575}_{0.3420}$	$0.9814^{1.5114}_{0.4513}$
van der Linde (2014)	NB	$0.1548^{0.3005}_{0.0091}$	$0.0792^{0.1435}_{0.0149}$	$0.1004^{0.1997}_{0.0011}$	$0.1475^{0.3187}_{-0.0237}$
	RB	$0.3319^{0.5432}_{0.1206}$	$0.2908^{0.4751}_{0.1065}$	$0.2971^{0.4817}_{0.1126}$	$0.3142^{0.4993}_{0.1291}$
	Hole	$4.4015^{4.6856}_{4.1174}$	$3.9578^{4.4551}_{3.4606}$	$3.9706^{4.503}_{3.4383}$	$3.9173^{4.5309}_{3.3037}$
van der Valk (2011)	NB	$0.1761^{0.2850}_{0.0672}$	$0.0951^{0.1002}_{0.0901}$	$0.1328^{0.1435}_{0.1222}$	$0.1676^{0.1928}_{0.1424}$
	RB	$0.5527^{0.7795}_{0.3259}$	$0.4544^{0.5483}_{0.3682}$	$0.4639^{0.5483}_{0.3794}$	$0.4897^{0.5741}_{0.4053}$
	Hole	$9.7963^{9.9226}_{9.6701}$	$9.7372^{9.7453}_{9.7291}$	$9.7440^{9.7513}_{9.7368}$	$9.7644^{9.7696}_{9.7588}$

Table D.5: Results from the linearized propagation of variance

	Location:	Scenario 1 1970 - 1980	Scenario 2 2007 - 2010	Scenario 3 Single Smart Well	Scenario 4 Full-scale design
Contribution from recharge	RB	51.6% $^{69.9\%}_{33.4\%}$	72.8% $^{86.7\%}_{58.9\%}$	70.5% $^{81.2\%}_{59.8\%}$	63.8% $^{79.5\%}_{48.0\%}$
	NB	55.0% $^{71.0\%}_{38.9\%}$	-	98.2% $^{119.8\%}_{76.6\%}$	95.0% $^{112.0\%}_{78.0\%}$
	NBQB	-	-	70.0% $^{195.0\%}_{-55.0\%}$	15.4% $^{45.5\%}_{-14.6\%}$
	GR	-	44.3% $^{53.8\%}_{34.8\%}$	44.0% $^{65.6\%}_{22.3\%}$	43.1% $^{68.6\%}_{17.7\%}$
	IN	-	84.5% $^{108.1\%}_{60.9\%}$	84.6% $^{96.1\%}_{73.1\%}$	89.8% $^{123.3\%}_{56.3\%}$
Contribution from Tegelen	RB	14.6% $^{22.2\%}_{7.0\%}$	7.7% $^{15.5\%}_{-0.2\%}$	9.2% $^{17.8\%}_{0.6\%}$	13.5% $^{23.5\%}_{3.4\%}$
	NB	8.8% $^{16.9\%}_{0.7\%}$	-	0.0% $^{0.0\%}_{0.0\%}$	0.7% $^{3.0\%}_{-1.6\%}$
	NBQB	-	-	10.5% $^{18.6\%}_{2.5\%}$	35.8% $^{56.5\%}_{15.1\%}$
	GR	-	5.1% $^{9.8\%}_{0.4\%}$	5.1% $^{10.3\%}_{-0.1\%}$	5.0% $^{9.7\%}_{0.4\%}$
	IN	-	1.4% $^{2.7\%}_{0.6\%}$	0.7% $^{2.6\%}_{-1.2\%}$	0.8% $^{2.8\%}_{-1.3\%}$
Contribution from hole	RB	6.8% $^{12.8\%}_{0.8\%}$	4.1% $^{7.7\%}_{0.5\%}$	4.5% $^{8.3\%}_{0.6\%}$	5.6% $^{10.2\%}_{1.1\%}$
	NB	0.0% $^{0.0\%}_{0.0\%}$	-	0.0% $^{0.0\%}_{0.0\%}$	0.0% $^{0.0\%}_{0.0\%}$
	NBQB	-	-	0.0% $^{0.0\%}_{0.0\%}$	0.0% $^{0.0\%}_{0.0\%}$
	GR	-	0.0% $^{0.0\%}_{0.0\%}$	0.0% $^{0.0\%}_{0.0\%}$	0.0% $^{0.0\%}_{0.0\%}$
	IN	-	0.0% $^{0.0\%}_{0.0\%}$	0.0% $^{0.0\%}_{0.0\%}$	0.0% $^{0.0\%}_{0.0\%}$
Contribution from boundaries	RB	27.0% $^{38.5\%}_{15.5\%}$	15.4% $^{22.4\%}_{8.5\%}$	15.9% $^{20.5\%}_{11.2\%}$	17.1% $^{26.7\%}_{7.6\%}$
	NB	36.2% $^{51.5\%}_{21.0\%}$	-	1.8% $^{23.4\%}_{-19.8\%}$	4.3% $^{21.8\%}_{-13.2\%}$
	NBQB	-	-	19.4% $^{151.8\%}_{-112.9\%}$	48.8% $^{78.3\%}_{19.2\%}$
	GR	-	50.5% $^{56.6\%}_{44.5\%}$	50.9% $^{70.0\%}_{31.8\%}$	51.8% $^{75.2\%}_{28.4\%}$
	IN	-	14.8% $^{38.7\%}_{-9.0\%}$	14.7% $^{27.9\%}_{1.5\%}$	9.4% $^{44.0\%}_{-25.2\%}$
Movement of the brackish front $[m]$	Top layer	2,071 $^{2,227}_{1,915}$	110 $^{358}_{-137}$	227 $^{504}_{-50}$	623 $^{977}_{269}$
	Middle Layer	1,816 $^{1,975}_{1,657}$	106 $^{298}_{-85}$	201 $^{412}_{-10}$	538 $^{815}_{261}$
	Bottom layer	2,167 $^{2,782}_{1,553}$	183 $^{472}_{-106}$	334 $^{686}_{-17}$	857 $^{1,253}_{460}$

Table D.6: Results from the Monte Carlo analysis

	Location:	Scenario 1 1970 - 1980	Scenario 2 2007 - 2010	Scenario 3 Single Smart Well	Scenario 4 Full-scale design
Contribution from recharge	RB	$50.2\%^{65.8\%}_{32.1\%}$	$72.6\%^{83.0\%}_{53.9\%}$	$69.5\%^{80.4\%}_{49.3\%}$	$63.2\%^{76.3\%}_{41.4\%}$
	NB	$53.4\%^{68.7\%}_{38.2\%}$	-	$98.2\%^{99.9\%}_{93.3\%}$	$91.9\%^{97.8\%}_{70.3\%}$
	NBQB	-	-	$74.7\%^{95.1\%}_{0.0\%}$	$7.1\%^{47.7\%}_{0.0\%}$
	GR	-	$37.7\%^{58.0\%}_{19.5\%}$	$37.5\%^{57.7\%}_{19.4\%}$	$36.8\%^{56.9\%}_{18.6\%}$
	IN	-	$84.2\%^{91.1\%}_{64.5\%}$	$84.7\%^{92.0\%}_{65.7\%}$	$87.6\%^{95.1\%}_{69.2\%}$
Contribution from Tegelen	RB	$14.6\%^{24.0\%}_{6.9\%}$	$8.2\%^{17.4\%}_{2.8\%}$	$9.9\%^{20.7\%}_{3.8\%}$	$14.1\%^{27.5\%}_{6.9\%}$
	NB	$9.1\%^{19.2\%}_{3.8\%}$	-	$0.0\%^{0.0\%}_{0.0\%}$	$0.7\%^{2.4\%}_{0.1\%}$
	NBQB	-	-	$7.7\%^{14.2\%}_{3.6\%}$	$38.3\%^{58.8\%}_{24.0\%}$
	GR	-	$4.5\%^{12.1\%}_{0.9\%}$	$4.5\%^{11.8\%}_{1.0\%}$	$4.3\%^{10.7\%}_{1.2\%}$
	IN	-	$0.6\%^{3.0\%}_{0.0\%}$	$0.6\%^{2.8\%}_{0.0\%}$	$0.5\%^{2.3\%}_{0.0\%}$
Contribution from hole	RB	$6.9\%^{14.3\%}_{2.4\%}$	$4.2\%^{8.8\%}_{1.5\%}$	$4.6\%^{9.4\%}_{1.6\%}$	$5.7\%^{11.3\%}_{2.2\%}$
	NB	$0.0\%^{0.0\%}_{0.0\%}$	-	$0.0\%^{0.0\%}_{0.0\%}$	$0.0\%^{0.0\%}_{0.0\%}$
	NBQB	-	-	$0.0\%^{0.0\%}_{0.0\%}$	$0.0\%^{0.0\%}_{0.0\%}$
	GR	-	$0.0\%^{0.0\%}_{0.0\%}$	$0.0\%^{0.0\%}_{0.0\%}$	$0.0\%^{0.0\%}_{0.0\%}$
	IN	-	$0.0\%^{0.0\%}_{0.0\%}$	$0.0\%^{0.0\%}_{0.0\%}$	$0.0\%^{0.0\%}_{0.0\%}$
Contribution from boundaries	RB	$27.4\%^{39.5\%}_{18.5\%}$	$14.5\%^{24.7\%}_{9.6\%}$	$15.6\%^{26.6\%}_{10.3\%}$	$16.2\%^{29.0\%}_{9.7\%}$
	NB	$36.5\%^{52.4\%}_{22.2\%}$	-	$1.8\%^{6.2\%}_{0.0\%}$	$7.3\%^{27.5\%}_{1.6\%}$
	NBQB	-	-	$17.2\%^{87.9\%}_{0.0\%}$	$50.0\%^{69.8\%}_{18.0\%}$
	GR	-	$56.8\%^{73.7\%}_{38.8\%}$	$57.2\%^{74.3\%}_{39.4\%}$	$58.0\%^{75.9\%}_{39.8\%}$
	IN	-	$15.0\%^{31.7\%}_{8.6\%}$	$14.5\%^{31.1\%}_{7.8\%}$	$11.8\%^{28.4\%}_{4.7\%}$
Movement of the brackish front $[m]$	Top layer	$2,105^{2,338}_{1,735}$	167^{444}_{-36}	291^{613}_{53}	$684^{1,043}_{334}$
	Middle Layer	$1,830^{1,958}_{1,523}$	146^{339}_{-10}	245^{461}_{61}	557^{819}_{304}
	Bottom layer	$2,231^{2,485}_{1,929}$	243^{585}_{11}	412^{798}_{102}	$917^{1,285}_{473}$

E

Sensitivity Coefficients of the chloride transport analysis

The different sensitivity coefficient of the parameters, calculated using Equation 4.9, are presented in this Appendix. The sensitivity coefficient for the different initial distributions and different scenarios are presented. Note that the original parameters form Table 4.1 are scaled to 1.0. The parameters in the tables are not named, but numbered:

Recharge [Parameter 1]
Semi-confining layer [Parameter 2]
Aquifer 1 [Parameter 3]
Tegelen clay [Parameter 4]
Aquifer 2 [Parameter 5]

Table E.1: Sensitivity coefficients for the different scenarios and locations of the chloride transport analysis (part 1). Here: NB = Noardburgum, RB = Ritskebos, and Hole is the hole in the Tegelen clay

Initial Distribution: B					
Scenario 1 1970 - 1980					
Parameter	1	2	3	4	5
NB	-0.04	-0.05	-0.25	0.10	0.04
RB	-0.02	-0.05	-0.30	0.04	0.16
Hole	0.06	0.05	0.41	0.05	0.77
Scenario 2 2007 - 2010					
Parameter	1	2	3	4	5
NB	0.00	-0.00	0.00	-0.00	-0.00
RB	-0.02	-0.03	-0.10	0.03	0.04
Hole	-0.14	-0.09	-0.88	0.10	0.39
Scenario 3 Smart Well					
Parameter	1	2	3	4	5
NB	0.00	-0.01	-0.00	0.00	0.00
RB	-0.02	-0.03	-0.12	0.04	0.04
Hole	-0.12	-0.08	-0.82	0.09	0.41
Scenario 4 Full-scale					
Parameter	1	2	3	4	5
NB	-0.02	-0.02	-0.05	0.02	0.00
RB	-0.03	-0.04	-0.16	0.05	0.07
Hole	-0.08	-0.06	-0.62	0.06	0.45

Initial Distribution: A					
Scenario 1 1970 - 1980					
Parameter	1	2	3	4	5
NB	-0.04	-0.05	-0.22	0.09	0.04
RB	-0.02	-0.05	-0.30	0.04	0.18
Hole	0.04	0.03	0.14	0.05	1.04
Scenario 2 2007 - 2010					
Parameter	1	2	3	4	5
NB	0.01	0.00	0.00	-0.00	-0.00
RB	-0.01	-0.02	-0.05	0.02	0.03
Hole	-0.12	-0.08	-0.71	0.02	0.77
Scenario 3 Smart Well					
Parameter	1	2	3	4	5
NB	-0.01	-0.01	-0.02	0.01	0.00
RB	-0.00	-0.01	-0.02	0.01	0.01
Hole	-0.05	-0.03	-0.20	-0.08	0.27
Scenario 4 Full-scale					
Parameter	1	2	3	4	5
NB	-0.02	-0.02	-0.04	0.02	0.00
RB	-0.02	-0.03	-0.12	0.04	0.05
Hole	-0.09	-0.07	-0.60	-0.03	0.94

F

Smart Well measurements and electrical conductivity

Using the water quality data a correlation between the electrical conductivity and the chloride concentration is found: (see Figure F.1)

$$CL = 3.83\ EC - 215.49 \tag{F.1}$$

Where
CL Is the chloride concentration in mg/L,
EC Is the electrical conductivity in mS/m,

This relation can be used to connect the electrical conductivity measurements of the Smart Well to a chloride concentration. Also, for future reference, the variable discharge based on electrical conductivity or chloride measurements is presented:

$$Q = 0.03\ EC + 2 \tag{F.2}$$

$$Q = 0.00783\ CL + 3.96 \tag{F.3}$$

Where
Q Is the extraction rate of the brackish extraction $[L^3\ T^{-1}]$,

The measurement location of the electrical conductivity for the Smart Well is located at -136 meters below ground surface, while the well screen is located at -143 to -154 meters. Therefore, an 600 mS m^{-1} is assumed, based on difference between Figure F.3 and measurements from lab analysis at the same time, as maximum electrical conductivity of the brackish water. This equals a concentration of 2.1 g per liter chloride (see Equation F.1)

The extractions and Electrical conductivity measurements are presented in Figure F.2 and Figure F.3. It can be seen that the brackish extraction causes the electrical conductivity to decline over time. A period without extraction causes the electrical conductivity to rise again.

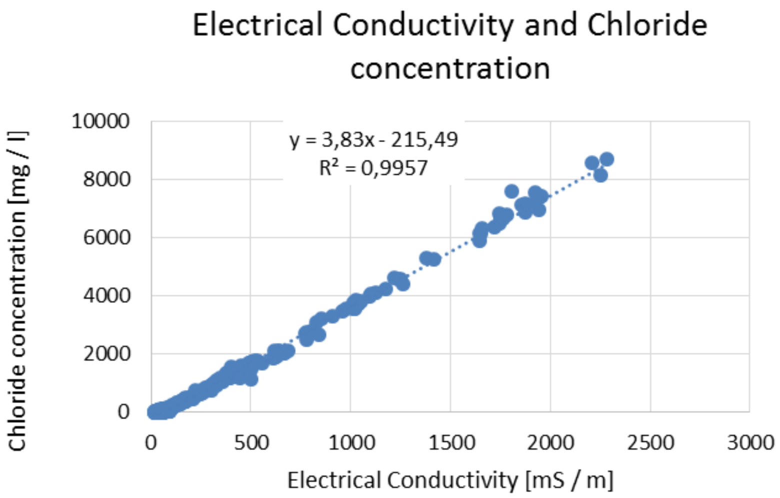

Figure F.1: Correlation between electrical conductivity and chloride concentration based on water quality measurements

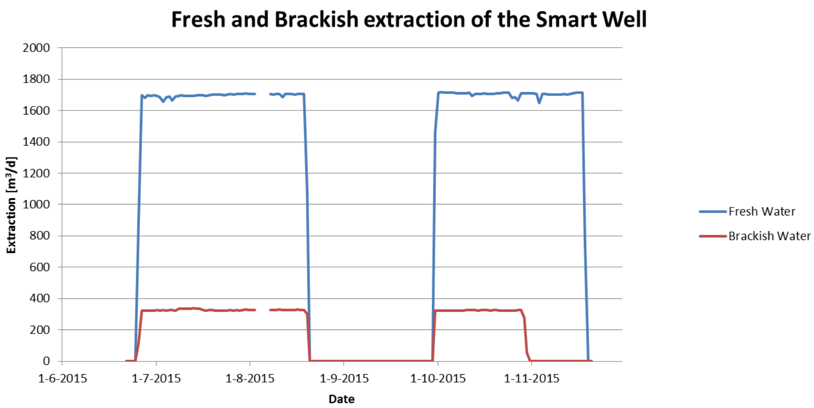

Figure F.2: The extractions of the Smart Well

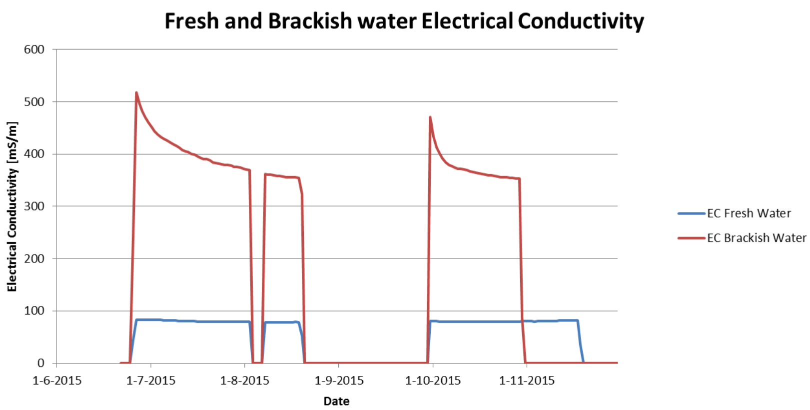

Figure F.3: The electrical conductivity measurements of the Smart Well

G

Comparison different initial chloride distributions

The different initial distributions are shown and compared to the conducted measurements. Also, cross-sections at different locations are shown, to visualize the differences between the initial distributions.

The dots in all presented Figures are scaled to the difference between observed and modeled chloride concentration. Positive indicates the modeled concentration is larger than the observed concentration. Negative indicates a larger observed concentration than modeled concentration.

A total of four different initial distributions are presented. The earlier presented distributions A and B, and the initial distributions created by van der Linde (2014) and van der Valk (2011). van der Linde (2014) continued with the Triwaco Model, and created a chloride distribution based on contour maps created by de Graaf et al. (2007) and the Triwaco inverse distance interpolator. van der Valk (2011) created the chloride distribution based on his cross-sectional model simulating historic salt water intrusion. First a top view of the first and second aquifer is given. Four different cross-section are also shown, since a top view cannot provide any information over the depth of the measurement in the aquifers.

Table G.1: Differences between the different initial chloride distributions compared to the chloride measurements (simulation - observation)

	Maximum difference [g/l]	Minimum difference [g/l]	Mean difference [g/l]	Absolute mean difference [g/l]	RMSE [g/l]
Distribution A	0.939	5.479	-0.050	0.081	0.40
Distribution B	1.444	5.479	-0.032	0.079	0.41
van der Linde (2014)	0.705	2.697	0.046	0.168	0.71
van der Valk (2011)	9.741	4.001	0.121	0.229	1.18

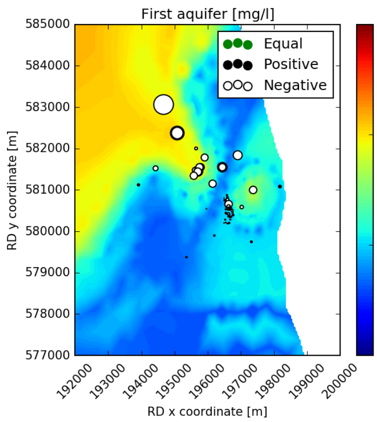

(a) First aquifer, distribution A

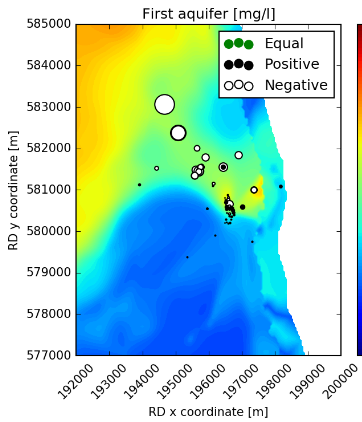

(b) First aquifer, distribution B

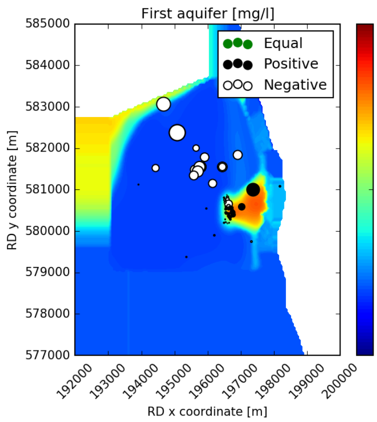

(c) First aquifer, initial distribution van der Linde (2014)

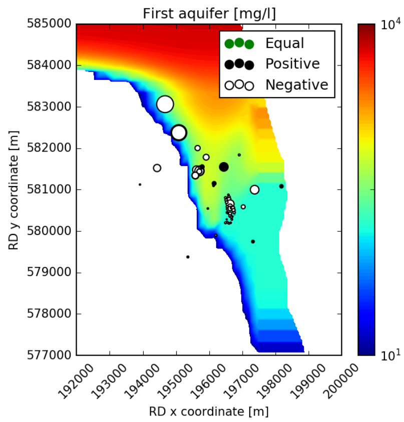

(d) First aquifer, initial distribution van der Valk (2011)

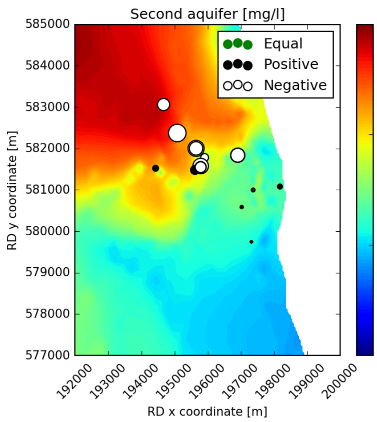

(e) Second aquifer, distribution A

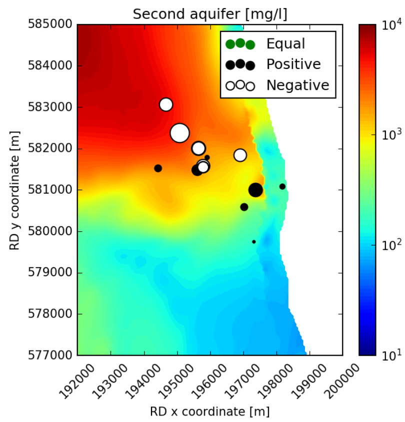

(f) Second aquifer, distribution B

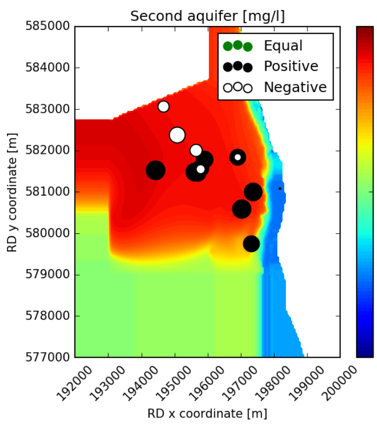

(g) Second aquifer, initial distribution van der Linde (2014)

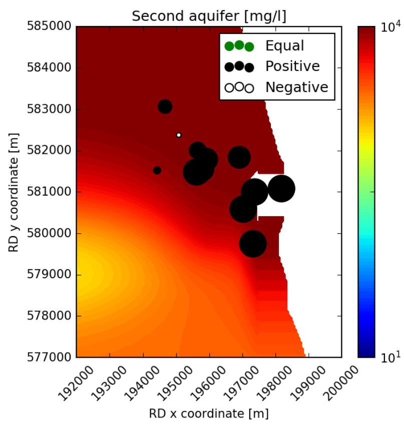

(h) Second aquifer, initial distribution van der Valk (2011)

Figure G.1: Top view of the first and second aquifer, comparing the different initial distribution to the measurements

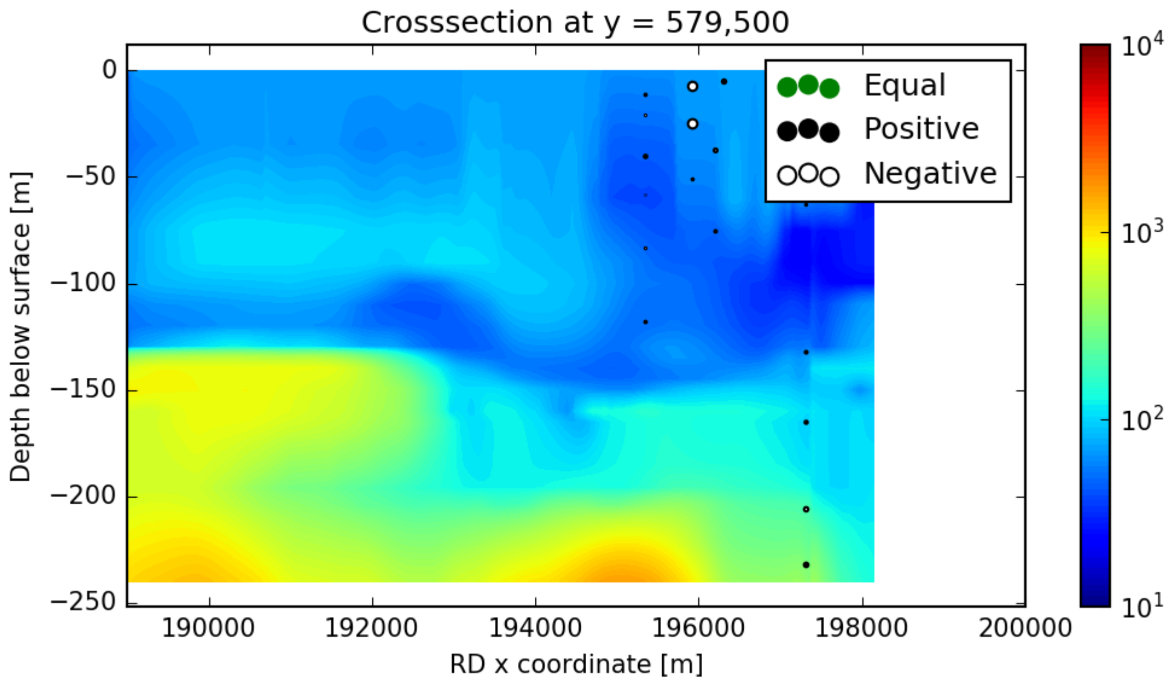

Figure G.2: Cross-section, created with distribution A

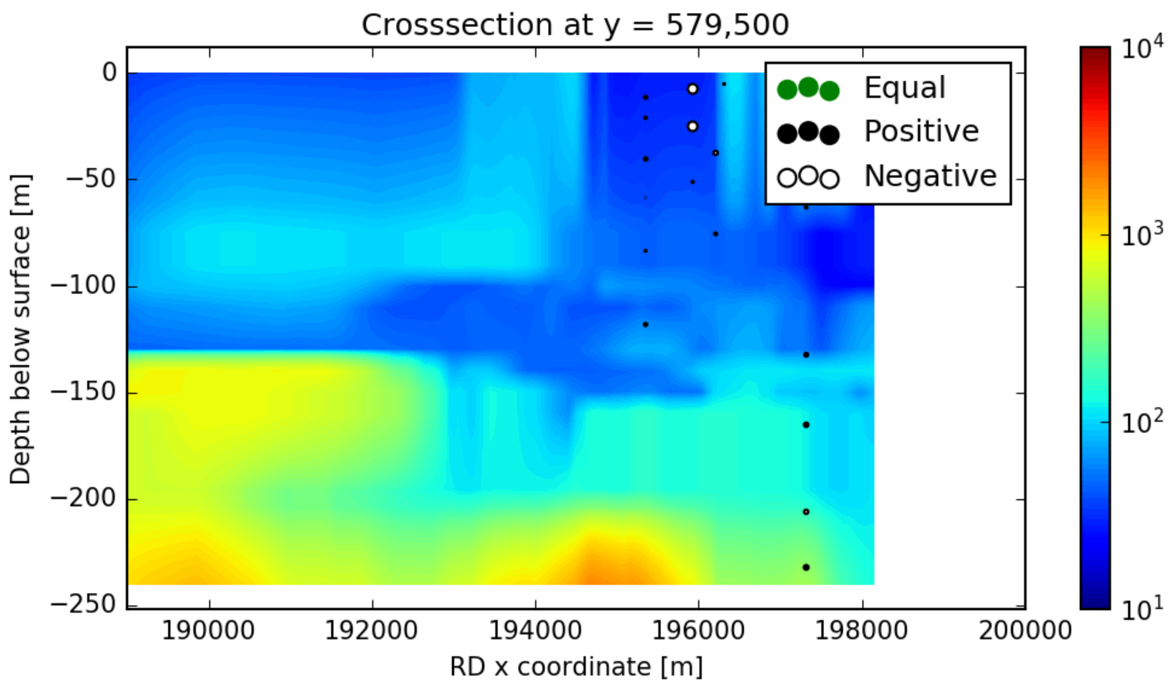

Figure G.3: Cross-section, created with distribution B

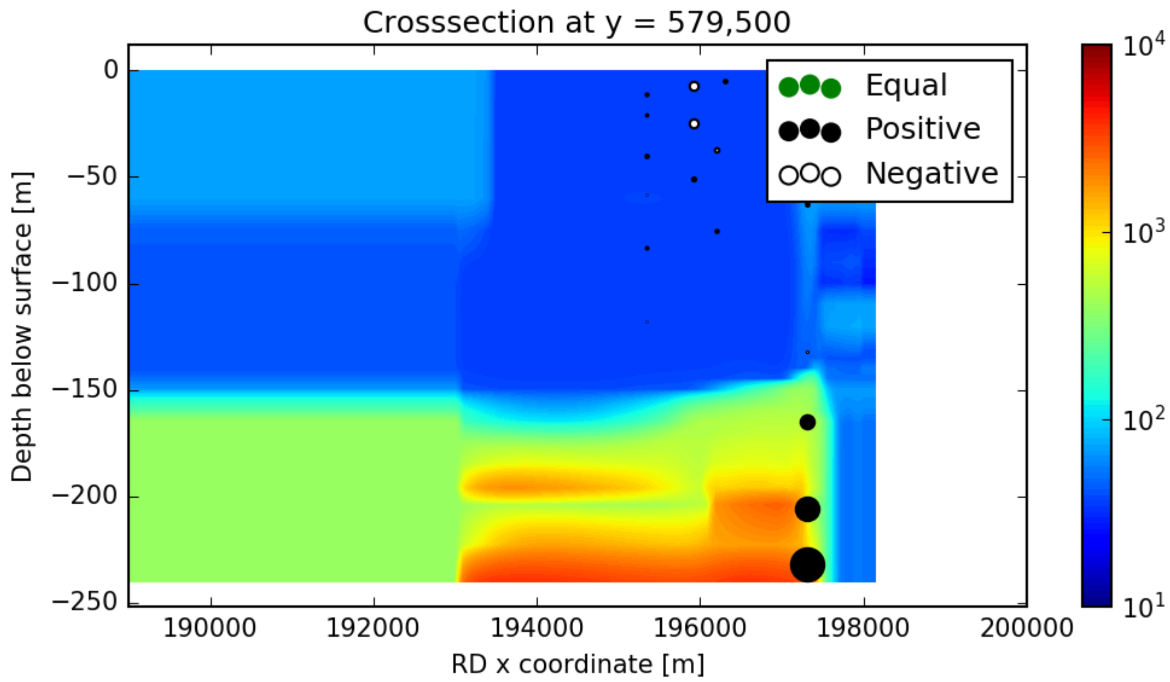

Figure G.4: Cross-section, created with the initial distribution van der Linde (2014)

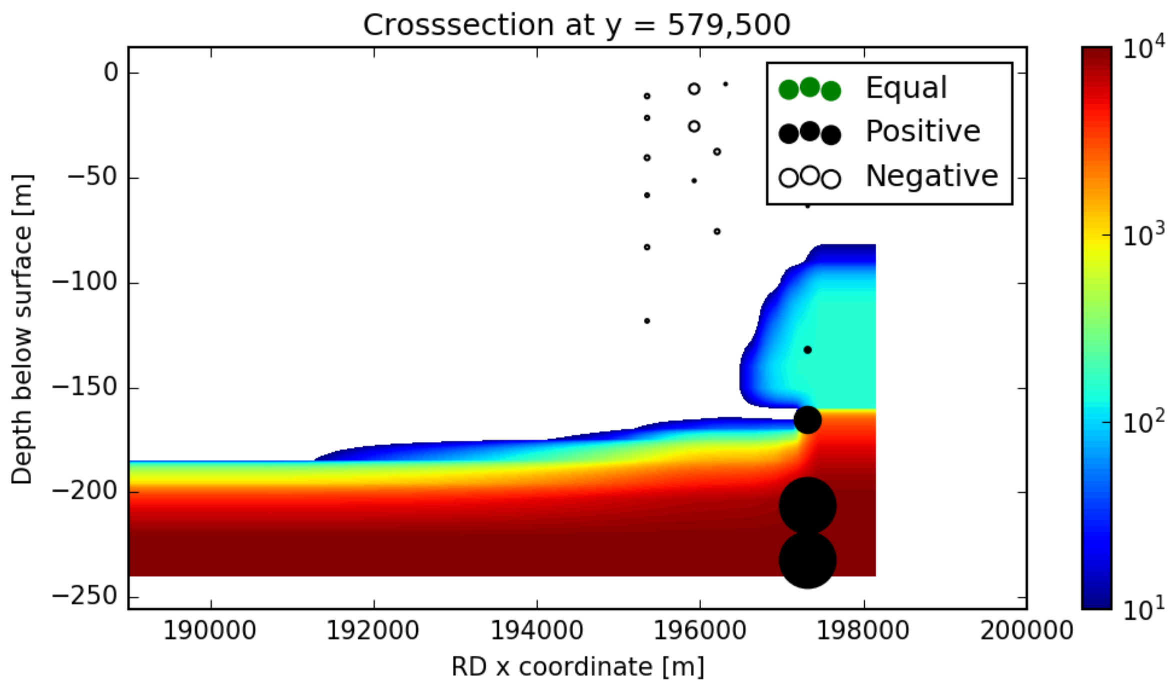

Figure G.5: Cross-section, created with the initial distribution van der Valk (2011)

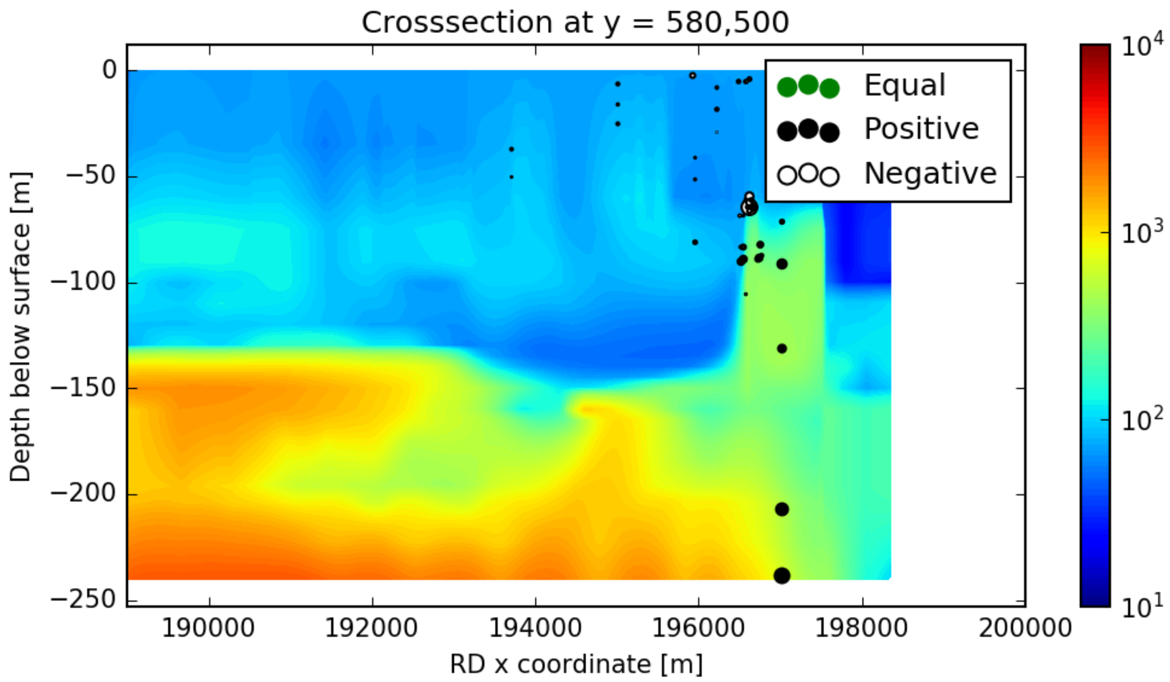

Figure G.6: Cross-section, created with distribution A

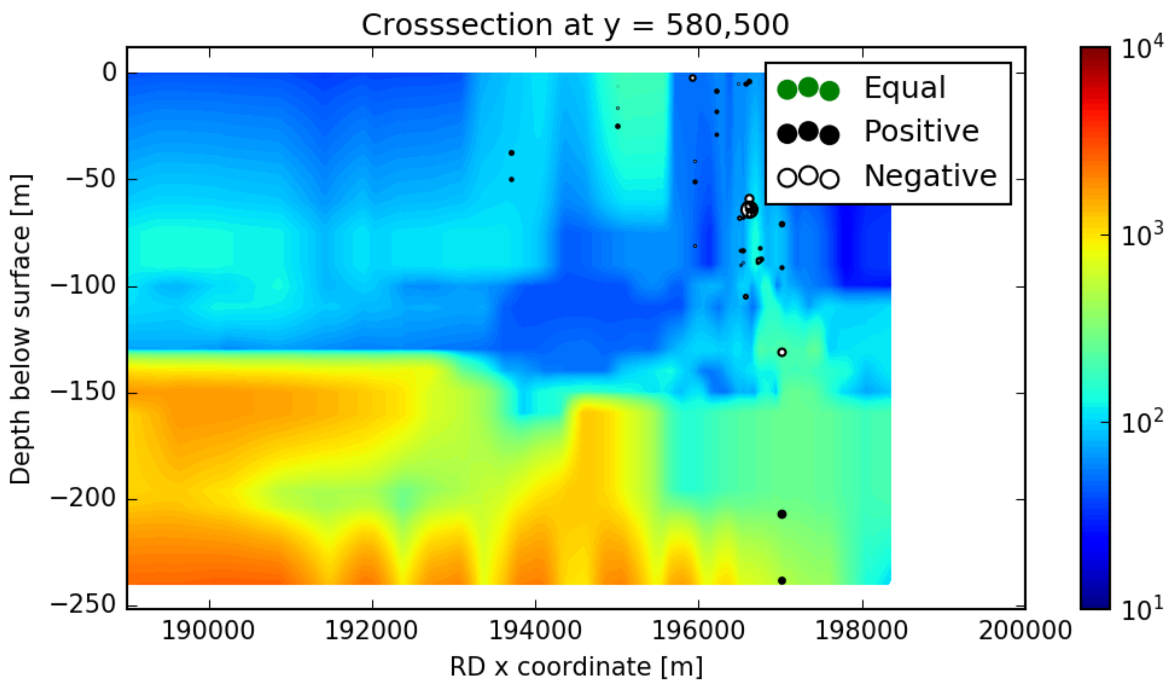

Figure G.7: Cross-section, created with distribution B

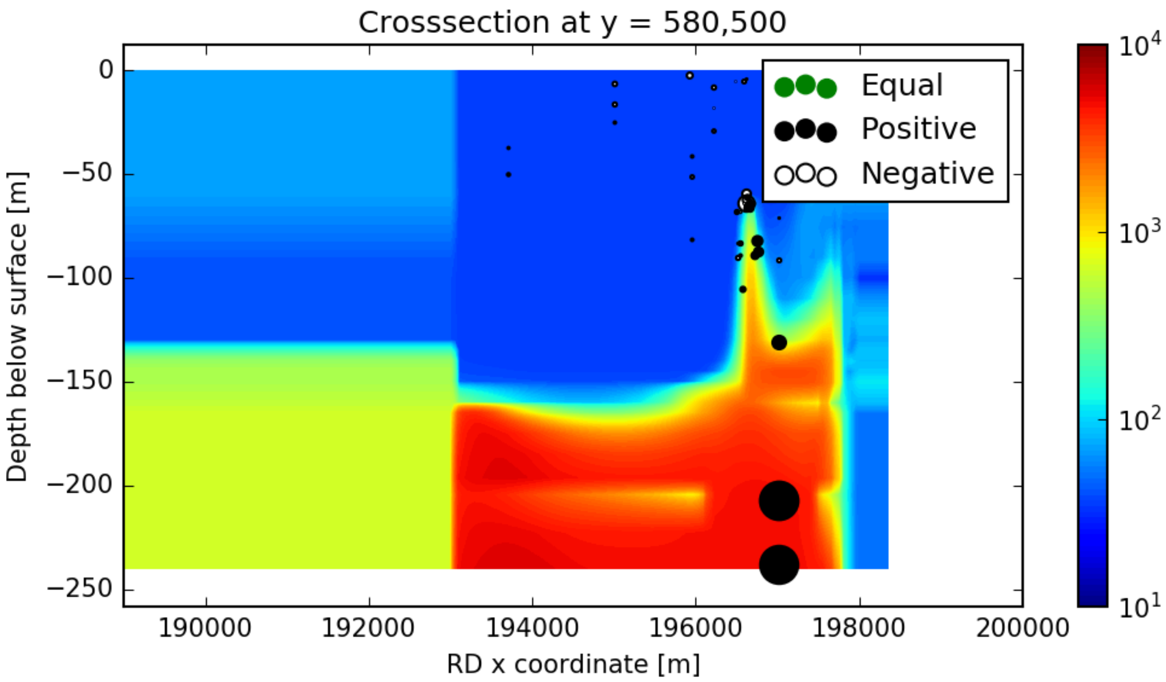

Figure G.8: Cross-section, created with the initial distribution van der Linde (2014)

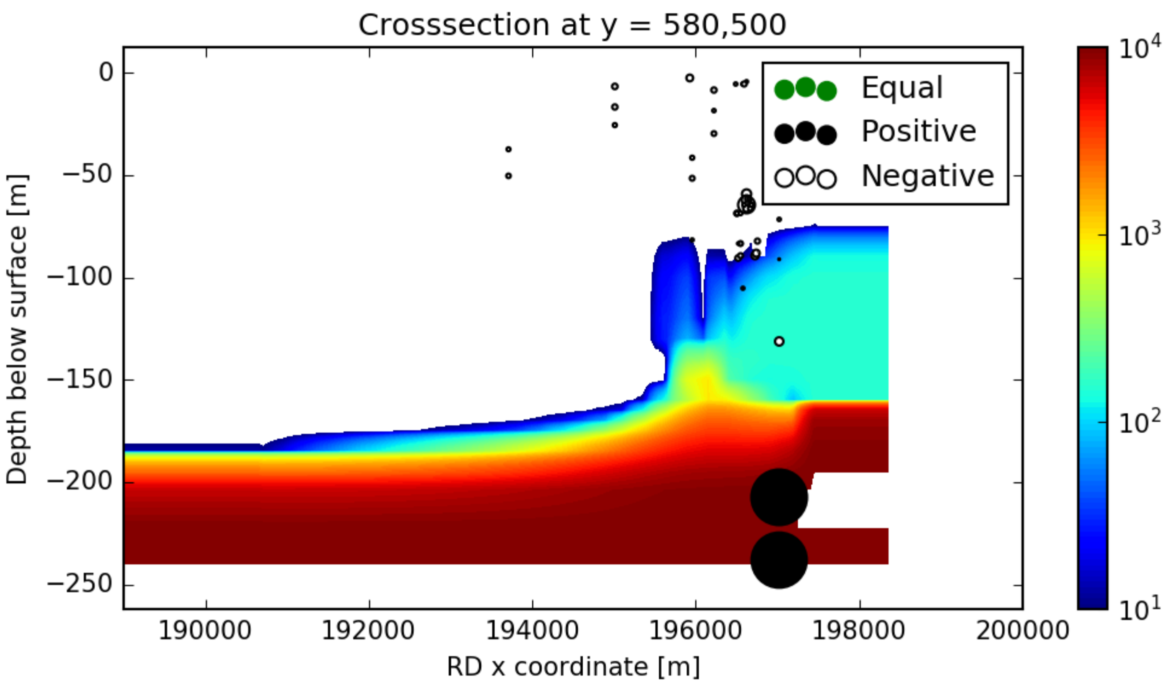

Figure G.9: Cross-section, created with the initial distribution van der Valk (2011)

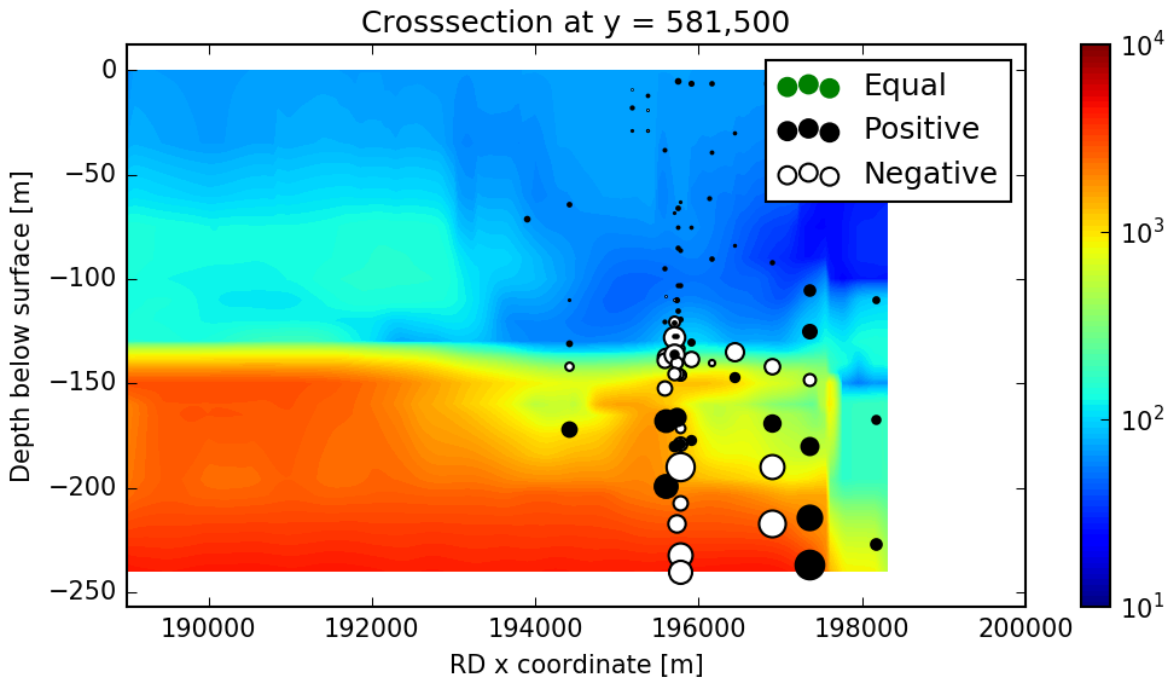

Figure G.10: Cross-section, created with the distribution A

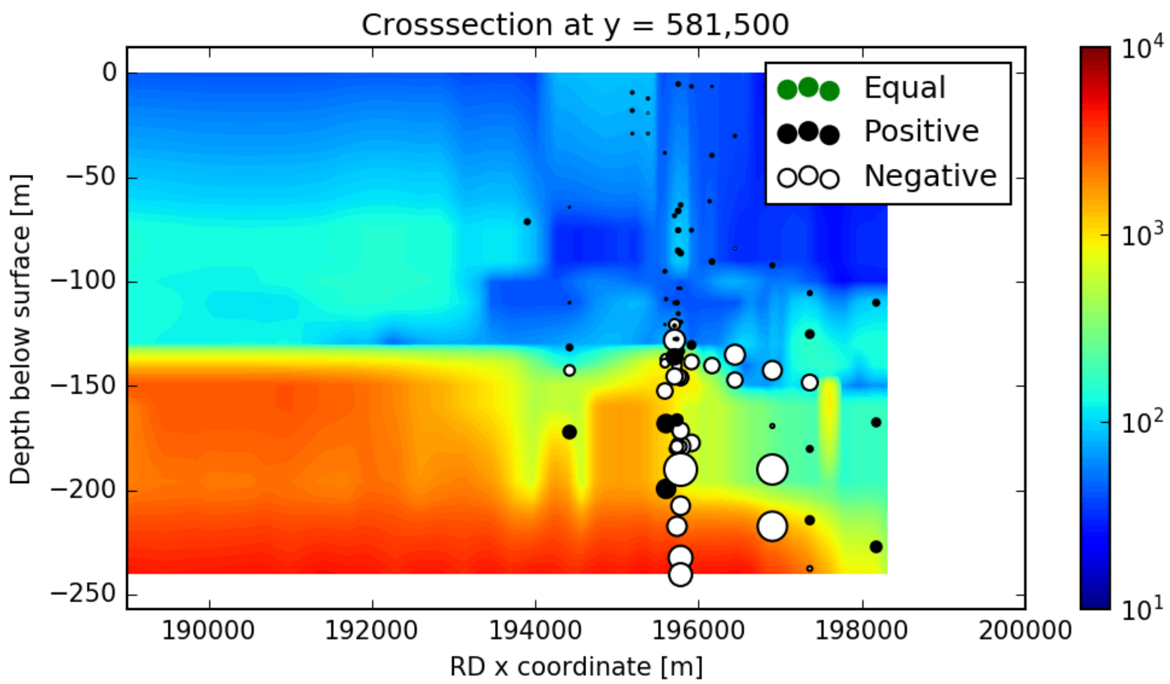

Figure G.11: Cross-section, created with distribution B

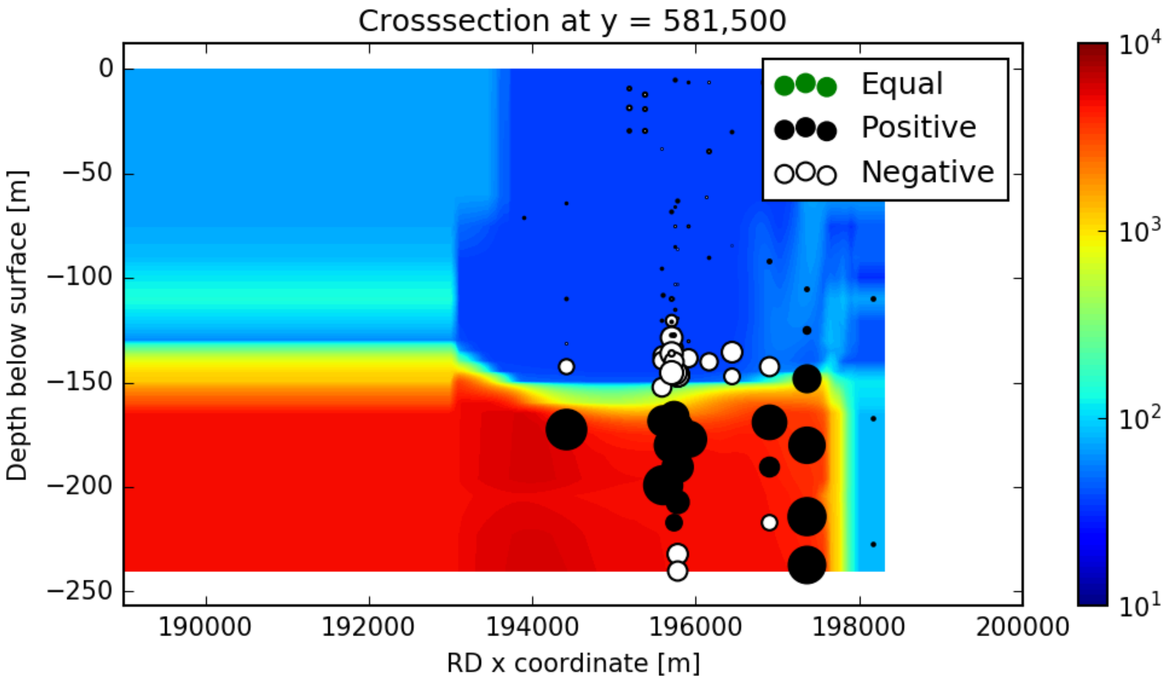

Figure G.12: Cross-section, created with the initial distribution van der Linde (2014)

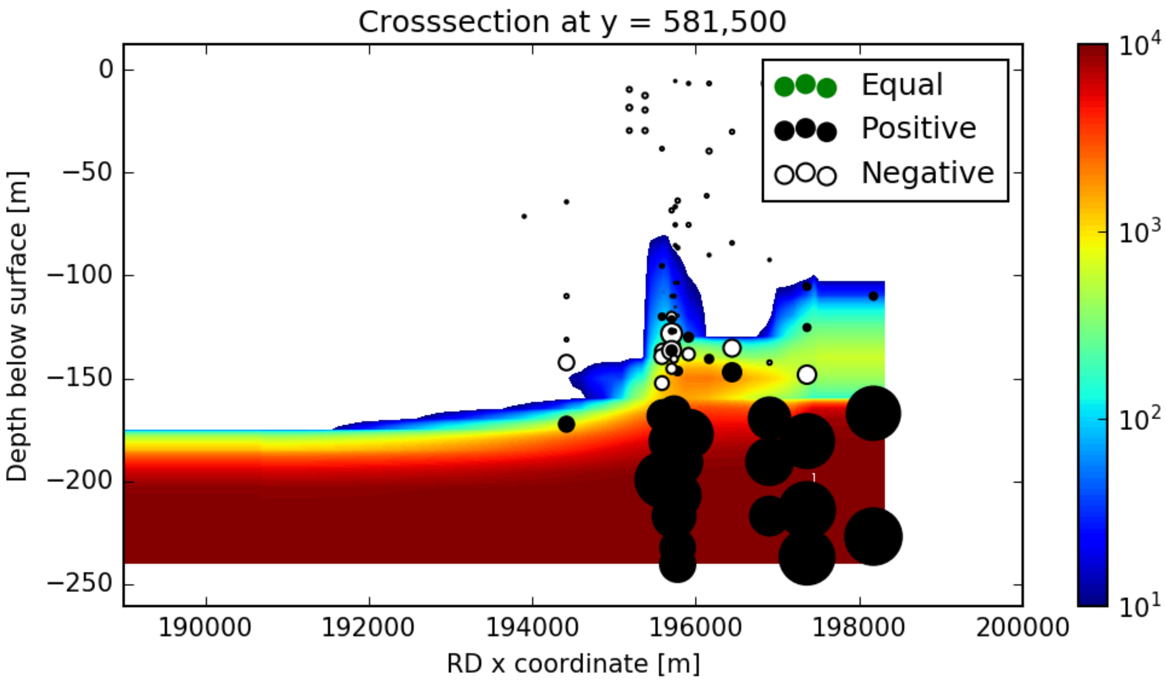

Figure G.13: Cross-section, created with the initial distribution van der Valk (2011)

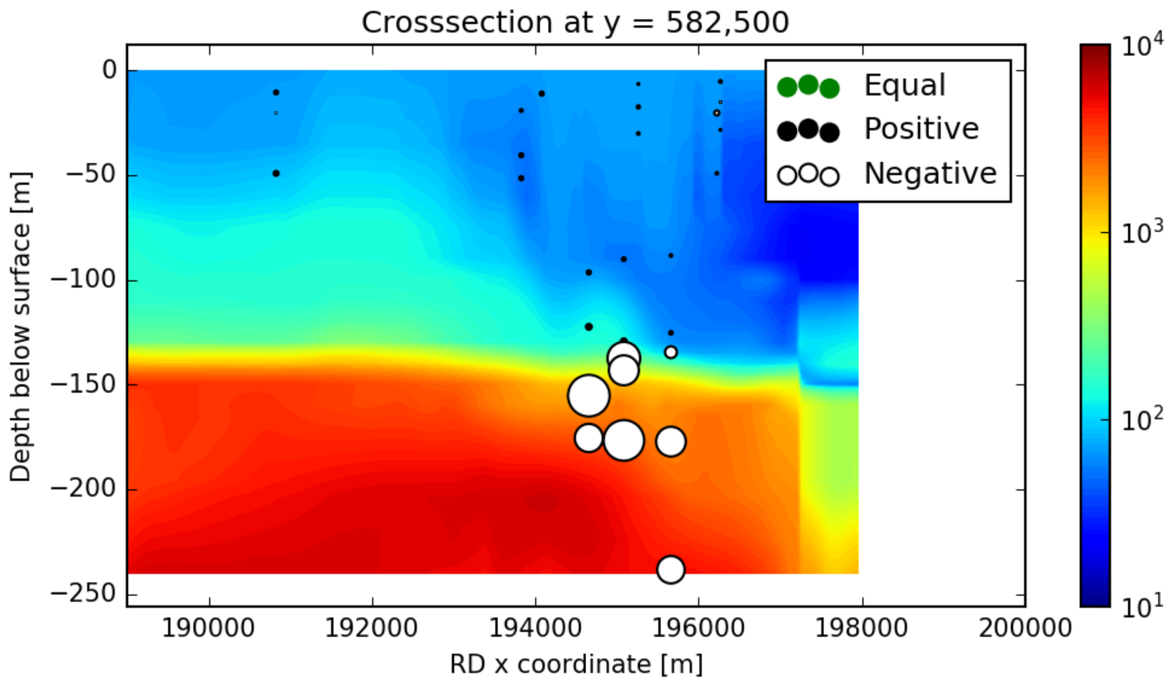

Figure G.14: Cross-section, created with the distribution A

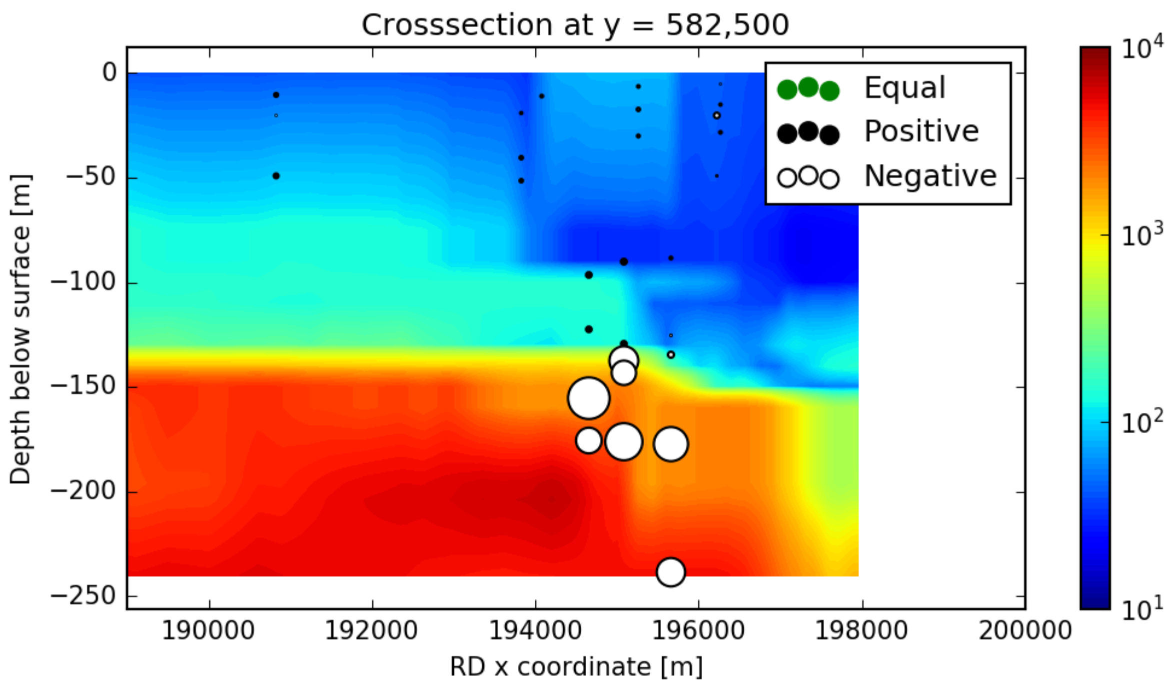

Figure G.15: Cross-section, created with distribution B

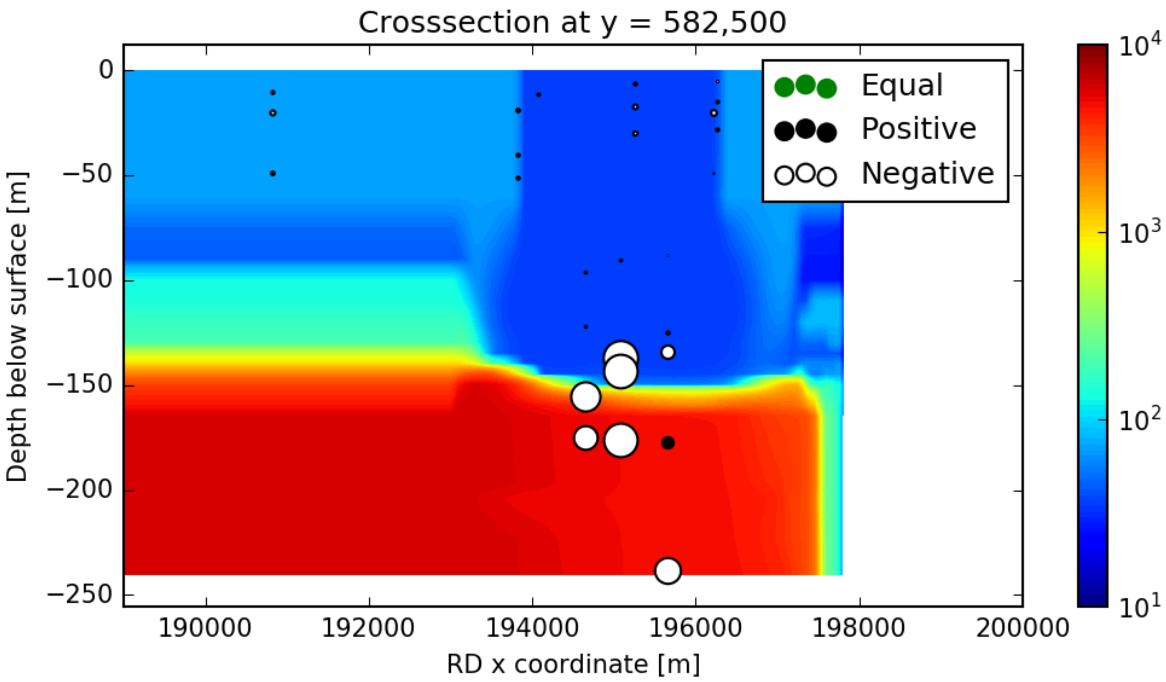

Figure G.16: Cross-section, created with the initial distribution van der Linde (2014)

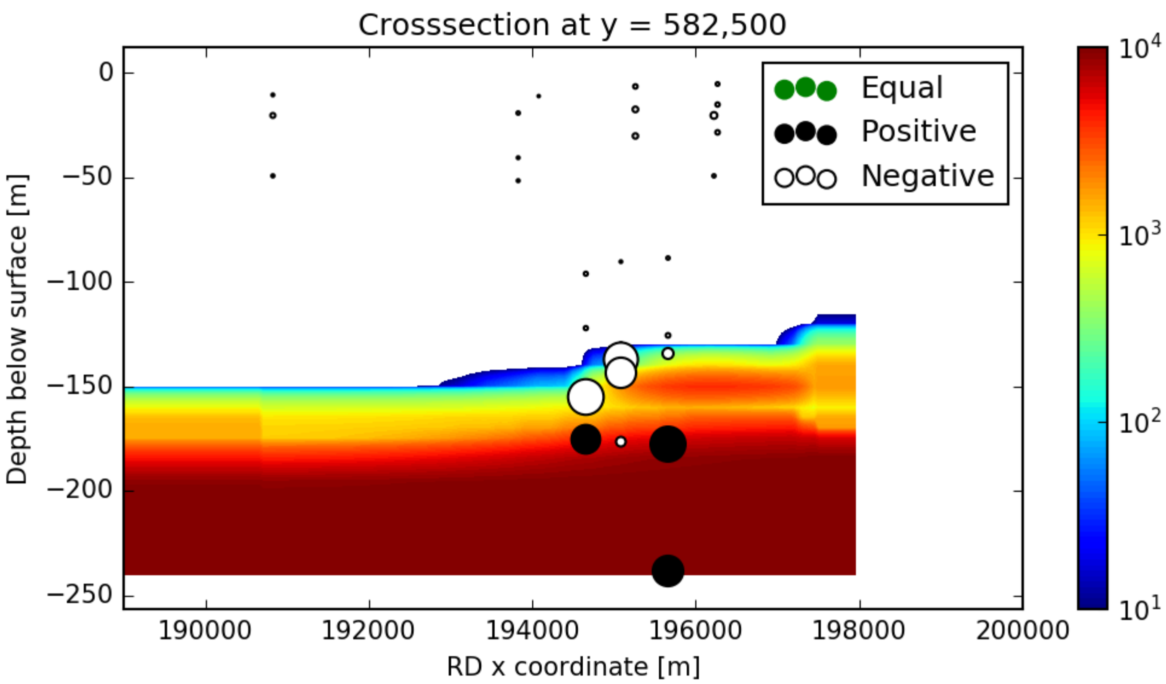

Figure G.17: Cross-section, created with the initial distribution van der Valk (2011)

H

Aquifer testing

One of the most efficient ways of obtaining reliable values for the hydraulic characteristics of geological formations is through aquifer testing. An aquifer test is performed by measuring the discharge of the pump and the drawdown of the water Table at known distances from the pump. Hydraulic characteristics of the aquifer can be calculated using these measurements. The following hydraulic characteristics of the aquifer can be determined using aquifer testing (Heath, 1983; Kruseman and de Ridder, 1979):

- **Transmissivity**
  Product of the average hydraulic conductivity (K) and saturated thickness of aquifer (D).
- **Leakage factor or characteristic length**
  This is a measure of leakage through the aquitard. Equation H.2 calculates the leakage factor. The leakage factor includes the hydraulic resistance of an aquitard.
- **Storage coefficient**
  Volume of water released or taken into storage per unit of surface area of the aquifer per unit change in head.

Two different methods developed to determine aquifer characteristics will be used. Also, the software MLU (Lite Version 2.25.68) can be used to calculate hydraulic characteristics. MLU includes different analytical methods, including the following presented methods (Hemker and Post, 2014).

H.1. De Glee method

This method is applied to steady-state drawdown (De Glee, 1930).

$$s = \frac{Q}{2\pi T} K_0\left(\frac{r}{\lambda}\right) \tag{H.1}$$

$$\lambda = \sqrt{Tc} \tag{H.2}$$

Where

s	is the drawdown (L),
Q	is the discharge (L^3 T^{-1}),
T	is the transmissivity (L^2 T^{-1}),
K_0	is the second kind zero order Bessel function (-),
r	is the radial distance (L),
λ	is the Leakage factor (L),
c	is the hydraulic resistance of an aquitard (T)

H.2. Hantush method

This method is applied for transient drawdown (Hantush, 1956).

$$s(r,t) = \frac{Q}{4\pi T} W\Big(u, \frac{r}{\lambda}\Big) \tag{H.3}$$

$$W = \int_u^\infty \frac{1}{y} \exp\Big(-y - \frac{r^2}{4\lambda^2 y}\Big) dy \tag{H.4}$$

$$u = \frac{r^2 S}{4Tt} \tag{H.5}$$

Where
W is the ‘Well function’ for leaky systems (-),
S is the Storage Coefficient (-),
t is the time since start of pumping (T)

The Well Function in Equation H.4 can be approximated by the follow function: (Maas and Veling, 2010)

$$F(\theta,\tau) = \begin{cases} 2 * K_0(\theta) - wE_1\Big(\frac{\theta}{2}\exp\tau\Big) + (w-1)E_1(\theta\cosh\tau) & \tau > 0 \\ wE_1(\frac{\theta}{2}\exp\tau) - (w-1)E_1(\theta\cosh\tau) & \tau \leq 0 \end{cases} \tag{H.6}$$

$$w = \frac{E_1(\theta) - K_0(\theta)}{E_1(\theta) - E_1(\frac{\theta}{2})} \tag{H.7}$$

Where
K_0 is the second kind zero order Bessel function (-),
E_1 is the Exponential integral (-),
θ and τ are variables (-)

Using Equation H.6 and Equation H.7, Equation H.3 becomes:

$$s(r,t) = \frac{Q}{4\pi T} F\Big(\frac{r}{\lambda}, \ln\Big(2\frac{\lambda}{r}\frac{t}{cS}\Big)\Big) \tag{H.8}$$

H.3. Aquifer test

During the first week of October in 2015 an aquifer test was performed with the Smart Well. The aquifer test took place after a period in which the Smart Well was not active (see Figure F.2). Over an period of 8 days the Smart well was extracting both fresh and brackish water at a rate of 1,700 m^3 d^{-1} and 350 m^3 d^{-1}, respectively. Infiltration was kept at the same rate as the extraction of brackish water. Ten locations were selected to monitor the variation of the water Table. Divers, sensors to measure water pressure, were used to for the monitoring of the water Table. The data from the weather station of the KNMI (Koninklijk Nederlands Meteorologisch Instituut) in Leeuwarden was used to account for precipitation, evaporation and air pressure differences. Using Menyanthes, software to analyze observed water head (Von Asmuth, 2012), the drawdown caused by the Smart Well can be calculated. The hydraulic characteristics of the aquifer can be calculated using the methods explained in Section **??**. The extraction at Ritskebos (± 1.3 kilometers from the Smart Well) was not known during this period. Variations of the extraction at Ritskebos can cause nuisance in the results.

H.4. Results of aquifer testing

The calibration of the parameters is performed using the methods explained in Section 4.1 and 4.2. The objective function, Equation 4.1, is minimized using the piezometer data. The results of the aquifer test are used as an indication of the reliability of the calibration process for the first aquifer. Also, the different initial

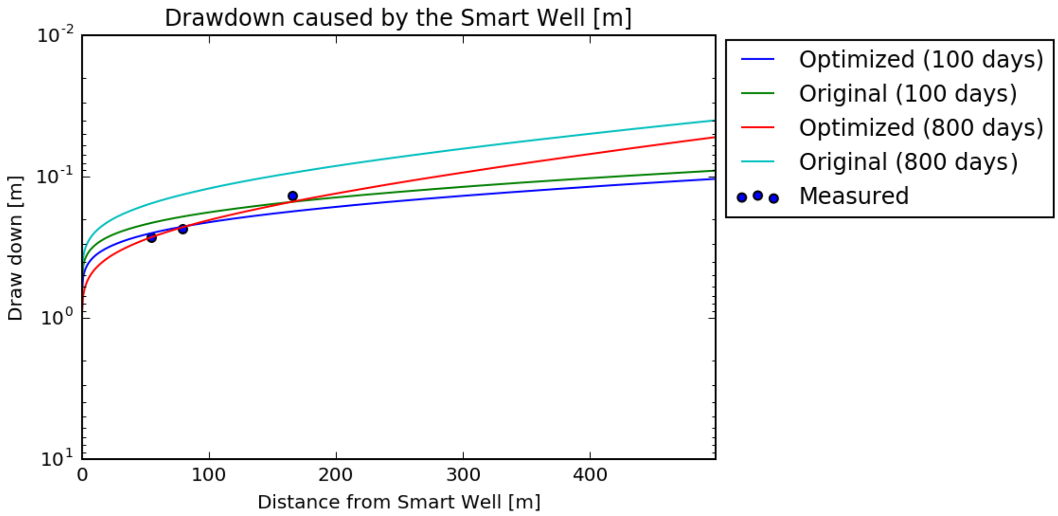

Figure H.1: Drawdown [m] caused by the Smart Well for the original and optimized transmissivity for different top layer resistances

chloride distributions are analyzed and compared. Lastly, the velocity and direction of the groundwater flow is presented using the optimal parameter values calculated in the calibration process.

The results of the aquifer test conducted in the first aquifer are analyzed. The calculated final drawdown using Menyanthes is presented in Table H.1. Some of the data is considered to be unreliable due to unrealistic results, such as a drawdown of 32 meters while the expected drawdown is just a few decimeters.

The optimal calculated transmissivity is presented in Table H.2. Using de Glee and Least Squares calibration method, and the free version of the MLU software, similar results are found for the different resistances of the semi-confining layer. The drawdown over a radial distance from the Smart Well using the original parameters and the optimal parameters from the calibration process is presented in Figure H.1.

Table H.1: Final drawdown results of the aquifer test for the different measurement locations

Name	Filter	Depth diver [m-NAP]	Radial distance to Smart Well [m]	Drawdown [m]	Reliable
06DP0002	1	5.8	361	0.0782	No
06DP0016	1	69.9	209	0.0272	No
06DP0017	2	59.8	79	0.2346	Yes
06DP0018	1	7.2	55	31.9957	No
06DP0018	2	70.2	55	0.2703	Yes
06DP0048	1	66.2	334	0.1581	No
06DP0127	2	7.4	228	4.2976	No
06DP0208	2	94.9	166	0.1377	Yes
06DP0208	4	138.9	166	0.1360	Yes
06DP0208	5	152.9	166	0.2159	No

Table H.2: Analytically calculated optimal transmissivity of the aquifer test for different resistances using results from Table H.1

Resistance Semi-confining layer	De Glee
c = 100 d	2,900 m^2/d
c = 325 d	4,000 m^2/d
c = 800 d	4,800 m^2/d

H.5. Discussion of the aquifer test

The results of the aquifer test are not equal to previous conducted aquifer tests. IWACO (1979) conducted an aquifer test in 1978 and used a resistance for the semi-confining layer of 365 days. Using the same resistance leads to different results (see Table H.2). A reason the results are different, may be that the new aquifer test is conducted over a short period (± 8 days) and disturbance by precipitation occurred. The precipitation is measured 20 kilometers west of Noardburgum at the KNMI station in Leeuwarden. Precipitation is spatial variable, thus the measured precipitation during aquifer test at Leeuwarden may not be representative for Noardburgum. Also, the exact extraction of Ritskebos is not known during the aquifer testing.

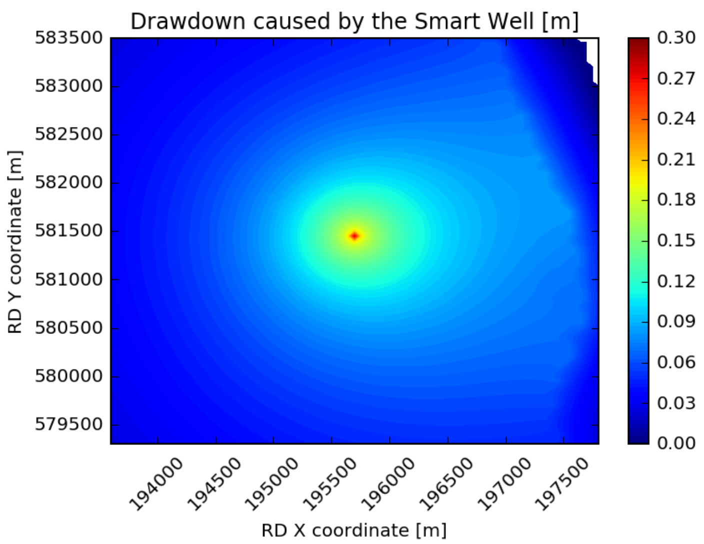

Figure H.2: Modeled drawdown caused by the Smart well

Just four results from the aquifer test are considered to be reliable. A result is considered reliable when the observed drawdown makes sense and is in line with the other observed drawdowns. The result of the aquifer test indicates the transmissivity is between 2,800 and 4,900 $m^2\ d^{-1}$. The Glacial tunnel valley east of the Noardburgum well field is modeled as an impermeable wall (or a no flow boundary). As can be seen in Figure H.2 additional drawdown occurs at the impermeable wall. This impermeable wall has an influence on the drawdown which cannot be accounted for by the presented analytical formulas. An image well can be used to account for an impermeable boundary (Fitts, 2002). However, this will result in negligible differences near the Smart Well. Negligible differences in drawdown at the measurement locations are observed when using the analytically calculated transmissivity in the model.